الجمهورية الجزائرية الديمقراطية الشعبية

REPUBLIQUE ALGERIENNE DEMOCRATIQUE ET POPULAIRE

وزارة التعليم العالي و البحث العلمي

Ministère de l'Enseignement Supérieur et de la Recherche Scientifique

جامعة أبي بكر بلقايد – تلمسان –

Université Aboubakr Belkaïd – Tlemcen –
Faculté de TECHNOLOGIE

MEMOIRE

Présenté pour l'obtention du **diplôme** de **MASTER**

En : Electrotechnique

Spécialité : Commandes Electriques

Par : OCHIENG Ehud Barack
&
KABUYE Vianney Ernest

Sujet

Study and Control of a Three-Phase Switched-Inductor Split Source Inverter (SI-SSI)

Soutenu publiquement, le 16 / 06 /2025, devant le jury composé de :

M. LOUCIF Mourad	MCA	Université de Tlemcen	Président
M. BENHABIB Mohamed Choukri	Professeur	Université de Tlemcen	Examinateur
Mme. GHLAM Karima	MCA	Université de Tlemcen	Encadreur

Année universitaire : 2024 /2025

Dedications

I dedicate this thesis to my parents, whose support, encouragement, and sacrifices have been the foundation of my academic journey.
To my thesis partner Kabuye Vianney Ernest.
To the friends and family we made along the way.
Most importantly, to our Almighty Lord our God, Alhamdulillah
- Ehud

I dedicate the thesis to my family for their encouragement and unconditional love and support they provided during this journey.
To my teachers and professors for their wisdom and patience during this academic journey.
To my thesis partner Ochieng Barack and all my classmates of electrical engineering of the year 2024/2025 for their help and experiences we shared.
-Vianney

Acknowledgements

First, we would like to thank The Almighty God who has enabled us to come this far. It is by His grace that we were able to succeed in our studies and attain this milestone.

We also express our deepest gratitude to the members of the jury, Dr. Mourad Loucif and Prof. Mohamed Benhabib Choukri for their time and valuable insights and feedback during the evaluation of this thesis. We thank our supervisor, Dr. Ghlam Karima, for her patience, availability, and invaluable guidance and mentorship through this thesis preparation. Moreover, we are grateful for her trust in us to be able to accomplish this thesis, even though we had some ups and downs.

We express our genuine gratitude to the members of the jury for their interest in reviewing the work that we are to present.

We also acknowledge the numerous professors that we consulted during the preparation of this thesis. Finally, our dear classmates with whom we studied and formed unbreakable bonds advancing from just classmates to lifelong friends.

Contents

List of Figures

List of Tables

Nomenclature

The principal notations and abbreviations used in this thesis are explained below in their most commonly used forms in electrical engineering. The symbols are grouped by their application domains for easier reference.

Nomenclature: Symbols and variables

Symbol	Description	Unit
V_{dc}	DC bus voltage	V
M_i	Modulation index ($0 \leq M_i \leq 1$)	–
ω	Angular frequency ($2\pi f$)	rad/s
f	Output frequency	Hz
D	Duty cycle	–
t_x	Inductor charging time	s
t_y	Inductor discharging time	s
$D_{\min}$	Minimum duty cycle	–
$D_{\max}$	Maximum duty cycle	–
D_{avg}	Average duty cycle	–
V_C	DC-link capacitor voltage	V
V_L	Inductor voltage	V
I_L	Inductor current	A
ΔI_L	Inductor current ripple	A
ΔV_C	DC-link voltage ripple	V
f_c	Carrier frequency	Hz
f_f	Fundamental frequency	Hz
K	Modulation technique constant	–
$\mathbf{V}_{abc}$	Phase voltage vector ($[V_{an}, V_{bn}, V_{cn}]^T$)	V
$\mathbf{V}_{ll}$	Line-to-line voltage vector ($[V_{ab}, V_{bc}, V_{ca}]^T$)	V
$\vec{V}_s$	Complex space vector	–
$\mathbf{S}$	Switching state vector	–
a	120° phase shift operator ($e^{j\frac{2\pi}{3}}$)	–
V_{pph}	Peak phase voltage	V
g	Inverter gain	–
B	Boosting factor (SSI)	–
B_{SL}	Boosting factor (SI-SSI)	–

Nomenclature: Abbreviations

Abbreviation	Description
VSI	Voltage Source Inverter
CSI	Current Source Inverter
SSI	Split-Source Inverter
SI-SSI	Switched-Inductor Split-Source Inverter
ZSI	Z-Source Inverter
q-ZSI	Quasi-Z-Source Inverter
SPWM	Sinusoidal Pulse Width Modulation
SVPWM	Space Vector Pulse Width Modulation
THIPWM	Third-Harmonic Injection PWM
DPWM	Discontinuous PWM
THD	Total Harmonic Distortion
EMI	Electromagnetic Interference
PV	Photovoltaic
EV	Electric Vehicle
IGBT	Insulated Gate Bipolar Transistor
MOSFET	Metal-Oxide-Semiconductor Field-Effect Transistor

GENERAL INTRODUCTION

Global shift towards renewable energy and electrification has generated increasing demands for efficient, reliable, and cost-effective power conversion solutions. The traditional voltage source inverters (VSIs) and current source inverters (CSIs) have been commonly adopted but they still suffer from some drawbacks, including acquiring limited voltage gain, being sensitive to the electromagnetic interference (EMI) as well as the requirement of additional DC-DC converters. These limitations have led to advanced topologies such as Z-source inverter and quasi-Z-source inverters, which provide single-stage power conversion while achieving better reliability. However, these approaches present their own set of issues such as complicated control programming and a large number of passive elements.

This thesis presents a comprehensive study of the switched-inductor split-source inverter, an emerging topology that incorporates a series of inductor networks to enhance its voltage boosting in a single stage. The SI-SSI is suitable for low-voltage renewable energy sources like photovoltaic (PV) systems. However, the SI-SSI still faces challenges when it comes to control optimization and operational efficiency that still need to explored. Traditional inverters that are commonly used are VSI and CSI. The V-source inverter is a buck (step-down) inverter for DC-to-AC conversion while the V-source converter is a boost(step-up) rectifier. On the other hand, I-source is a boost inverter for DC-to-AC power conversion and I-source converter is a buck rectifier for AC-to-DC conversion [1]. However, these converters suffer from limitation such as restricted voltage gain, vulnerability to EMI noise and need for additional DC-to-DC converters. The additional DC-to-DC boost converter necessitates a second switching device that increases the system's footprint and cost and reduces its efficiency [2]. To address these challenges , Z-source inverter and quasi-Z-source inverter have been developed offering single-stage power conversion with improved reliability. However, these topologies introduce issues such as complex control requirements and high passive component count.

To address these challenges, the Switched Inductor Split-Source Inverter(SI-SSI) has been introduced, which integrates a switched inductor network to enhance the voltage-boosting capability without additional active switches, which makes it particularly attractive for applications involving low-voltage renewable energy sources such as photovoltaic(PV) systems [2].

However, despite its potential, challenges related to control strategy optimization, operational efficiency, and implementation feasibility still arise. This study explores these issues to establish the SI-SSI as an effective, high-efficiency, and innovative solution for modern power conversion applications. The SI-SSI presents an alternative integrating boosting and inversion in a single stage, reducing the component count and improving its overall efficiency.

By addressing these objectives and scope, the study aims to enhance the efficiency and reliability of power conversion technologies, particularly enabling seamless integration of renewable energy into the power grid.

The objective of this project is to design and investigate the operation and performance of the new three-phase switched-inductor split source inverter (SI-SSI). In the earlier stages of development, this new topology has demonstrated improved energy efficiency.

1. Analyze the SI-SSI topology :To investigate the operational principles and structural advantages compared to the traditional inverters.

2. Evaluate the voltage boosting capacity: assess the voltge gain performance of SI-SSI and benchmark it against existing boost inverter topologies to determine its effectiveness in achieving higher output voltage levels.

3. Investigate control strategies: develop and explore advanced control methodologies such as SPWM to optimise the performance of the SI-SSI.

4. Assess the efficiency and power quality: Examine the efficiency metrics and power quality output of the SI-SSI under varying operating conditions including different load profiles and input voltage variations.

5. Explore potetntial applications: Identify and evaluate the sustainability of SI-SSI for renewable energy systems, electric vehicles and industrial motor drives.

6. Validate Through Simulation and Hardware Implementation: Use MATLAB/Simulink tools to model te SI-SSI, where feasible, develop hardware prototype to experimentally validate

Scope of the study

- Theoretical and Simulation Analysis: The research will focus and mathematical modelling and simulation studies to comprehensively understand the performance of the SI-SSI and its behaviour.
- Control Techniques: SPWM will be implemented as an efficient modulation scheme for the SI-SSI.
- Comparative Analysis: A detailed comparison will be conducted between the SI-SSI topology and other inverter topologies to highlight the performance improvements in terms of voltage gain, efficiency, and component stress. Voltage range and applications.
- Hardware implementation constraints: any hardware development will be limited to lab oratory-scale prototypes, with a focus on proof-of-concept rather than commercial deployment.

The study is organized in chapters as follows:

- Chapter 1: In this chapter the fundamentals of power electronics and inverters, classification, operation principles, various control strategies, performance parameters of three-phase inverters, switched-inductor topology, mathematical modeling and operation of both the Split-Source Inverter (SSI) and switched-inductor SSI (SI-SSI) topologies are discussed.

- Chapter 2: Discussed in this chapter is the MATLAB/Simulink implementation of the three inverter topologies and interpretation of results. Comparative analysis of the performance metrics of each topology is also presented here.
- Chapter 3: describes the hardware implementation of the SI-SSI in Proteus software and presents the general conclusion and findings of this study with key findings and recommendations for future work.

The research aims to establish the SI-SSI as an effective, high-efficiency solution to renewable energy applications, integration, and in electric vehicles due to its robustness and high boosting capabilities in medium to high-power applications.

Chapter 1

INTRODUCTION TO POWER ELECTRONICS AND INVERTERS

1.1 Introduction

This chapter explores the fundamentals of power electronics and inverters. The key concepts include an overview of power electronics, the importance of three-phase inverters in renewable energy and industrial applications.

Power electronics is a branch of electrical engineering that deals with the conversion and control of electric power using electronic devices [3]. Inverters are very essential components that are mainly used for the conversion of DC power to AC power, enabling compatibility with grid systems and AC powered devices [4]. In recent studies, it has been shown that power electronic systems achieve conversion accuracy exceeding 95% in three-phase inverter applications [5], making them indispensable for the integration of renewable energy.

1.2 Fundamentals of power electronics

Power electronics encompasses three key aspects [3, 6]. Modern power electronic systems are based on three fundamental elements that work together to facilitate efficient power conversion. Semiconductor devices form the backbone of these systems, with ttransistors,mainly IGBTs and MOSFETs being the predominant choices due to their exceptional fast-switching capabilities and high-efficiency characteristics [6]. Diodes and thyristors are also used depending on the application requirements.These devices allow for various operations in power converters including AC to DC, DC to AC, DC to DC, and AC to AC conversions. The performance of these systems is further enhanced by advanced control methodologies, particularly the PWM technique, which are critical to maintaining power quality [7].

1.3 Inverters

Power inverter is a power electronic device that converts electrical energy from DC to AC for both domestic and industrial application. This conversion is essential for integrating renewable energy systems such as solar panels into the AC power grid [8]. The rise in Electric Vehicles also lead to the rise for the need for efficient inverters to convert the energy DC energy stored in batteries into usable AC energy needed to run the motors. With the energy revolution towards renewable and sustainable energy, inverters have become more popular in the recent years.

1.4 Classification of inverters

Power inverters can mainly be classified into:

1. Voltage Source Inverters (VSI)
2. Current Source Inverters (CSI)
3. Variable DC linked Inverter

In VSI, the input DC source has negligible impedance, while CSI is fed with an adjustable current from a high-impedance DC source.

A standard single-phase voltage or current source inverter can be in a half-bridge or full-bridge configuration. Single-phase units can be joined to have three-phase or multi-phase topologies [9].

1.5 Autonomous inverters

An autonomous inverter, commonly referred to as a stand-alone or off-grid inverter, is a power electronic device that converts direct current (DC) from sources like batteries or solar panels into alternating current (AC) for use in electrical appliances, operating independently of the main electrical grid. In addition to their functional independence, off-grid energy storage inverters are typically more economical than their grid-tied counterparts. Their simpler design and manufacturing process make them cost-effective, especially for residential or small-scale commercial users seeking affordable solar energy solutions. These characteristics make off-grid inverters a practical and efficient choice for decentralized energy systems [10].

1.5.1 Current source inverters

Current source inverter (CSI) is a type of power electronic converter that primarily focuses on maintaining a nearly constant output current, while allowing the output voltage to vary with changes in the load. In contrast to a Voltage Source Inverter (VSI), where the voltage is kept constant, the CSI operates such that the current remains stable despite fluctuations in load conditions, making it ideal for applications where current control is paramount.

CSIs are widely used in applications such as motor drives for Iinduction motors where load torque can fluctuate, and precise current control is essential for efficient operation. The CSI design allows for the seamless adjustment of the output current, ensuring that the motor receives the necessary current to meet varying load conditions without compromising performance [11].

1.5.2 Voltage source inverters

Voltage Source Inverters as the name indicates, receives DC voltage and then converts it to AC voltage. The AC voltage and frequency may be variable depending on the application. It operates using high-speed switching devices, such as MOSFETs or IGBTs, controlled by modulation techniques such as PWM and SPWM. In VSI, power semiconductor devices always remain forward biased due to DC supply voltage [3]. They are widely used in applications such as motor drives, renewable energy systems, and uninterruptible power supply (UPS). Their benefits include high efficiency, precise voltage control, and adaptability for both grid-connected and standalone systems, making them essential in modern power electronics.

1.5.2.1 Single-phase half-bridge voltage source inverters

A single-phase half-bridge voltage source inverter (VSI) is a fundamental power converter that transforms a constant DC voltage into an alternating AC voltage. It consists of two power electronic switches (Q1 and Q2) and two equal DC-link capacitors (C1 and C2 that split the DC voltage into two equal parts, providing a neutral reference point for the AC output.

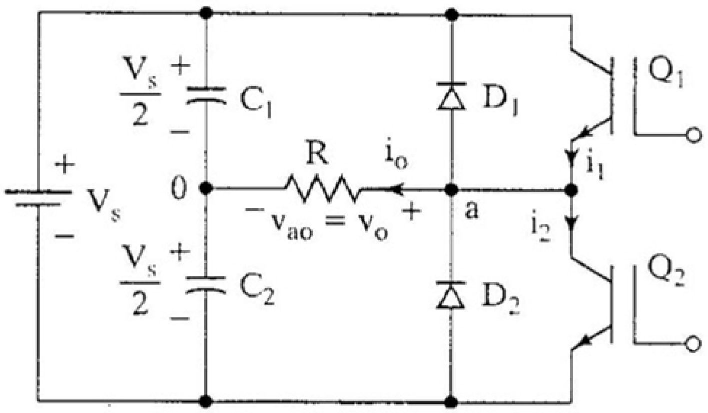

Figure 1.1: Single-phase half-bridge voltage source inverters

Operating Principle

The inverter operates by alternately switching Q1 and Q2. When Q1 is ON and Q2 is OFF, the output voltage across the load is $+\frac{V_{dc}}{2}$. When Q1 is OFF and Q2 is ON, the output becomes $-\frac{V_{dc}}{2}$ creating a two-level square waveform. In practical applications, Pulse Width Modulation (PWM) is applied to modulate the switching pattern, improving the output waveform and reducing harmonic content.

This topology is commonly used in low-power applications such as small induction motor drives, domestic inverters, and power electronics training kits due to its structural simplicity and cost-effectiveness. However, its output power is limited compared to full-bridge inverters, and it requires a split DC supply or balanced capacitors to maintain symmetry in operation [3].

1.5.2.2 Single-phase full-bridge voltage source inverter

A single-phase full-bridge voltage cource snverter (VSI) is a widely used inverter topology that converts a constant DC input into an alternating AC output by employing four power electronic switches, typically labeled Q1 to Q4. Unlike the half-bridge configuration, the full-bridge inverter can apply the full DC voltage $\pm V_{dc}$ across the load, resulting in higher output power and better utilization of the DC supply.

The inverter operates in a two-step switching sequence. In the first half of the cycle, switches Q1 and Q3 are ON-stated, allowing current to flow through the load in one direction and producing a positive output voltage $+V_{dc}$. In the second half of the cycle, Q2 and Q4 conduct, reversing the current direction through the load and generating a negative output voltage $-V_{dc}$. This switching action produces a bipolar square wave across

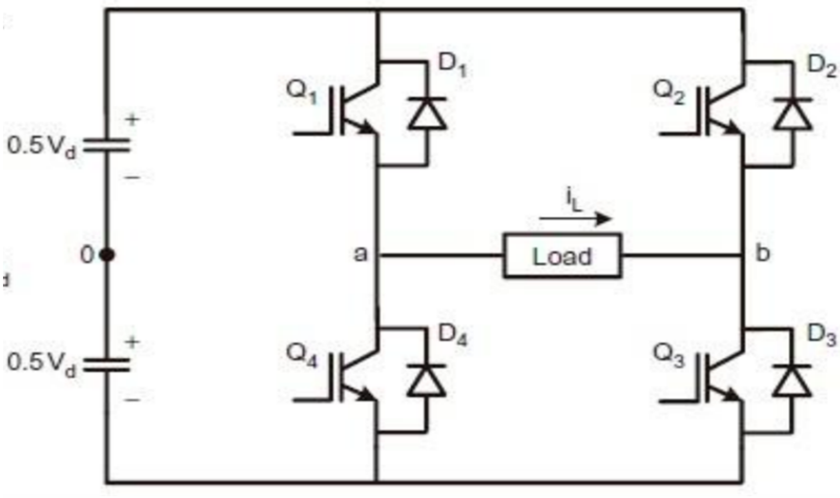

Figure 1.2: Single-phase full-bridge voltage source inverter

the load. To enhance waveform quality, Pulse Width Modulation (PWM) techniques are typically used, enabling better control over the output frequency and voltage, as well as reduced harmonic distortion.

The full-bridge VSI is commonly used in applications such as industrial motor drives, solar inverters, UPS systems, and electric vehicle (EV) inverters, due to its efficient use of the DC bus and ability to deliver higher power levels [3].

1.6 Resonant inverters

A resonant inverter is a type of power electronic converter that transforms direct current (DC) into alternating current (AC) using a resonant circuit, typically consisting of inductors and capacitors. Unlike conventional square-wave or PWM-based inverters, resonant inverters operate by driving a load at or near the natural resonant frequency of the circuit, allowing sinusoidal current or voltage output with high efficiency.

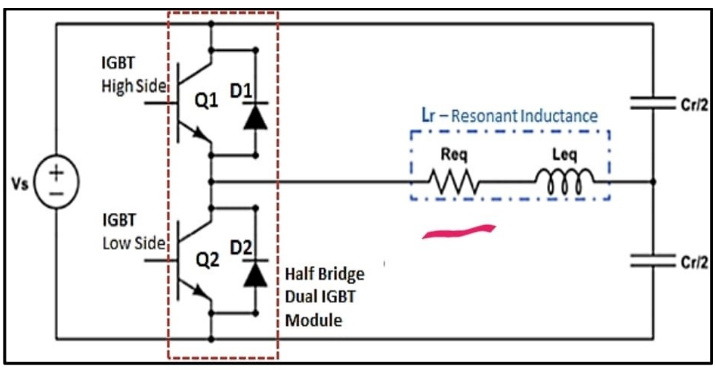

Figure 1.3: Resonant half-bridge inverter

The key principle of operation lies in the resonance of LC components, which enables soft-switching conditions, such as zero–voltage switching (ZVS) or zero–current switching (ZCS) —-thereby minimizing switching losses and reducing electromagnetic interference (EMI). Due to these benefits, resonant inverters are commonly employed in high-frequency applications such as induction heating, wireless power transfer, electronic ballasts, and high-efficiency DC-DC converters. Despite their advantages in efficiency and noise reduction, resonant inverters require more complex control strategies and are often sensitive to load variations, which must be considered in design [12].

1.7 Grid-connected (non-standalone) inverters

1.7.1 Three-phase inverters

Three-phase inverters convert DC into three-phase AC output, which are uniformly separated in phase angle shift by 120° from each other. Three-phase VSI cover medium- to high-power applications. They are widely used in motor drives, active filters and unified power flow in power systems and uninterrupted power supplies to generate controllable frequency and AC voltage magnitude using various PWM strategies [9]. The standard three-phase inverter has six switches. The input DC is usually obtained from a single-phase or three-phase utility power supply through a diode-bridge rectifier or and LC or C filter.

1.7.2 Three-phase inverter phase voltage output equations

The three-phase inverter with modulation techniques like SPWM converts DC to AC. The output voltages are typically represented as functions of switching states and DC bus voltage.

For a three-phase voltage source inverter (VSI) with sinusoidal PWM modulation, the output voltages are given by:

1.7.3 Phase Voltages (relative to DC bus midpoint)

$$\begin{bmatrix} V_{an} \\ V_{bn} \\ V_{cn} \end{bmatrix} = \frac{V_{dc}}{2} M_i \begin{bmatrix} \sin(\omega t) \\ \sin\left(\omega t - \frac{2\pi}{3}\right) \\ \sin\left(\omega t + \frac{2\pi}{3}\right) \end{bmatrix} \tag{1.1}$$

1.7.4 Line-to-line voltage transformation

The line-to-line voltages are obtained through the transformation [13]:

$$\begin{bmatrix} V_{ab} \\ V_{bc} \\ V_{ca} \end{bmatrix} = \begin{bmatrix} 1 & -1 & 0 \\ 0 & 1 & -1 \\ -1 & 0 & 1 \end{bmatrix} \begin{bmatrix} V_{an} \\ V_{bn} \\ V_{cn} \end{bmatrix} = \sqrt{3}\frac{V_{dc}}{2} M_i \begin{bmatrix} \sin\left(\omega t + \frac{\pi}{6}\right) \\ \sin\left(\omega t - \frac{\pi}{2}\right) \\ \sin\left(\omega t + \frac{5\pi}{6}\right) \end{bmatrix} \tag{1.2}$$

1.7.5 Space vector representation

The voltage space vector can be expressed as:

$$\vec{V_s} = \frac{2}{3}\left(V_{an} + aV_{bn} + a^2 V_{cn}\right) = V_\alpha + jV_\beta \tag{1.3}$$

where $a = e^{j\frac{2\pi}{3}}$ is the 120° phase shift operator.

1.7.6 Fundamental output voltage (RMS)

$$V_{ph(RMS)} = \frac{\sqrt{3}}{2\sqrt{2}} \cdot M_i \cdot V_{dc} \approx 0.612 \cdot M_i \cdot V_{dc} \tag{1.4}$$

1.7.7 Switching state matrix

The inverter's switching states can be represented by:

$$\mathbf{S} = \begin{bmatrix} S_a \\ S_b \\ S_c \end{bmatrix}, \quad S_x \in \{0, 1\} \tag{1.5}$$

where S_x represents the switching state of each phase leg (1 for upper switch ON, 0 for lower switch ON).

Notes:

- These equations assume ideal switching and balanced three-phase operation.
- For overmodulation ($M_i > 1$), the output becomes non-sinusoidal.
- Third harmonic injection can increase maximum M_i to 1.15.

1.8 Importance of three-phase inverters

Three-phase inverters have become very crucial in modern power electronic systems due to their superior performance characteristics. They are widely used in renewable energy due to their significant advantages over single phase systems, particularly in utility-scale solar installations, where they achieve lower Total Harmonic Distortion (THD) while maintaining 2%-3% more efficiency [14]. This improved power quality is critical for grid integration, as discussed in IEEE Std 1547-2018 for distributed energy resource interconnection [7].

In industrial applications, three-phase inverters are revolutionizing motor drives, with modern multilevel topologies that reduce torque ripple by a significant percentage (60%) and improve efficiency by 8-12% [5].

In addition, three-phase inverters are used in electric vehicle charging systems infrastructure where the Z-source inverters are utilized in fast-charging stations. They have demonstrated 15% reduction in component count while maintaining a 95.9% peak efficiency [11].

1.9 Control strategies of inverters

1.9.1 Introduction

The main issues concerning PV inverters include the DC-output nature of PV devices, intermittent fluctuations, output voltage regulation, harmonic content, and conversion efficiency [15].Inverters like any other power conversion electronics are not immune to this issues which challenges the inverter design [16]. Thus the need to setup various control strategies to mitigate the various challenges. Though certain features have to be taken into consideration when designing controllers for the inverters. First, to ensure the inverter system design remains simple and not bulky, likewise reliable and also low cost. The design should ensure flexibility control of the inverter, relatively easy maintenance and testing of the inverter [17]. Plus, the systems should be small and light [18].

The inverter control system should aim to minimize the impact of output fluctuation on the stability and power quality of the inverter. Thus the need to continously upgrade inverters and controllers to ensure higher efficiency in inverter applications. Types of controllers include basic control methods, modulation techniques, closed-loop methods and finally AI and adaptive control.

1.9.2 Modulation techniques

The following are some of the most commonly used modulation techniques in inverters:

1. Variable Width Slot Control (VWSC)
2. Square Wave Control (RWC)
3. Pulse Width Modulation (PWM)

1.9.2.1 Variable Width Slot Control

Uses phase shifted rectangle pulses. Allows for control of RMS output voltage by adjusting pulse width.

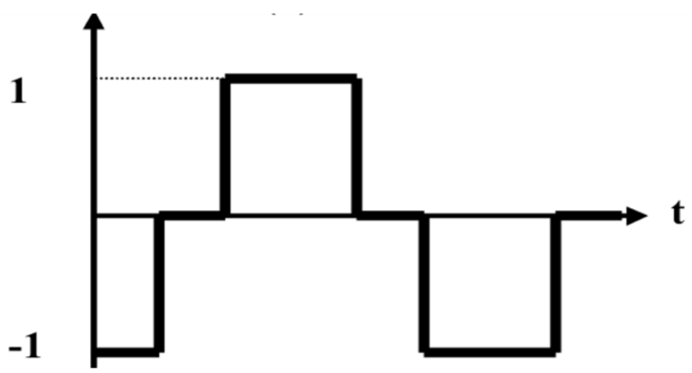

Figure 1.4: Variable width slot control

1.9.2.2 Square Wave Control

Consists of an oscillator (usually nearly sinusoidal), whose waveform is converted to rectangular by some kind of square wave forming circuit followed by digital frequency dividers [19]. The RMS voltage is not adjustable and depends on the input DC voltage. It is simple to implement but results in higher harmonic distortion.

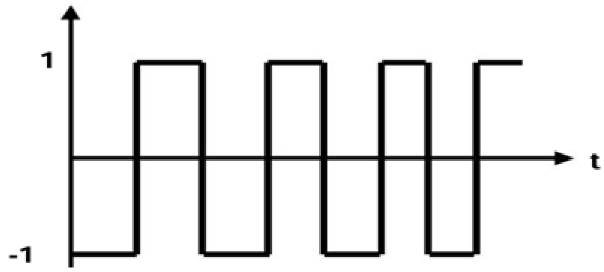

Figure 1.5: Square wave modulation

1.9.2.3 Pulse width modulation

Also known as pulse duration modulation (PDM). Pulse width modulation serves as the fundamental control mechanism for modern power electronic converters.The evolution of PWM techniques has been driven by the need for improved efficiency, reduced harmonic distortion, and better utilization of DC bus voltage [3].
The duty cycles of these inverters are adjusted according to the PWM technique applied. The frequency and amplitude of the output voltage are controlled to meet the load requirement.

Amplitude modulation or modulation index (M_i) is defined as the ratio of the amplitude of the sinusoidal wave form (reference signal), A_s to the amplitude of the carrier signal, A_c. The modulation index can be controlled by varying the amplitude of the reference signal. Consequently, the width of pulses that control the inverter switches can be controlled and consequently the RMS values[20].

Modulation Index:

$$M_i = \frac{A_s}{A_c} \tag{1.6}$$

The frequency modulation is referred to as the ratio of the frequencies of the carrier wave f_c to the frequency of the sinusoidal wave f_s. The frequency index is sometime called the frequency modulation:

$$M_f = \frac{f_c}{f_s} \tag{1.7}$$

The frequency of the carrier wave determines the number of pulses in one cycle n:

$$n = M_f \tag{1.8}$$

Key PWM methods include:

1. Sinusoidal PWM (SPWM)
2. Space Vector PWM (SVPWM)

3. Third-Harmonic Injection PWM (THIPWM)
4. Discontinuous PWM (DPWM)

Space vector pulse width modulation

SVPWM emerged as an alternative representation of three-phase voltages. This provide provides approximately 15% higher DC bus utilisation compared to the conventional SPWM while simultaneously improving harmonic performance. Though complex in its nature, the SVPWM produces superior waveform quality and enhanced voltage utilization. Its applocation ares include in motor drives and grid-tied systems [21].

Third-harmonic injection PWM

THIPWM addresses the utilization limitations of the basic SPWM by strategic injection of zero-sequence component. This method extends the linear modulation index range up to M = 1.15 without entering overmodulation. THIPWM are widely used in areas where additional voltage headroom is valuable, such as in motor drive systems and uninterruptible power supply (UPS) [22].

Discontinuous PWM

DPWM reduces switching losses by 30%-50% through clamped switching patterns that eliminate transitions in one phase per switching cycle. This technique is particularly effective in high-power inverters where switching losses dominate. However, it increases harmonic distortion compared to continuous PWM methods. [23]

Sinusoidal PWM

This technique operates by comparing a sinusoidal reference signal with a high-frequency triangular carrier wave. This technique delivers a high performance within its linear modulation range, where $M_i \leq 1$ making it suitable for basic applications. However, it is limited to approximately 78.5% DC bus utilization in three-phase systems, constraining its efficiency in high-power applications [3].

1.9.2.4 Selection of SPWM technique

In this research, SPWM was adopted due to its simplicity of implementation in both analogue and digital systems, well-documented harmonic characteristics that facilitate theory analysis and its compatibility with standard three-phase inverter topologies [3, 24].

1.9.3 Basic control methods

Under this type of control we have two main types Voltage-Frequency control and Hysteresis current Control. These strategies are relatively simple and some of their applications include stand alone inverters.

1.9.3.1 Voltage-frequency control

Voltage freqeuncy control or commonly abbreviated as V/f control, is a control technique of an inverter used mainly used in inverters to control a motor by supplying a specific current to the coil of the motor to provide a specific torque. Thus the voltage and frequency are proportional which is called V/f characteristics[25]. Therefore, the voltage and frequency are in a proportional relationship. This is called the V/f characteristics. The main principe of this control is that the magnetic flux should be proportional to V/f. This ensures that the magnetic flux is constant and thus preventing saturation.

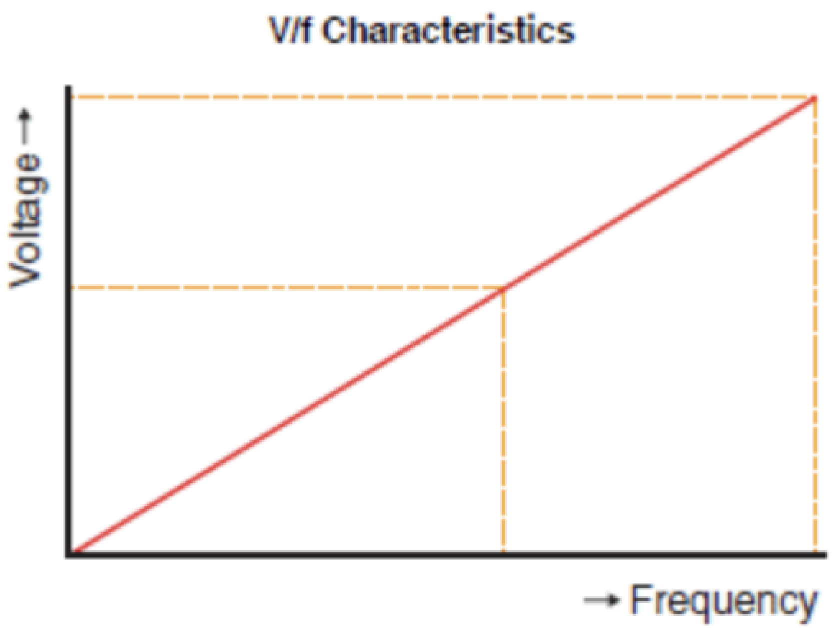

Figure 1.6: V/f characteristics graph

Principe operation
In this controller system, there exists two types of control, the open loop and also the closed cloop. A desired frequency is set, and then the corresponding voltage is calculated from

$$\frac{V^*}{f^*} = \frac{V_{\text{rated}}}{f_{\text{rated}}} \quad \Rightarrow \quad V^* = V_{\text{rated}} \cdot \frac{f^*}{f_{\text{rated}}}$$

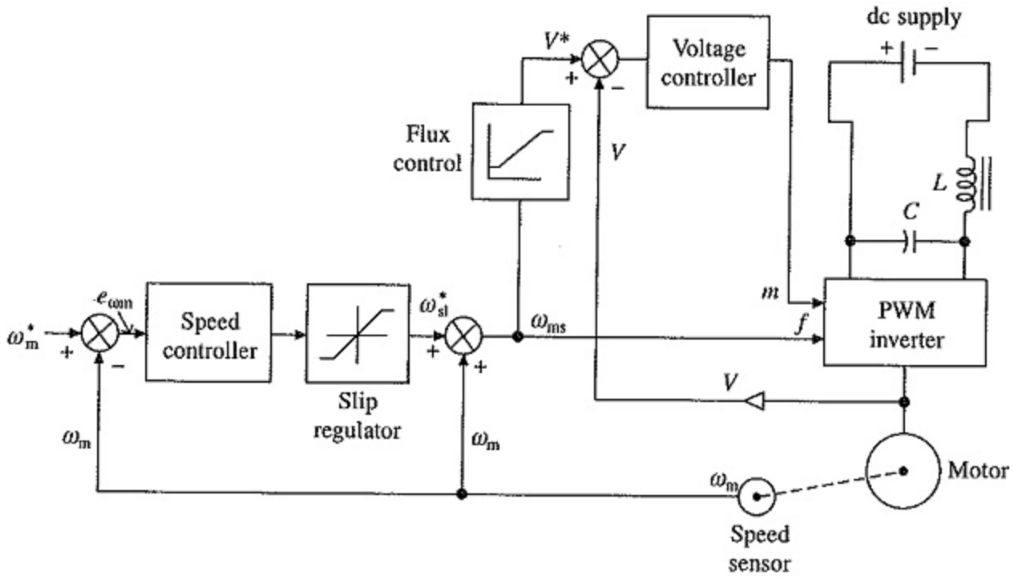

Figure 1.7: Closed loop of the V/f controller

1.9.3.2 Hystersis current control

This one of the most popular control strategy for inverters. It´s mainly focused in the current control of Voltage source inverters. One of the reasons its popular is its simplicity, fast response and high efficiency. It works continously by adjsuting the currrent with a reference value. Under varying load conditions and/or command current, hysteresis current controllers have a variable switching frequency[26]. Though its mainly effective in single/three-phase systems or two/three-level inverters. And can cause a lot of problems in multilevel inverters, since it normally operates on switching frequency which can lead to uneven switching for example the inner switches having a different frequency than the outer ones.

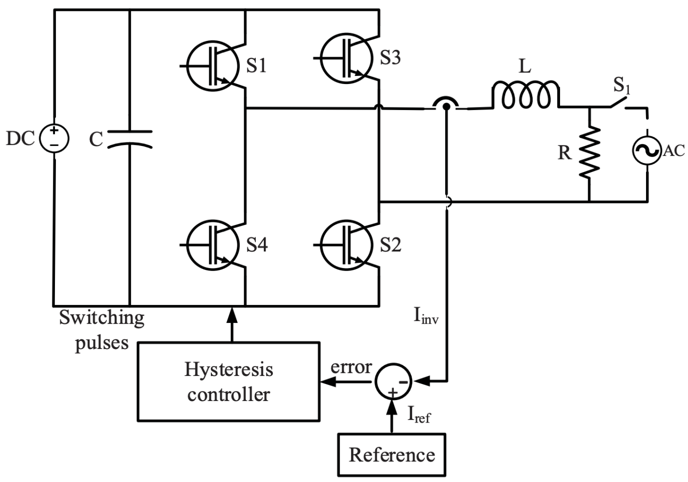

Figure 1.8: Hystersis Scheme

Working principle

Under this control strategy, the current output of the inverter is controlled by the inverter switches(IGBTs or MOSFETS). the corresponding phase current is kept within a defined hysteresis band Δi. Then the actual output Iactual is generated and compared to our Iref and the error is measured. If this error tends to pass the hysteresis band lower limit, the top power switch of the corresponding phase is turned off, turning on the lower one. On the contrary, if the error tends to be greater than the higher limit, the top power switch is turned on and the bottom one is deactivated.

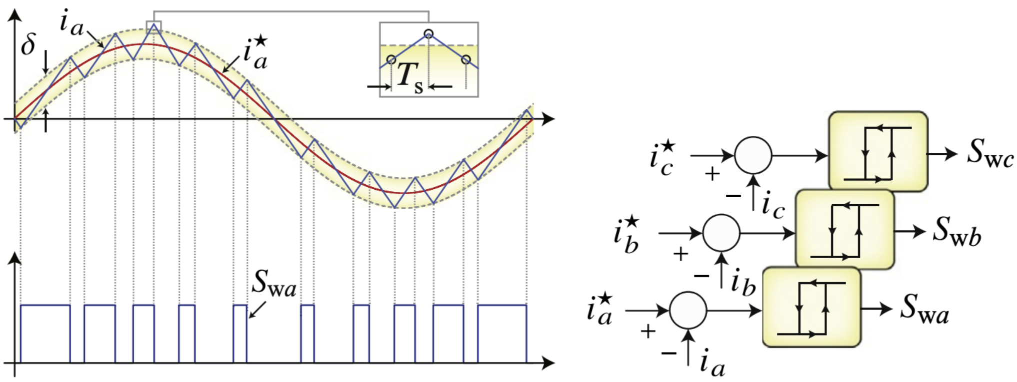

Figure 1.9: Hystersis current control

1.9.4 Intelligent and adaptive control

Traditional controllers for example Proportional-Integral (PI) are common due to their simplicity, but aren't very effective in non-linear and time varying environments. AI control strategies incorporate human reasoning for example fuzzy logic controller, that mimics how the human brain thinks by interpreting the information as imprecise terms [27].

1.9.4.1 Fuzzy logic control

Fuzzy logic was first introduced by Lotfi Zadeh in 1965, was introduced as a computation system that, instead of using binary values, uses partial truth values (True, False). It does not require mathematical models; rather, it uses human-like reasoning by processing uncertain data through linguistic variables (high, medium, low).

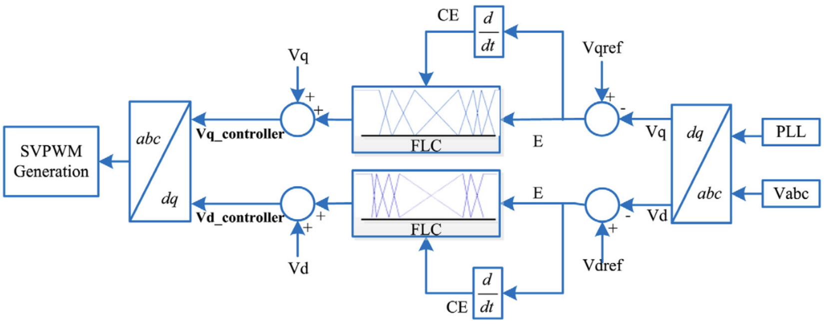

Figure 1.10: Voltage control using fuzzy controller

Working principle
The working principle of a fuzzy logic controller can be broken down into 3 parts, fuzzification, fuzzy interference and finally defuzzification. During fuzzification, the controller processes two sets of input variables, error voltage and the rate of change of this error. Before the input is processed by the fuzzy system, the numerical inputs are converted into fuzzy sets through membership functions that define the degree to which each input belongs to various linguistic categories such as "Negative Big," "Negative Small," "Zero," "Positive Small," and "Positive Big." [28]. While fuzzy intereference, which acts as the brain of the controller is where the fuzzified inputs are processsed. The inference process produces a fuzzy output set according to the IF–THEN rule logic. In particular, it maps the input to an output by utilizing the theory of fuzzy sets [29]. And finally, defuzzification extracts the crisp output value from a fuzzy output set. This process takes the aggregate output fuzzy set and produces a single-number output which can be used to control the PWM of an inverter.

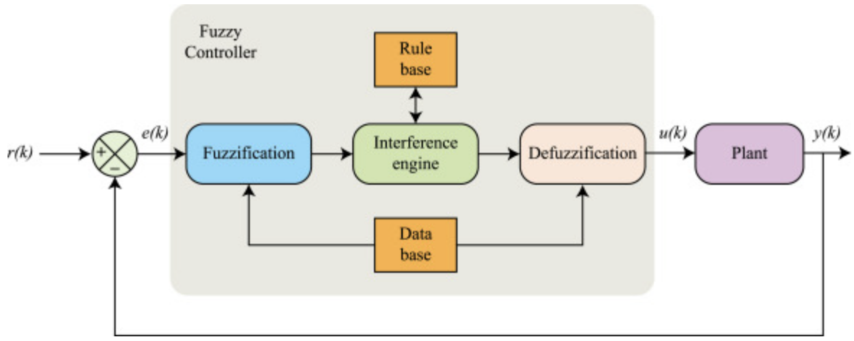

Figure 1.11: Fuzzy logic system overview

1.10 Performance parameters of three-phase inverters

Three-phase inverters are evaluated on critical performance metrics that define their efficiency, power quality, and operational robustness. Some of the key performance metrics include total harmonic distortion (THD) of the output waveforms(typically required to be ¡5% for grid compliance),switching losses(linked to semiconductor characteristics), dynamic response during load transient and efficiency. These characteristics are often independent; for example, reducing THD often increases switching losses-necessitating trade-offs through modulation strategies and topology selection [7, 21].

1.10.1 Total Harmonic Distortion

Total Harmonic Distortion (THD) is a critical parameter that quantifies the deviation of the output waveform from an ideal sine wave. A lower THD indicates a purer sinusoidal output, which is essential for improving the efficiency and reliability of power systems. High THD can lead to excessive heating, reduced efficiency, and potential damage to sensitive loads [22].

$$THD(\%)_{current} = \sqrt{\sum_{n=1,2,\ldots,n}^{n=n} \left(\frac{I_n}{I_1}\right)^2 \times 100} \tag{1.9}$$

$$THD(\%)_{Voltage} = \sqrt{\sum_{n=1,2,\ldots,n}^{n=n} \left(\frac{V_n}{V_1}\right)^2 \times 100} \tag{1.10}$$

Where I_n and V_n are the nth harmonic voltages and current components respectively. V_1 and I_1 are the fundamental frequency voltage and current respectively.

1.10.2 Harmonic Filtering

Harmonics generated by inverters can introduce unwanted noise and losses in power systems. Higher-frequency harmonics are easier to filter using passive or active filtering techniques. Passive filters, such as LC filters, are commonly used to attenuate harmonic distortion, while active power filters (APFs) dynamically compensate for harmonics in real-time [30].

1.10.3 Power Losses

Harmonics in inverter-fed systems cause power losses in motor windings, cores, and switching devices, reducing efficiency and increasing heat. Advanced PWM techniques like SHE-PWM can minimize these losses and improve system performance [31].

1.10.4 Efficiency and Power Factor

The efficiency of an inverter is influenced by switching losses, conduction losses, and thermal dissipation. Optimized modulation strategies and high-efficiency semiconductor devices (such as SiC and GaN transistors) are widely researched to enhance inverter efficiency. Additionally, maintaining a high power factor ensures efficient power transfer, reducing reactive power losses.

1.11 Switched-Inductor Topology

Introduction

Switched inductor topologies have emerged as a vital innovation in power electronics, enabling high step-up or step-down voltage conversion without the use of bulky transformers. These topologies utilize dynamically reconfigurable inductor networks to improve voltage gain and efficiency while reducing voltage and current stress on the switches. Initially applied in DC-DC converters, switched inductor structures have increasingly been integrated into AC-DC systems, particularly in power factor correction (PFC) rectifiers and single-phase inverters [32].

1.11.1 Switched Inductor Topologies in DC-AC Applications

In DC-AC conversion, particularly in applications like grid-tied inverters and renewable energy systems, maintaining a stable and high output voltage is essential. Switched inductor topologies are ideal for these applications as they provide an efficient method to step up the voltage of the DC source, ensuring that the inverter can generate a reliable AC output. By alternating the inductor configuration between series and parallel modes during the switching cycle, these topologies enhance voltage gain without the need for extreme switching ratios or transformer isolation. As a result, they offer significant advantages in terms of size, efficiency, and performance[33].

1.11.2 General Working Principle

Switched inductor topologies function by dynamically altering the configuration of inductors during different phases of the switching cycle to achieve high voltage gain and efficient energy transfer. The essential principle involves the use of inductors that are alternately charged in parallel and discharged in series, enabling a boost in voltage without the need for high duty cycles or magnetic isolation. When implemented in DC-AC systems, this approach is combined with active control methods such as average current mode control or peak current mode control to maintain output regulation and input current shaping[34].

During the charging phase (ON-state), the inductors are connected in parallel to the input DC supply, and each inductor stores energy independently. In the subsequent discharging phase (OFF-state), the inductors are reconfigured in series and deliver their stored energy to the output load or a DC-link capacitor, resulting in a cumulative voltage contribution. This reconfiguration enables a significantly higher output voltage than conventional boost converters, making it suitable for low-voltage sources such as photovoltaic panels or batteries feeding into DC-AC inverters [33, 35].

The topology typically employs controlled semiconductor switches (e.g., MOSFETs or IGBTs) and diodes to manage the state transitions. Careful timing of the switching signals ensures that current paths are controlled precisely, preventing short circuits and minimizing switching losses. Additionally, the use of multiple inductors reduces current ripple and enhances the system's electromagnetic compatibility (EMC).

In DC-AC inverter applications, the switched inductor stage acts as a high-gain preregulator that boosts the input voltage to a level suitable for AC waveform synthesis, enabling stable operation even under varying load conditions. The reduced voltage stress across switches and improved energy transfer efficiency make the switched inductor topology a compelling solution for next-generation inverter designs [35].

1.11.3 Benefits of Switched Inductor Topology

Switched inductor topologies offer numerous advantages that make them particularly attractive in modern power conversion systems, especially in applications requiring high voltage gain and compact design. One of the most notable benefits is the enhanced voltage boosting capability. By reconfiguring inductors between parallel and series connections during different switching intervals, these topologies achieve significantly higher voltage conversion ratios compared to traditional boost converters, without requiring extreme duty cycles or bulky transformer components[33, 35]. Another major advantage is improved efficiency. The staged charging and discharging of multiple inductors reduce conduction losses and distribute the current more evenly across components. This not only enhances thermal performance but also extends the operational life of power electronic components.

Additionally, switched inductor topologies can be designed to achieve lower voltage stress across switching devices and diodes, thereby allowing the use of lower-rated, more efficient, and cost-effective components[33]. Scalability and modularity are also key benefits. These topologies can be adapted to meet various voltage and power requirements by altering the number of inductors and switching configurations, making them suitable for both low-power and high-power applications. Furthermore, they support high power density designs due to the absence of large magnetic elements, which is critical in applications where space and weight are constrained, such as electric vehicles and portable renewable energy systems [35].

Finally, in DC-AC applications, switched inductor topologies help maintain a stable intermediate DC-link voltage, which is crucial for generating consistent and high-quality AC waveforms in inverter stages. This makes them especially effective in renewable energy systems, where input voltages can fluctuate significantly due to environmental conditions.

1.12 Previous Works and Findings on Switched Inductor Split Source Inverter

The evolution of switched input split source inverters (SI-SSI) emerged as a solution to overcome the limitations of the conventional voltage source and current source inverters. These inverters have limited voltage gain and hence require additional DC-DC inverters to boost their input voltage to produce the desirable output [36]. This poses a problem for their overall efficiency and increases the system complexity.

Single-stage boosting was first introduced by M.Mubeen [1] in his article "Design of Z-Source Inverter for Voltage Boost Application." This is an inverter design that uses a complex impedance network to achieve relatively higher voltage gain compared to the VSIs and the CSIs. However, subsequent studies showed that despite its advantages, the inverter design required complex control algorithms. Furthermore, it had a larger number of passive elements that affected its efficiency. Further studies suggested that a new inverter design that would not only deliver a high voltage gain but would also be less complex to design, implement, and control should be developed.

Development of the split-source inverters (SSI) was further addressed the shortcomings of the CSIs, VSIs and the Z-source inverters. The SSI showed improved performance metrics. Fashil Abas et al. (2017) conducted a comprehensive simulation of the SSI and compared its performance under different modulation techniques (THPWM, SPWM). The results were promisisng althought the SSI showed high THD levels with both modulation techniques, 13.63% and 23% respectively [37]. Further study was conducted by M. A. Ismeil and his colleagues in the subsequent years to further improve the performance of the SSI inverter. In their articles [38](2022), [39](2023), it is evident how the SSI has improved in harmonic management and its efficiency. Their findings highlighted the potential for renewable energy sytems.

The recent advancements in power electronics, especially in swithed-inductor technology, has brought about improvements in the SSI inveters. The integration of swithed-inductor network into the already existing SSI improved its performance and voltage boosting ability by 30%. This is how the switched-inductor split source inverters (SI-SSI) came about. Acomparative study was conducted by Ismeil et al.(2024) between the SSI and the SI-SSI and the latter produced more reliable and efficient performance compared to the SSI. The SI-SSI showed improved THD levels of less than 5% as required by the [7] IEEE standards. This improved performance and voltage boosting capabilities make the SI-SSI more suitable for applications in renewable energies or low power input systems. Further research are underway to ensure the integration of this technology in high-power application areas.

1.13 Three-phase split-source inverter operation, modulation and mathematical derivation

1.13.1 Introduction to Split-Source Inverter

The Split-Source Inverter (SSI) is a single-stage power conversion topology that combines the advantages of traditional Voltage Source Inverters (VSI) with an integrated boost capability. Unlike conventional inverters that require an external DC-DC converter for voltage boosting, the SSI topology allows voltage boosting within the inverter structure itself, reducing component count and improving efficiency. The SSI consists of a three-phase bridge, an inductor, and a capacitor, forming a DC-L-C circuit that enables the voltage boost operation. This structure provides better performance in renewable energy applications and motor drive systems by enhancing power conversion efficiency.

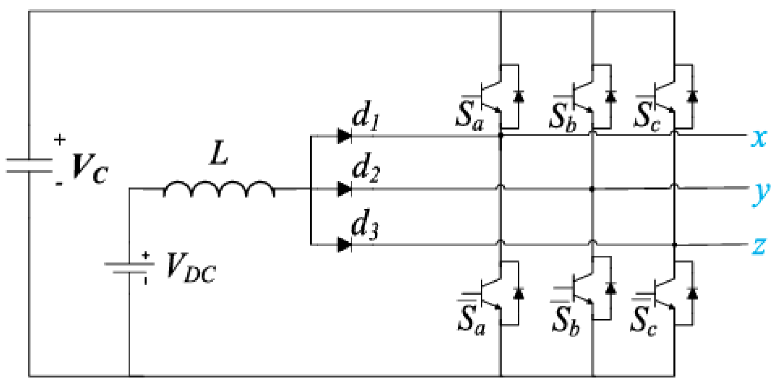

Figure 1.12: Basic Structure of a Three-Phase Split-Source Inverter

1.13.2 Operation

The three-phase SSI as shown in figure 1 uses the same B6 bridge of the traditional three-phase VSI and the same eight states (000, 001, . . . ,111). Table 1 provides a summary of the switching states, including both charging and discharging modes. When at least one of the lower switches (Sa, Sb, or Sc) is in the ON state, the inductor L is charged. During the 111 state, all upper switches are turned ON simultaneously, leading to the inductor's discharge, which in turn charges the DC-L-C network via freewheeling diodes[38]. This results in a boosted DC voltage, which is then converted into an AC output through the H-bridge circuit. One of the primary advantages of the SSI is its compatibility with various modulation schemes [2].

1.13.3 SSI Modulation Technique

The SSI can operate with conventional modulation schemes used in VSI structures. In this study, the Sinusoidal Pulse Width Modulation (SPWM) technique is employed. Figure 2 illustrates the reference and carrier signals used for the SPWM technique.

Table 1.1: Switching states of the three-phase split-source inverter

State	Sa	Sb	Sc	Inductor State
000	0	0	0	-
001	0	0	1	Charge
010	0	1	0	Charge
011	0	1	1	Charge
100	1	0	0	Charge
101	1	0	1	Charge
110	1	1	0	Charge
111	1	1	1	Discharge

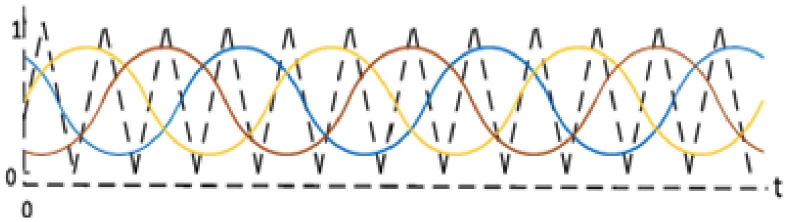

Figure 1.13: SPWM modulation Technique

1.13.4 SSI Mathematical derivation

The duty cycle ratio D at which the inductor L of the SSI is charged can be calculated by:

$$D = \frac{t_x}{t_x + t_y} \tag{1.11}$$

where t_x is the inductor charging time and t_y is the discharging time. The minimum duty cycle D_{min} can be derived from:

$$D_{\text{min}} = \frac{1}{4}M + \frac{1}{2} \tag{1.12}$$

where M is the modulation index. The maximum duty cycle D_{max} can be derived from:

$$D_{\text{max}} = \frac{1}{2}M + \frac{1}{2} \tag{1.13}$$

or

$$D(\theta) = \frac{1}{2} - \frac{M}{2}\sin(\theta) \quad [38] \tag{1.14}$$

The inductor is charged with an average duty cycle given by:

$$D_{\text{avg}} = \frac{3\sqrt{3}M.}{4\pi} + \frac{1}{2} \tag{1.15}$$

During the charging period, the inductor voltage V_L equals V_{DC}:

$$V_L = V_{DC} \tag{1.16}$$

where V_{DC} is the input DC voltage. During the discharge period:

$$V_L = V_{DC} - V_C \tag{1.17}$$

where V_C is the DC-L-C voltage. The DC-L-C voltage V_C will be given by:

$$V_C = \frac{1}{1 - D_{\text{avg}}} V_{DC} \tag{1.18}$$

Therefore, the SSI boosting factor B can be formulated as:

$$B = \frac{1}{1 - D_{\text{avg}}} \tag{1.19}$$

Substituting equation (5) in (8) gives the DC link capacitor voltage, which also equals the inverter voltage, expressed as:

$$V_C = V_{DC} \cdot \frac{4\pi}{2\pi - 3\sqrt{3}M} \tag{1.20}$$

From equation (1.22), the output fundamental peak phase voltage V_{pph} will be given by:

$$V_{pph} = V_{DC} \cdot \frac{2\pi M}{2\pi - 3\sqrt{3}M} \tag{1.21}$$

The overall inverter gain g can be indicated by:

$$g = \frac{2\pi M}{2\pi - 3\sqrt{3}M} \tag{1.22}$$

The required inductance L and capacitance C values can be calculated by (1.24) and (1.25) respectively, assuming low variations of capacitor voltage [2] and [38]:

$$L \approx \frac{D_{\max} V_{DC}}{2 f_c \Delta I_L} + \frac{K M V_C}{6\pi f_f \Delta I_L}$$

(1.23)

$$C \approx \frac{(1 - D_{\min}) I_L}{2 f_c \Delta V_C} + \frac{K M I_L}{6\pi f_f \Delta V_C} \tag{1.24}$$

where f_f and f_c are the fundamental and carrier frequency consecutively, ΔI_L is the inductor current ripple, and ΔV_C is the DC-L-C voltage ripple. K is a constant, its value depends on the modulation technique, and it is equal to $\frac{3\sqrt{3}}{8\pi}$ for SPWM [2].

1.14 Three-phase switched-inductor split source inverter, modulation and mathematical derivation

Introduction to SI-SSI

Switched inductor technology plays a key role in advanced inverter systems such as the Impedance Source Inverter (ZSI), Quasi-Z-Source Inverter (q-ZSI), and Switched-Inductor Single-Stage Inverter (SL-SSI). By integrating switched inductors, these topologies enhance efficiency, reduce component count, and achieve higher voltage gains without the complexity of multi-stage designs. This innovation has become a crucial advancement in power electronics, offering a reliable and high-performance solution for applications requiring efficient voltage conversion. Its ability to significantly boost DC voltage in single-stage converters has led to widespread adoption across various inverter configurations.

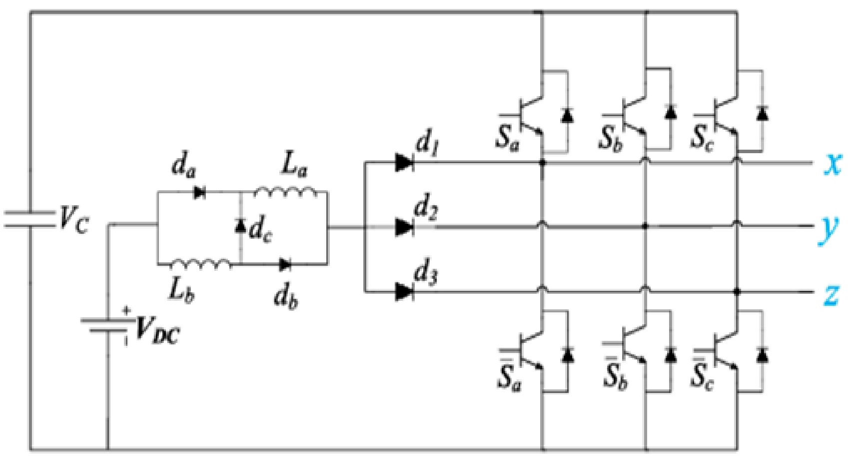

Figure 1.14: Basic Structure of a Three-Phase Split-Source Inverter

1.14.1 Operation

Similar to the conventional SSI, the SL-SSI operates in two fundamental switching states: charging and discharging. These states are detailed in Table 1.3. During the charging state, when at least one of the lower switches (Sa, Sb, or Sc) is in the ON state, the switched inductor which functions as two parallel inductors is charged. The parallel configuration reduces the effective inductance. Conversely, during the discharging state, simultaneous activation of upper switches allows the input source and the switched-inductor to jointly charge the DC-L-C. In this state the switched-inductor operates as two inductors in series, increasing the effective inductance.

The Switched Inductor Split Source Inverter (SI-SSI) outperforms conventional SSI by delivering higher voltage gain, better efficiency, and a simpler design, all while removing the need for an extra DC-DC converter. Though it uses additional inductors, the SI-SSI still manages to keep the total number of components lower than multi-stage alternatives.

This makes it an excellent choice for high-performance applications where both power and compactness matter.

Table 1.2: Switched-inductor split-source switching states

State	Capacitor State	Switched-Inductor La	Switched-Inductor Lb
000	Discharge	Charge	Charge
001	Discharge	Charge	Charge
010	Discharge	Charge	Charge
011	Discharge	Charge	Charge
100	Discharge	Charge	Charge
101	Discharge	Charge	Charge
110	Discharge	Charge	Charge
111	Charge	Discharge	Discharge

1.14.2 SI-SSI mathematical derivation

SL-SSI has the same maximum, minimum, and average duty cycle as in SSI, which are mentioned in (1.12), (1.13), and (1.14). The main difference is that during the charging period, as in [2].

$$V_{La} = V_{Lb} = V = V_{DC} \tag{1.25}$$

where V_{La} and V_{Lb} are the inductors L_a and L_b voltage. During the discharging period:

$$V_{La} + V_{Lb} = 2V = V_{DC} - V_C \tag{1.26}$$

When implementing the inductor voltage balance,

$$D \cdot V_{\mathrm{DC}} + \frac{1}{2} \cdot (1 - D)(V_{\mathrm{DC}} - V_C) = 0 \tag{1.27}$$

Hence,

$$V_C = \frac{1 + D_{avg}}{1 - D_{\mathrm{avg}}} \cdot V_{DC} \tag{1.28}$$

Therefore, the SI-SSI boosting factor B_{SL} can be formulated as:

$$B_{SL} = \frac{1 + D_{avg}}{1 - D_{avg}} \tag{1.29}$$

When comparing B_{SL} with the boosting factor in SSI in (1.20), this shows the increase in the boosting factor as shown in figure 1.7 [2].

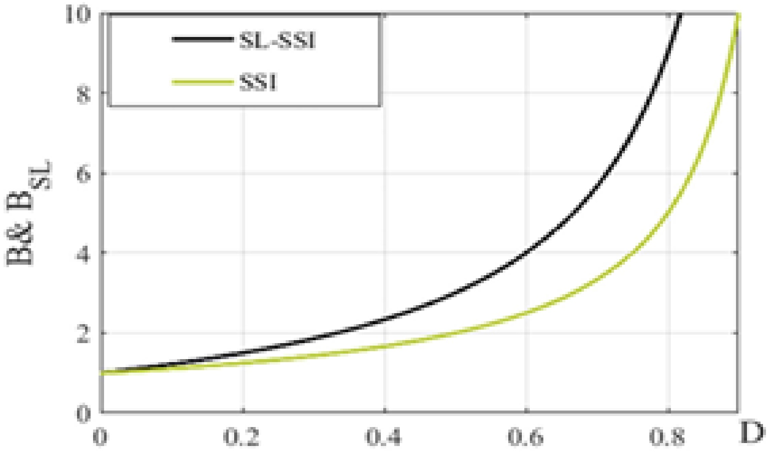

Figure 1.15: Comparison betwen the boosting factor of SSI and SI-SSI (also known as SL-SSI)

where D is the duty cycle

$$V_C = V_{DC} \cdot \frac{6\pi + 3\sqrt{3}M}{2\pi - 3\sqrt{3}M} \tag{1.30}$$

By substituting the average duty cycle(1.16) V_{pph} will be given by:

$$V_{pph} = V_{DC} \cdot \frac{M}{2} \cdot \frac{6\pi + 3\sqrt{3}M}{2\pi - 3\sqrt{3}M} \tag{1.31}$$

The overall inverter gain g_{SL} becomes

$$g_{SL} = \frac{M}{2} \cdot \frac{6\pi + 3\sqrt{3}M}{2\pi - 3\sqrt{3}M} \tag{1.32}$$

The desired inductance L_a, L_b and capacitance C magnitudes can be indicated from [37],

$$L_a = L_b \approx \frac{D_{\max} V_{DC}}{4 f_c \Delta I_L} + \frac{K M V_C}{12\pi f_f \Delta I_L} \tag{1.33}$$

$$C \approx \frac{(1 - D_{\min}) I_L}{4 f_c \Delta V_C} + \frac{K M I_L}{12\pi f_f \Delta V_C} \tag{1.34}$$

Where f_f and f_c are the fundamental and carrier frequencies respectively, ΔI_L is the inductor current ripple, and ΔV_C is the DC-L-C voltage ripple. K is a constant whose value depends on the modulation technique and equals $\frac{3\sqrt{3}}{8\pi}$ for SPWM [2].

Chapter 2

MATLAB SIMULATION OF VSI, SSI AND SI-SSI TOPOLOGIES

2.1 Introduction

This chapter presents comprehensive simulation results of the two inverter topologies discussed in this study. Split Source Inverter and the Switched Inductor Split Source Inverter obtained through the MATLAB/Simulink implementation. A simulation-based strategy was adopted to allow for detailed analysis with restrictions on hardware prototyping. The key performance indicators included output voltage, voltage gain, output current, waveform quality, and total harmonic distortion (THD) sinusoidal pulse width modulation (SPWM) technique was used to control the switching devices in both inverters. Identical components, parameters, and control techniques were used to ensure an unbiased comparison. For R and RL loads(R = [15.87 Ω, 22 Ω], L =[10 mH, 22 mH]) , Vdc = 100 V.

To generate the gate signals, the sinusoidal pulse width modulation technique was implemented for both topologies, SSI and SI-SSI. This method compares a sinusoidal reference signal to a high-frequency triangular carrier signal to control the switching of the inverters, ensuring smooth output waveforms. The SPWM block was configured to operate at a switching frequency of 10 kHz with a modulation index of 0.881 and 0.725 for the SSI and SI-SSI respectively, as shown in Figure 2.1.

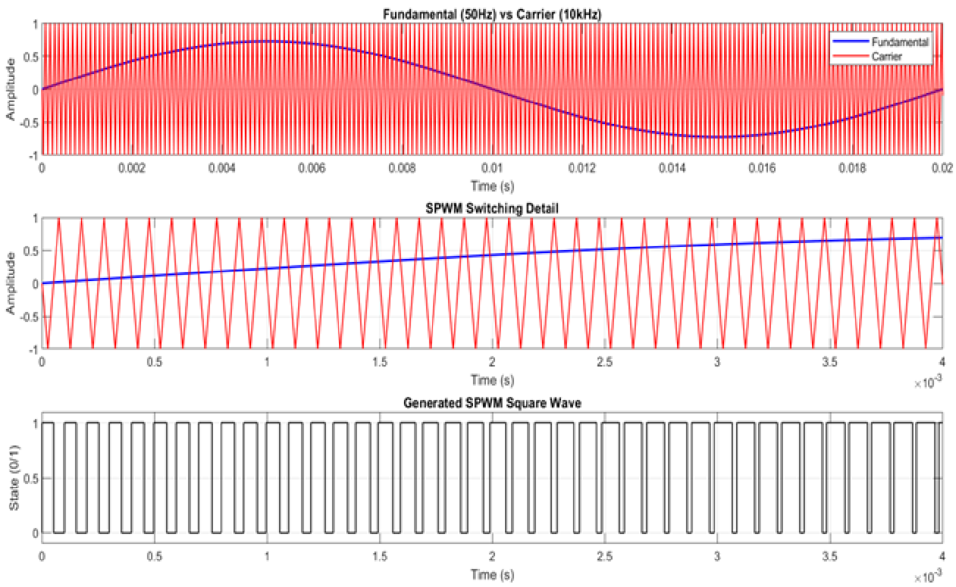

Figure 2.1: SPWM modulation for the SI-SSI control.

Table 2.1 presents the simulation parameters used in all the simulation setups. The values were designed based on the typical application requirements and to ensure accurate representation of real-world operating conditions for a 10 kW system. Both simulation setups targeted a three-phase output of 230 V RMS per phase across 15.87 Ω and 22 Ω resistive loads and RL loads. The DC input was maintained at 100 V and $\Delta V_C = 2.5\%$ and $\Delta I_L = 10\%$.

Table 2.1: Simulation parameters of SSI and SI-SSI

Parameter	**Symbol**	**SSI**	**SI-SSI**
Input DC Voltage	V_{DC}	100 V	100 V
Input inductor current (theory)	I_L	100 A	100 A
Input inductor current + ΔI_L(Simulation)	I_L	99.7 A	110.8 A
Peak phase output voltage	V_{pph}	$230\sqrt{2}$ V	$230\sqrt{2}$ V
Fundamental frequency	f_f	50 Hz	50 Hz
Carrier frequency	f_c	10 kHz	10 kHz
Switching device	–	IGBT (ideal)	IGBT (ideal)
Modulation index	M	0.881	0.726
Modulation technique	–	SPWM	SPWM
Maximum duty cycle	D_{max}	0.941	0.863
Minimum duty cycle	D_{min}	0.720	0.682
Average duty cycle	D_{avg}	0.864	0.8
Input inductance	L	15 mH	7.5 mH x 2
DC-link capacitor	C	1100 µF	100 µF

Theoretical modeling, design assumptions, and their practical limitations

Theoretical Modeling

The system was considered ideal with perfect power transfer:

$$P_{\text{in}} = P_{\text{out}} \tag{2.1}$$

which implies that:

$$P_{\text{in}} = V_{\text{dc}} \times I_{\text{dc}} \tag{2.2}$$

$$P_{out} = \sqrt{3} \times V_{ll} \times I_a \times \cos\theta \tag{2.3}$$

For a purely resistive load ($\cos\theta = 1$) with $P_{\text{in}} = 10\,000\,\text{W}$ and $V_{\text{dc}} = 100\,\text{V}$:

$$I_{\text{dc}} = \frac{P_{\text{in}}}{V_{\text{dc}}} = \frac{10000}{100} = 100\,\text{A} \tag{2.4}$$

$$I_a = \frac{P_{\text{out}}}{\sqrt{3} \times V_{ll}} = \frac{10000}{\sqrt{3} \times 400} = 14.43\,\text{A (RMS)} \tag{2.5}$$

$$I_{\text{dc}} = \frac{\sqrt{3} \times V_{ll} \times I_a}{V_{\text{dc}} \times \eta} = \frac{\sqrt{3} \times 400 \times 14.43}{100 \times 1} \approx 100\,\text{A} \tag{2.6}$$

For the three-phase resistive load with phase voltage $V = 230\,\mathrm{V}$:

$$P_{\text{out}} = 3 \times \frac{V_{\text{rms}}^2}{R} \tag{2.7}$$

Solving for the load resistance:

$$R = \frac{V_{\text{rms}}^2}{P_{\text{out}}/3} = \frac{230^2}{10000/3} = 15.87\,\Omega \tag{2.8}$$

Design Assumptions

Additional ideal conditions include zero conduction losses, ideal energy storage components, perfect SPWM generation, no electromagnetic interference (EMI) and an ideal system efficiency. Based on these assumptions, the expected output characteristics for both inverter topologies (SSI and SI-SSI) are

Table 2.2: Expected output characteristics

Parameter	Value
Output current (RMS)	14.43 A
Output current (peak)	20.41 A
Output voltage (RMS)	230 V
Output voltage (peak)	400 V

These values represent the theoretical performance under the idealized conditions specified above. The identical expected outputs for the SSI and SI-SSI topologies provide a common baseline for comparative analysis of their actual simulation results. From the equations 1.31 and 1.32, we were, through MATLAB, able to determine the optimal modulation index M for SI-SSI using the Newton method as in [40].

Newton-Raphson calculation of modulation index for SI-SSI

```
%% SL-SSI Modulation Index Calculator
% Finds the optimal M

clear; clc;
targetVoltage = 325 V; %  peak output
Vdc = 895.3; % capacitor voltage value
n = 20; % maximum iterations
tol = 0.000001; % tolerance
%newton method function
voltageError = @(M) targetVoltage - (capacitorVoltage * M / 2);
% derivative of the function
voltageErrorDerivative = @(M) -capacitorVoltage / 2;

Initial_guess = 0.7; %initial guess
fprintf('Starting with guess: M = %.3f\n', Initial_guess);
% Newton-Raphson iteration
for i = 1:n
    %calculate the margin of error
```

```
    error = voltageError(Initial_guess);
    slope = voltageErrorDerivative(Initial_guess);
    % Newton's  formula
    nextGuess = Initial_guess - (error / slope);

    % Check if the answer is  close enough
    change = abs(nextGuess - Initial_guess);
    fprintf('Iteration %d: M = %.6f (change: %.6f)\n', i, nextGuess, change);

    if change < tolerance
        fprintf('\nConverged after %d iterations\n', i);
        break;
    end

    % Update for next round
    Initial_guess = nextGuess;

    % Safety check
    if i == n
        warning('Hit max iterations without converging!');
    end
end

%% Final Results
finalM = Initial_guess;
achievedVoltage = capacitorVoltage * finalM / 2;

fprintf('\n=== Final Results ===\n');
fprintf('Optimal M: %.6f (%.2f%%)\n', finalM, finalM*100);
fprintf('Achieved Vpp: %.3f V (Target: 325 V)\n', achievedVoltage);
fprintf('Error: %.6f V\n', abs(achievedVoltage - targetVoltage));
% Verification of results
if abs(achievedVoltage - targetVoltage) < 0.1
    fprintf('Success! \n');
else
    warning('Missed the target voltage!');
end
```

Listing 2.1: Newton method MATLAB implementation

MATLAB results

```
Starting with guess: M = 0.700
Iteration 1: M = 0.726000 (change: 0.026000)
Iteration 2: M = 0.726000 (change: 0.000000)

Converged after 2 iterations

=== Final Results ===
Optimal M: 0.726000
Achieved Vpp: 325.000 V (Target: 325 V)
Error: 0.000000 V
Success! .
```

Practical limitations

The assumptions in section 2.1 simplified the simulation process. However, it is important to note that these idealized assumptions do not fully reflect the behavior of practical systems. Factors such as switching losses, conduction losses, and parasitic inductances influence the general performance of inverter systems. In real systems, voltage drop across switching devices is observed, harmonic contents are also evident, and there is distortion due to the dead-time effect and electromagnetic interference (EMI) [41]. This raises the need for filters and thermal management strategies to be implemented to ensure efficiency. The SPWM is assumed to generate perfect signals. However, in practical systems, signal noise, clock jitter, and analog circuit imperfections can affect pulse precision.

2.2 Simulation of the traditional VSI

To evaluate the performance of the SISSI, a traditional VSI model was implemented in MATLAB/Simulink under the same simulation conditions as the SSI and the SISSI to evaluate its steady state performance, quality of power, assess voltage regulation and efficiency. An input $V_{dc} = 100V$, an optimum modulation index of 0.8, for best performance and similar resistive load profile, R = 22 Ω.

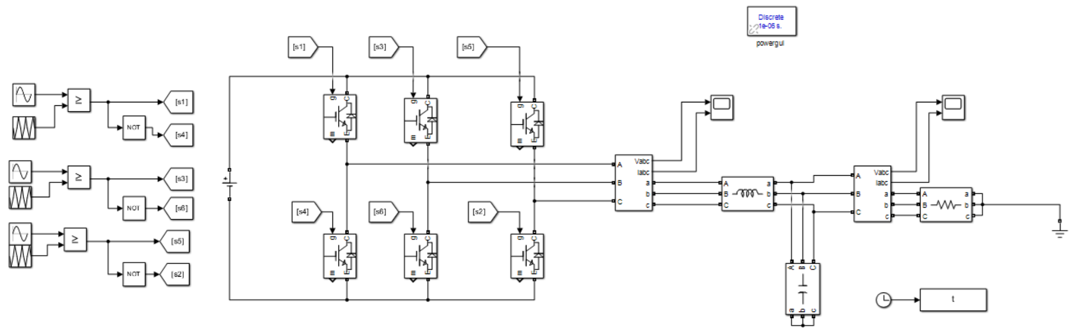

Figure 2.2: Simulink model of traditional VSI.

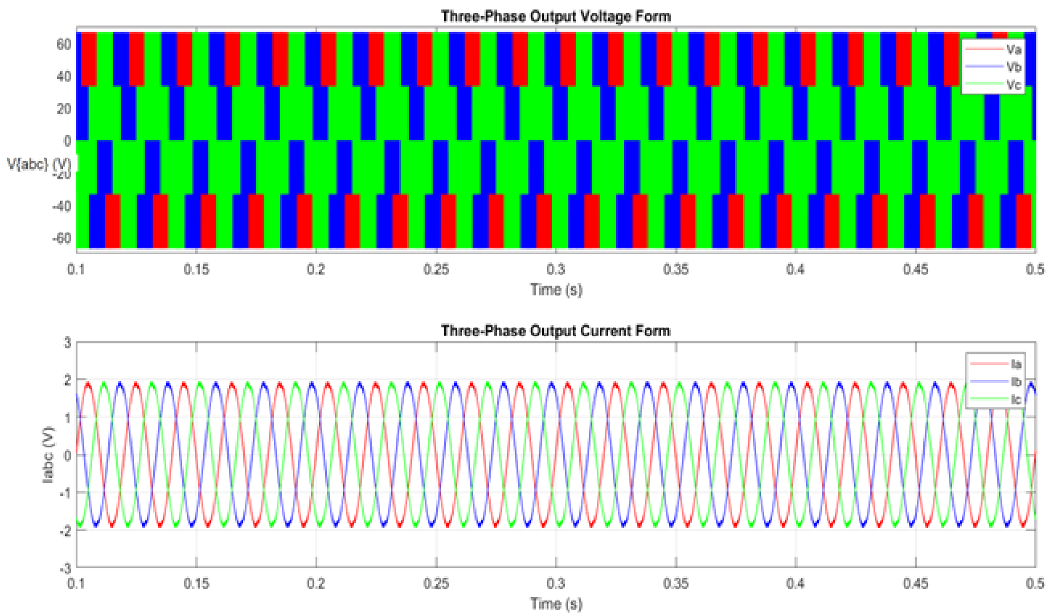

Figure 2.3: Unfiltered output waveform of the VSI.

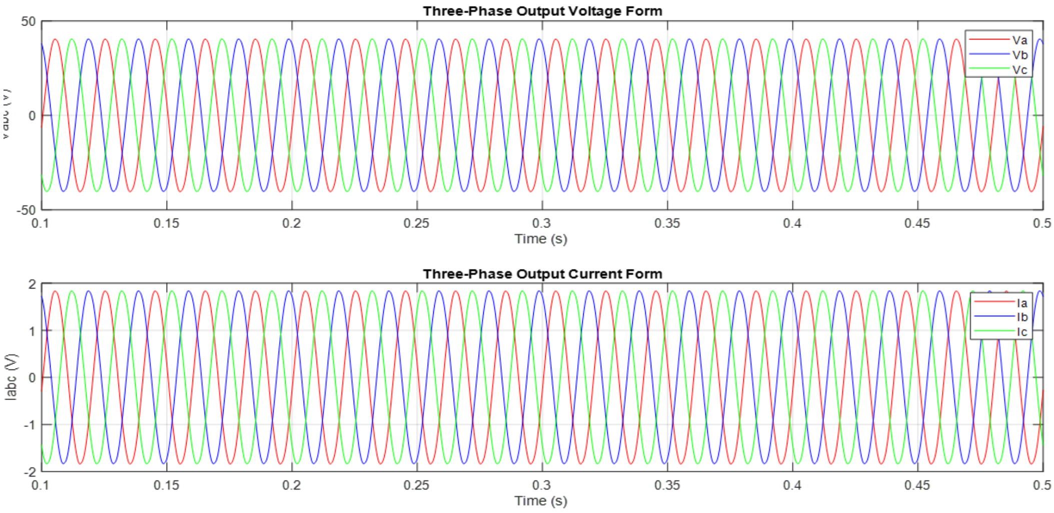

Figure 2.4: Filtered output of the VSI.

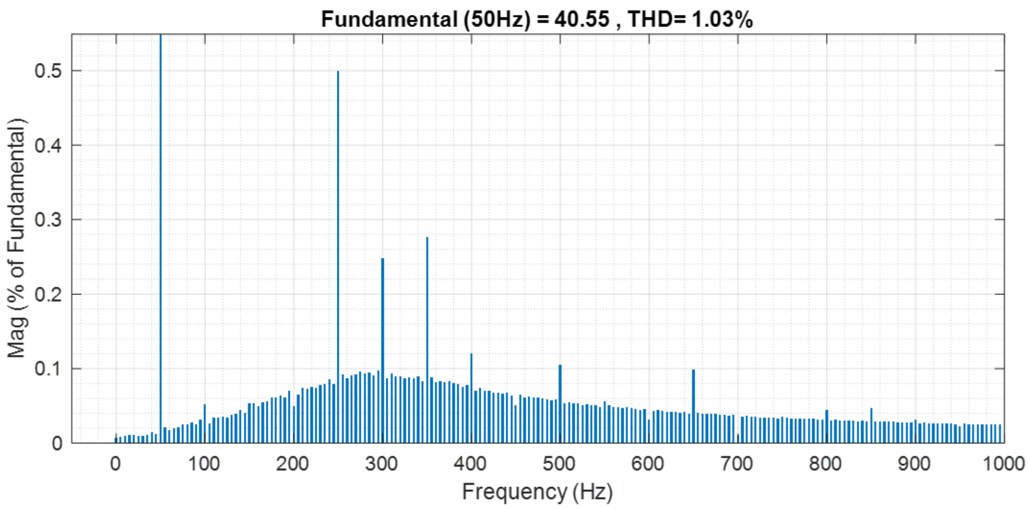

Figure 2.5: THD analysis of VSI output.

2.3 Simulation Results of SSI Topology

Figure 2.6 illustrates the Simulink implementation of the Split-Source Inverter (SSI) topology used for simulation and performance evaluation. The model integrates a DC input source, the split-source impedance network, the SPWM generation block, switching devices, a DC-Link capacitor, three-phase V-I measurement block, LC filter and the three-phase output stage. This setup also includes the Simscape's Powergui block (discrete) to allow for THD analysis, and the inverter behavior under various conditions with or without output filtering. In addition, resistive loads of $15.87\,\Omega$ and $R = 22\,\Omega$ were used.

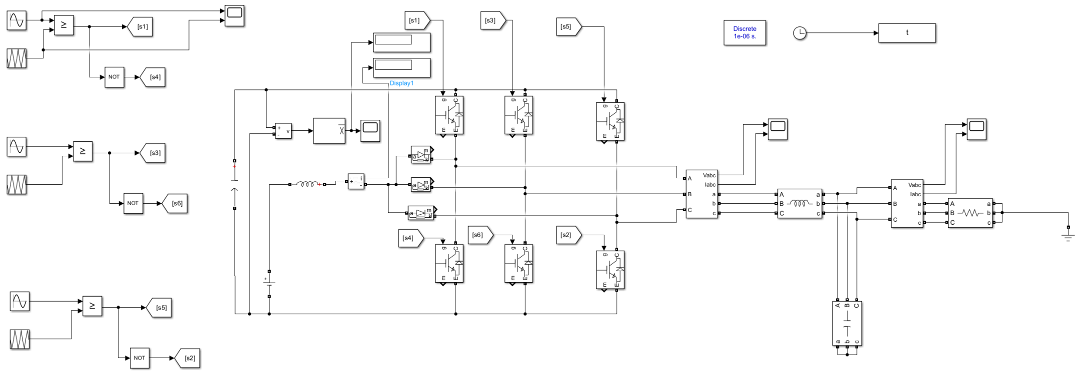

Figure 2.6: Simulink model of the split source inverter (SSI).

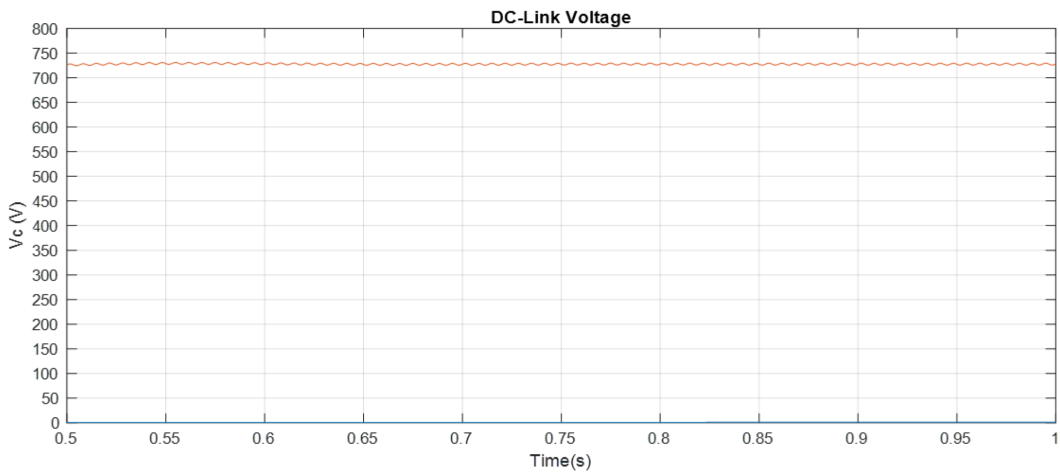

Figure 2.7: Capacitor voltage (Vc) of SSI.

Resistive load R $= 15.87\,\Omega$**.**

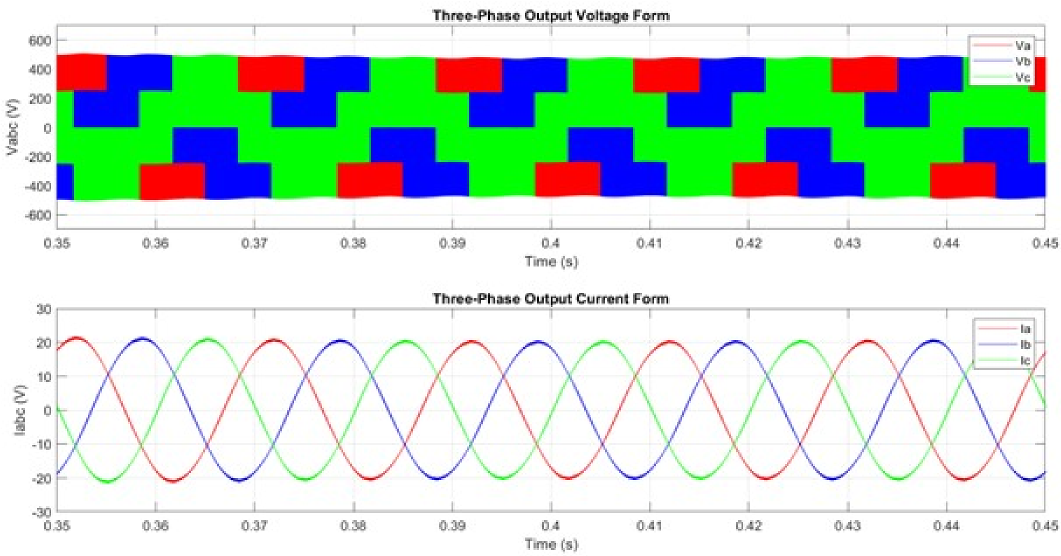

Figure 2.8: Unfiltered three-phase output waveforms SSI .

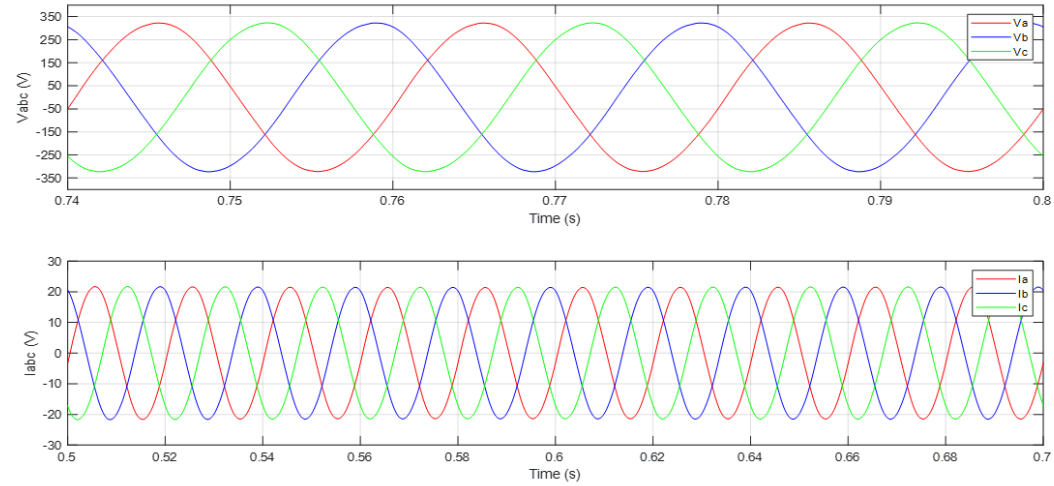

Figure 2.9: Filtered three-phase waveforms SSI.

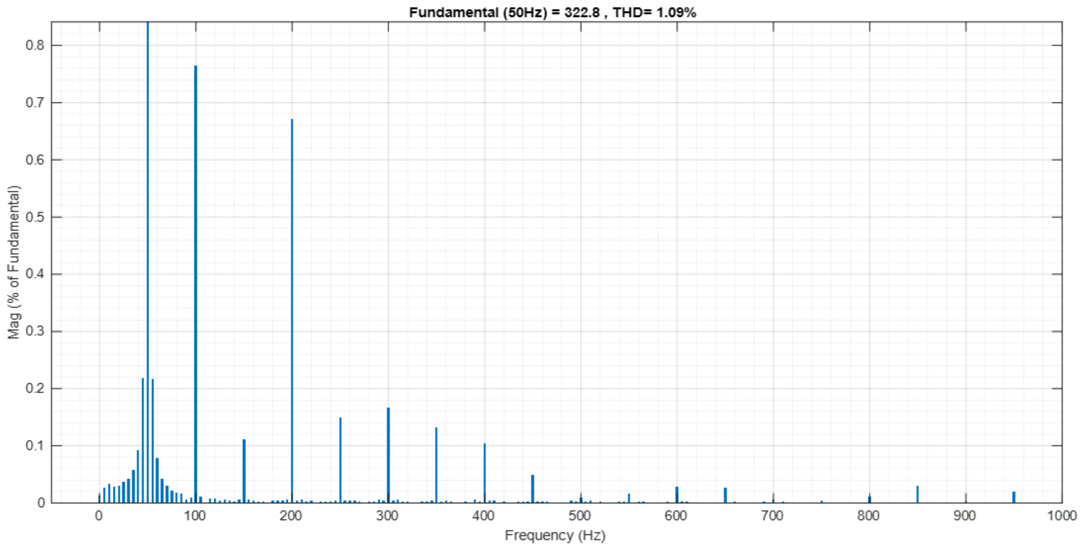

Figure 2.10: THD profile of SSI.

Resistive load R $= 22\,\Omega$**.**

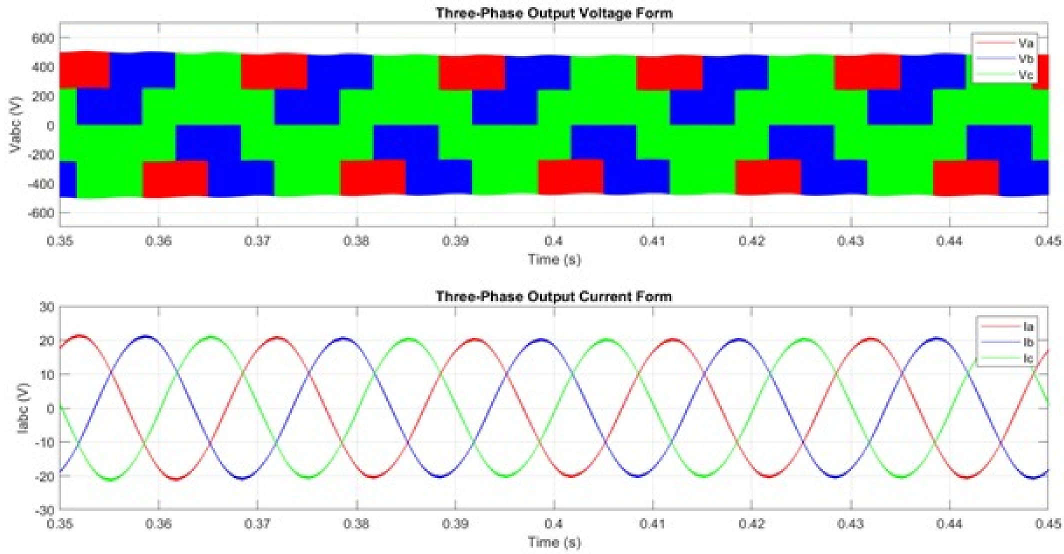

Figure 2.11: Unfiltered three-phase output voltage and current waveforms SSI.

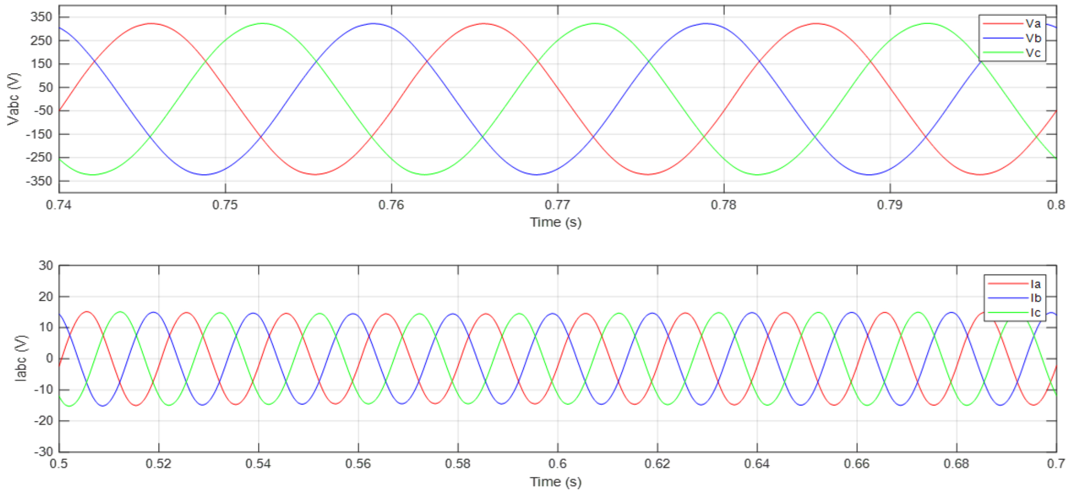

Figure 2.12: Filtered three-phase output voltage and current waveforms SSI.

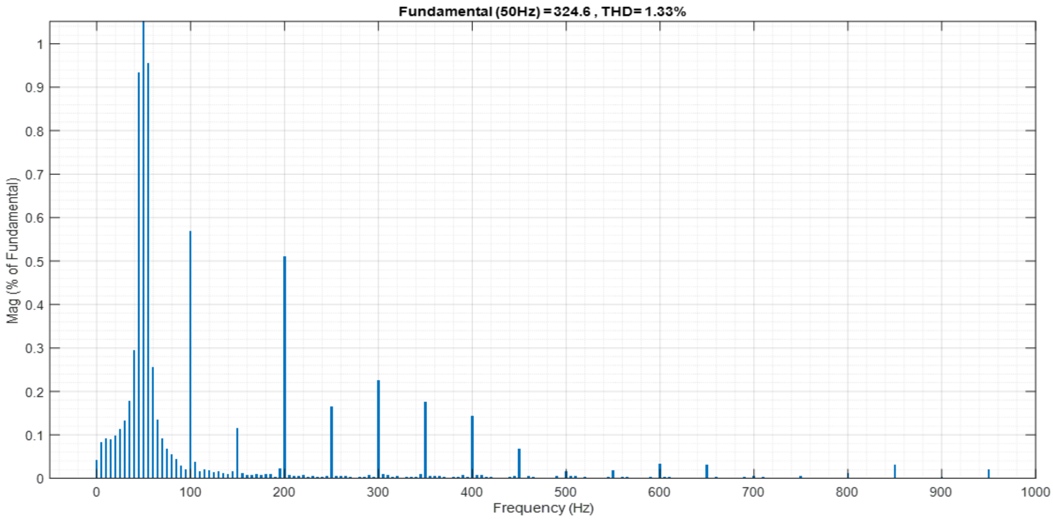

Figure 2.13: THD profile of SSI.

2.4 Simulation of the SI-SSI topology

The switched inductor split source inverter (SI-SSI) was modeled the same way as the standard split source inverter with a few modifications to incorporate the switched inductor network. The modifications contribute to its higher boost factor while maintaining a single-stage power conversion architecture.Figure 2.14 demonstrates the simulink model of the SI-SSI under the same input values and modulation technique, the SI-SSI was tested with pure resistive load R = 15.87 Ω and R = 22 Ω. The model was also subjected to different RL loads to investigate its performance in realistic operational conditions. This section involved the use of four RL loads (R = 15.87 Ω, L = 22 mH), (R = 22 Ω, L = 10 mH) and (R = 22 Ω, L = 22 mH) representing applications such as motor drives. The key performance metrics investigated in this section were voltage gain, boosting factor, THD and dynamic response under the steady-state operating condition.

2.4.1 SI-SSI with pure resistive load

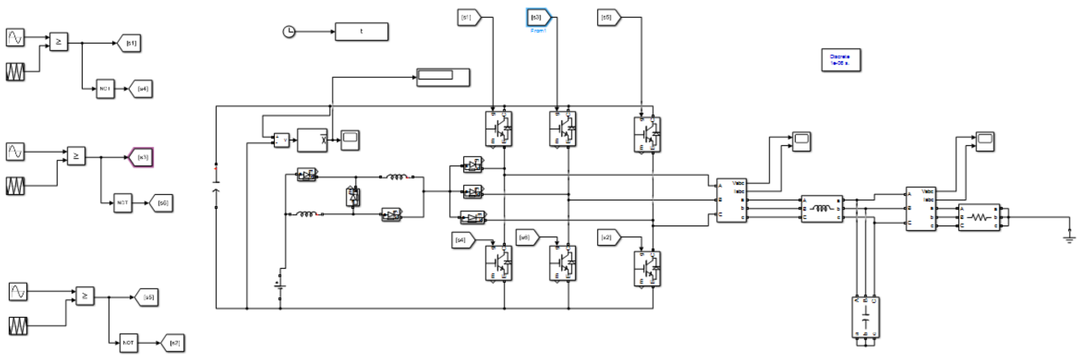

Figure 2.14: Simulink model of Switched Inductor Split Source Inverter (SI-SSI).

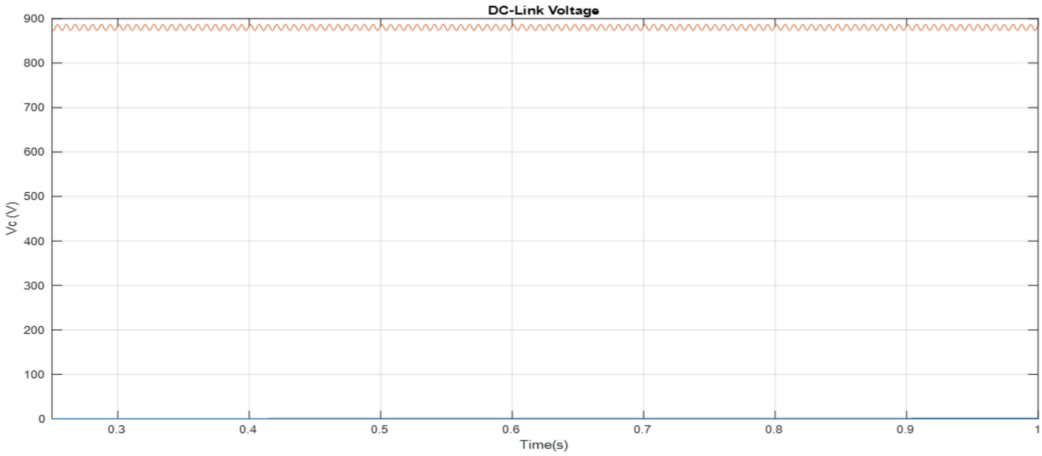

Figure 2.15: Capacitor voltage Vc of SI-SSI

Resistive load R $= 15.87\,\Omega$**.**

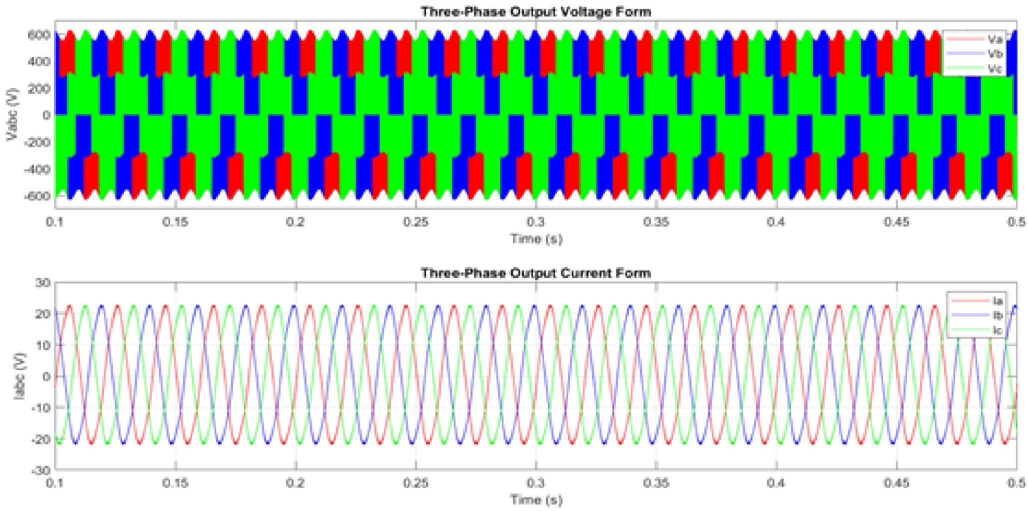

Figure 2.16: Unfiltered output waveforms SI-SSI (R $= 15.87\,\Omega$).

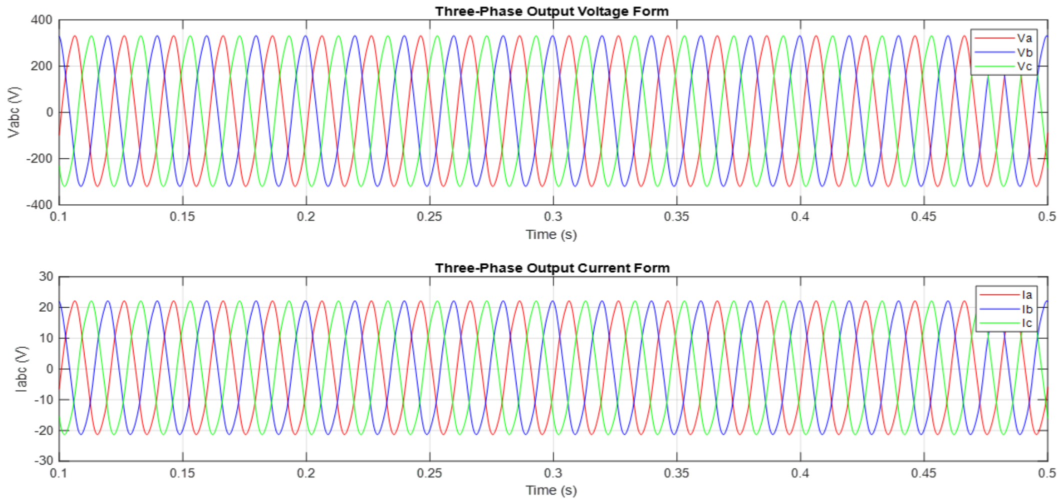

Figure 2.17: Filtered output waveforms SI-SSI (R = 15.87 Ω).

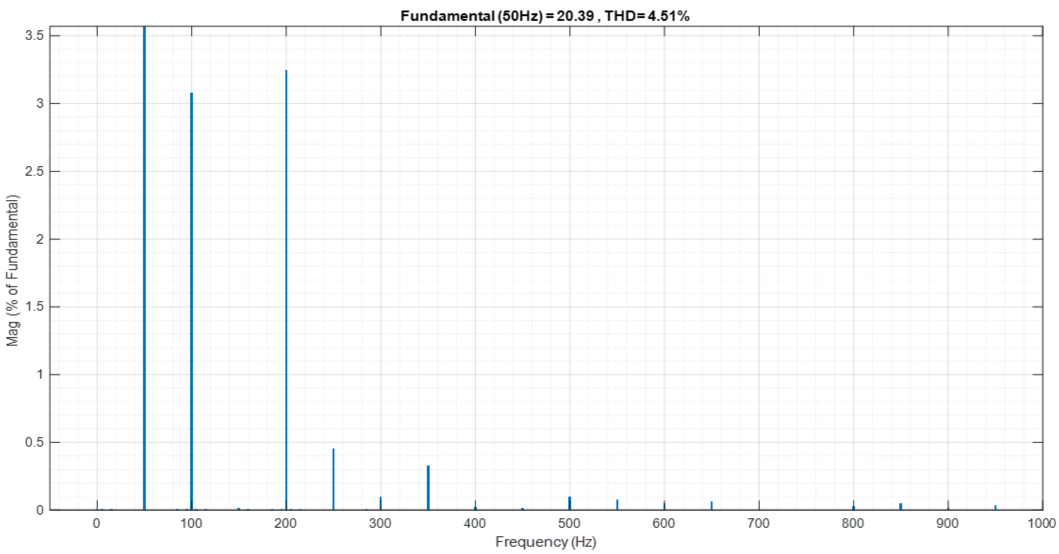

Figure 2.18: THD profile of SI-SSI (R = 15.87 Ω).

Resistive load R $= 22\,\Omega$**.**

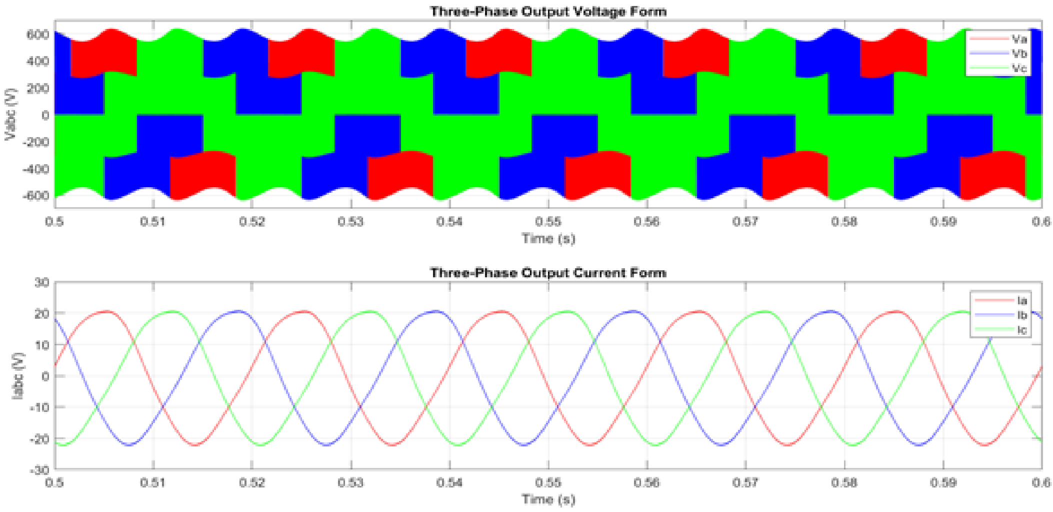

Figure 2.19: Unfiltered output SI-SSI (R $= 22\,\Omega$).

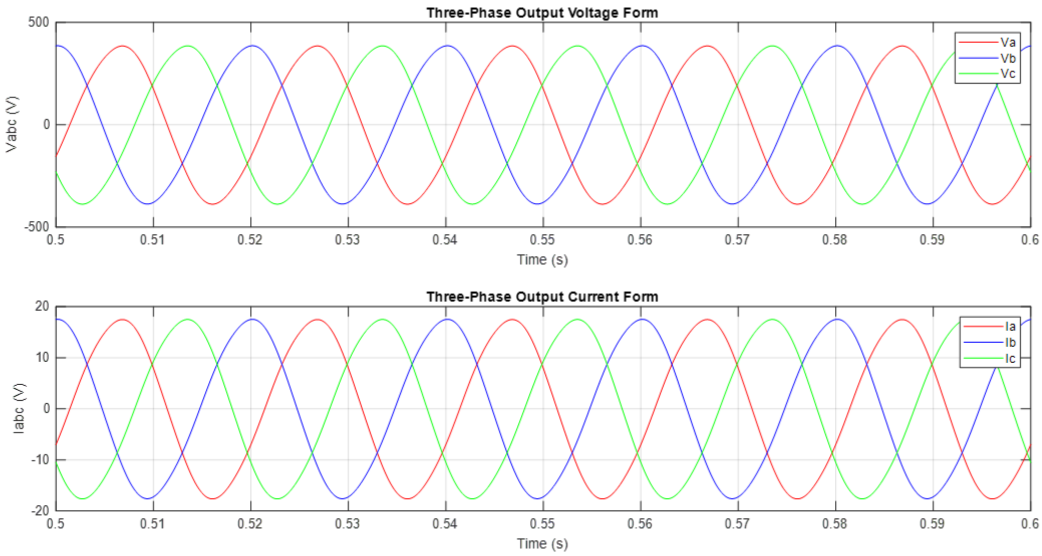

Figure 2.20: Filtered output waveforms SI-SSI (R $= 22\,\Omega$).

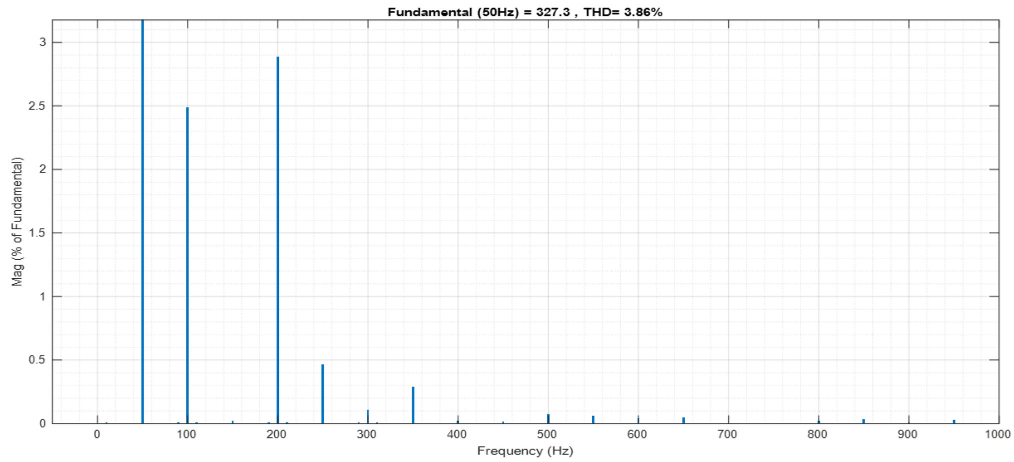

Figure 2.21: SI-SSI THD profile (R = 22 Ω).

2.4.2 SI-SSI with resistive-inductive load, RL load

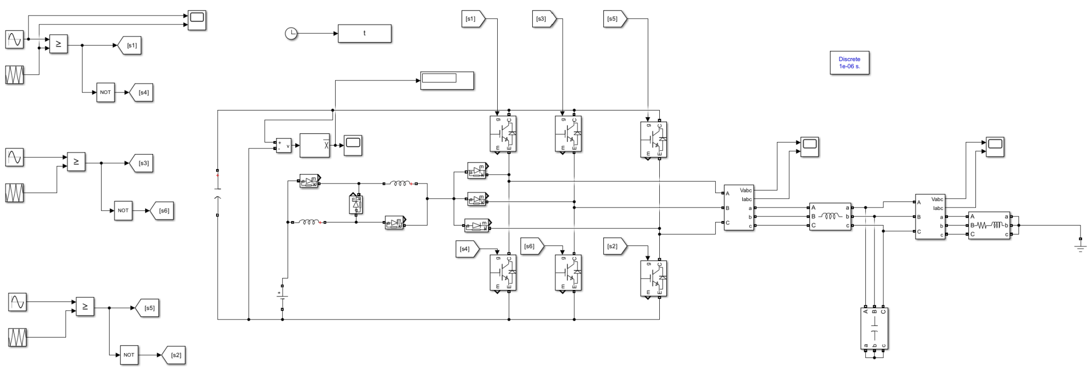

Figure 2.22: SI-SSI model with RL load

R = 15.87 Ω, L = 10 mH

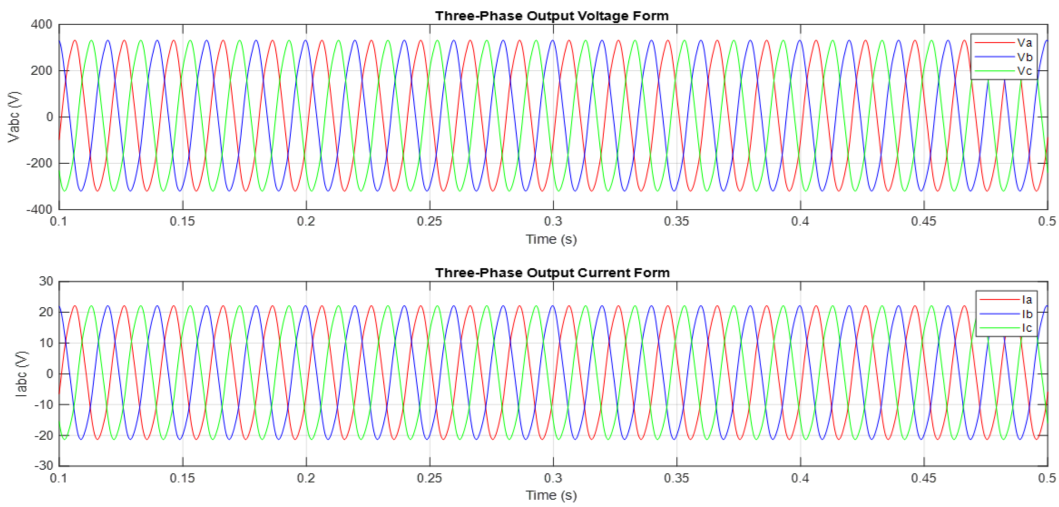

Figure 2.23: Filtered SI-SSI (R = 15.87 Ω, L = 10 mH).

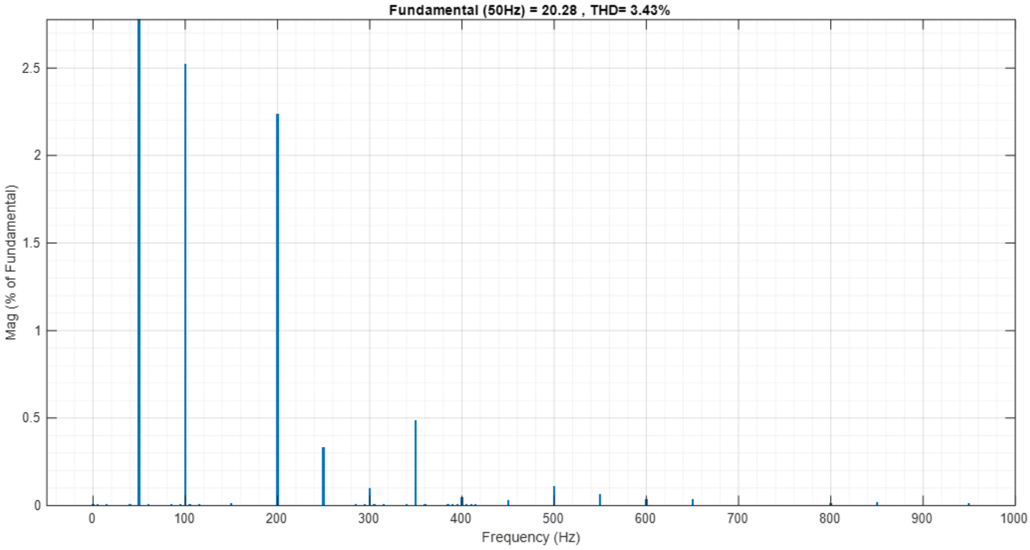

Figure 2.24: THD profile (current).

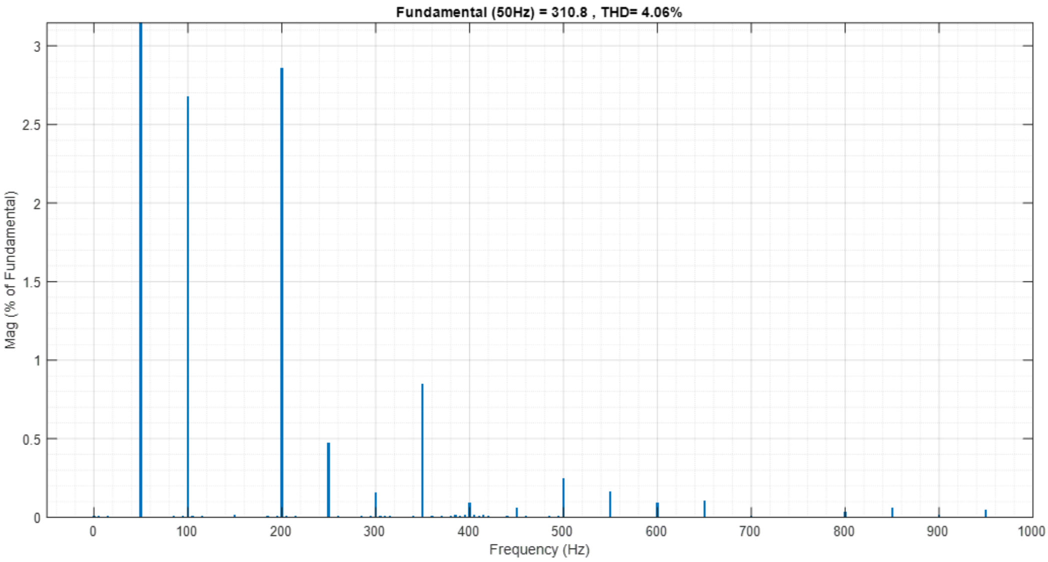

Figure 2.25: THD profile (voltage).

R $= 15.87\,\Omega, \mathrm{L} = 22\,\mathrm{mH}$

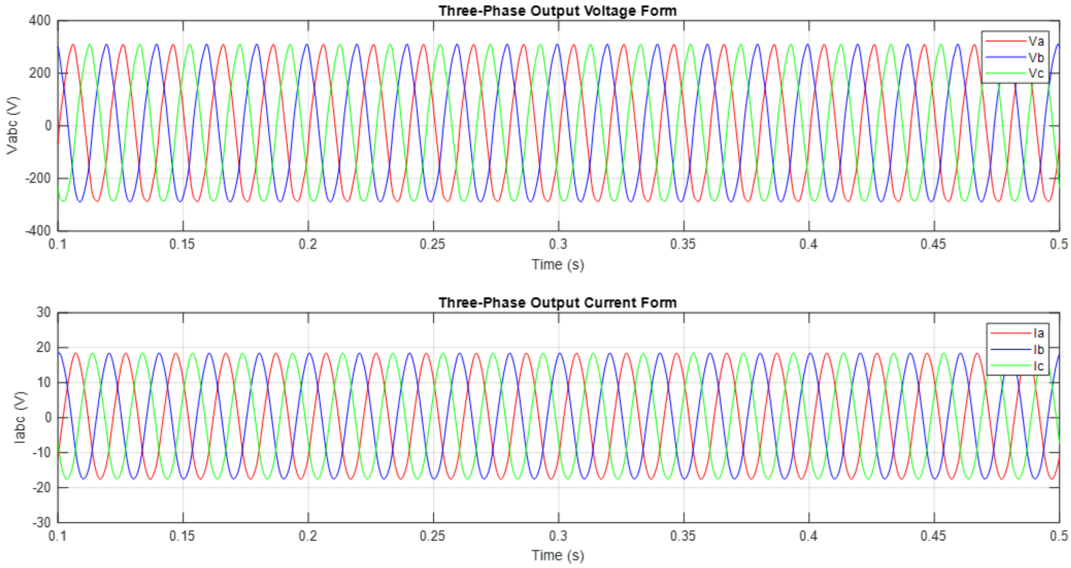

Figure 2.26: Filtered output waveforms ($\mathrm{R} = 15.87\,\Omega, \mathrm{L} = 22\,\mathrm{mH}$).

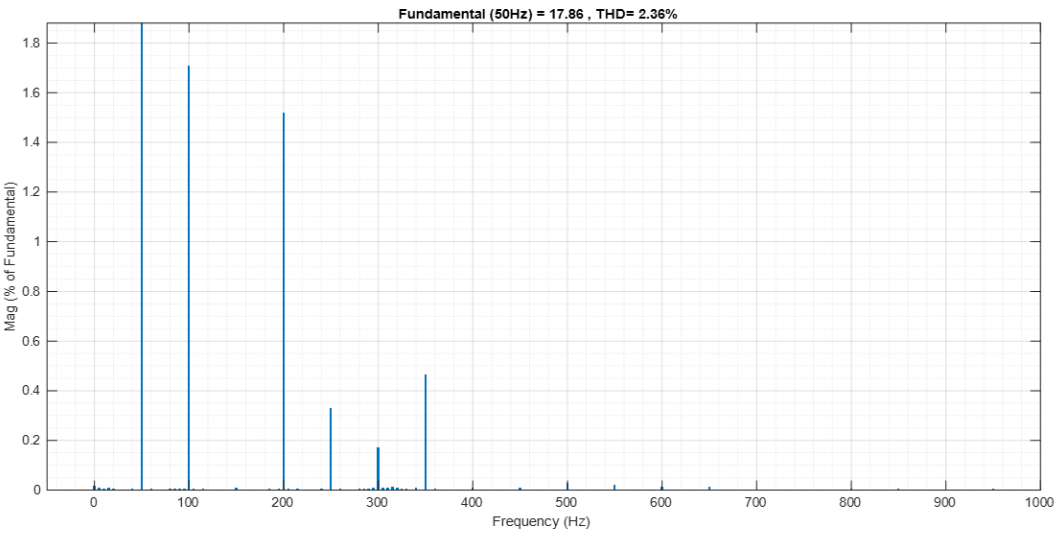

Figure 2.27: THD profile (current) $\mathrm{R} = 15.87\,\Omega, \mathrm{L} = 22\,\mathrm{mH}$.

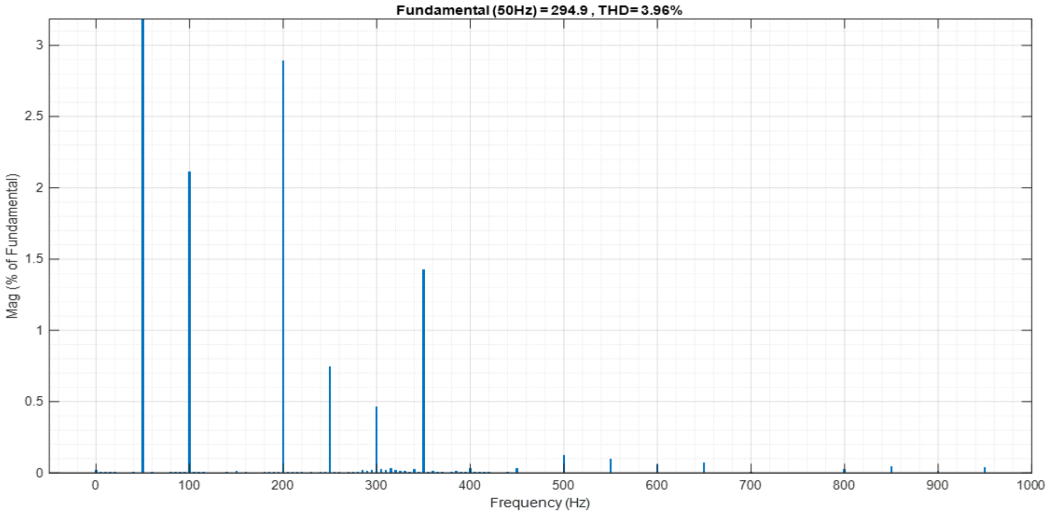

Figure 2.28: THD profile (voltage) $\mathrm{R} = 15.87\,\Omega, \mathrm{L} = 22\,\mathrm{mH}$.

$\mathbf{R} = 22\,\Omega, \mathrm{L} = 10\,\mathrm{mH}$

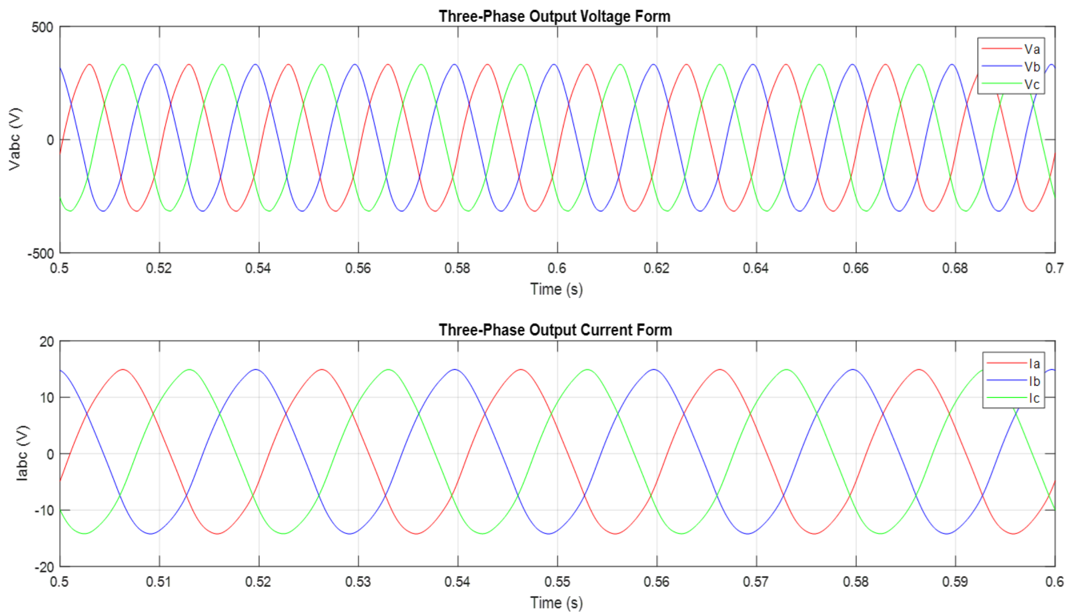

Figure 2.29: SI-SSI output waveforms

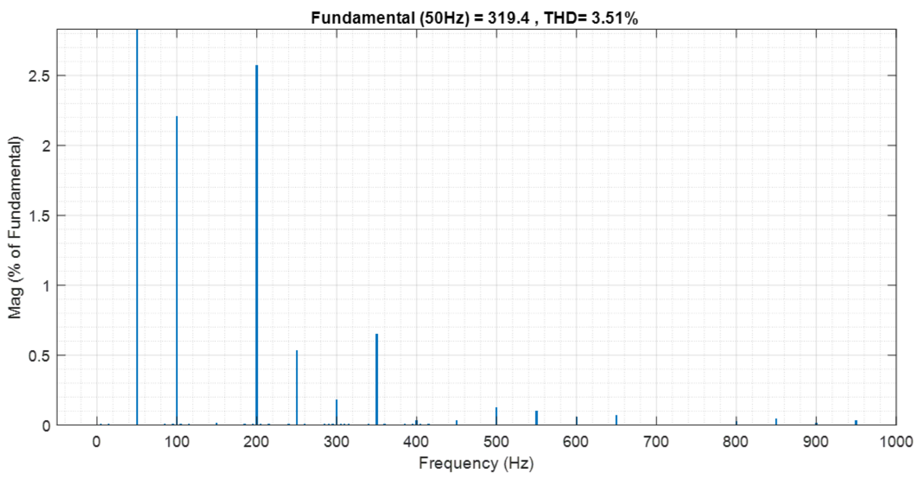

Figure 2.30: SI-SSI voltage THD profile

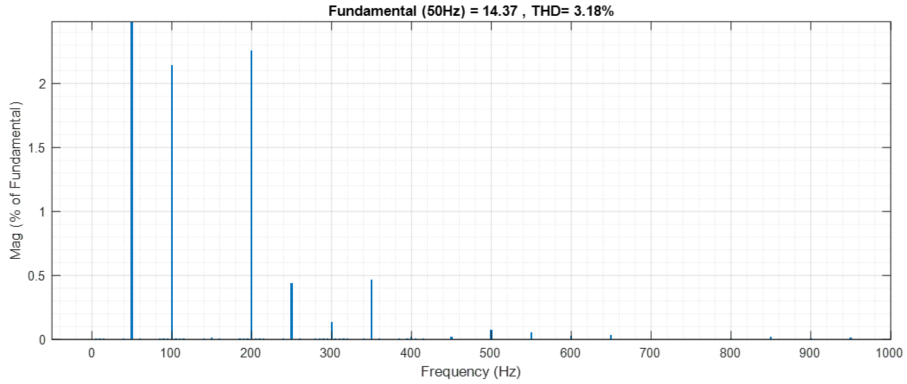

Figure 2.31: SI-SSI current THD profile

$\mathbf{R} = 22\,\Omega, \mathrm{L} = 22\,\mathrm{mH}$

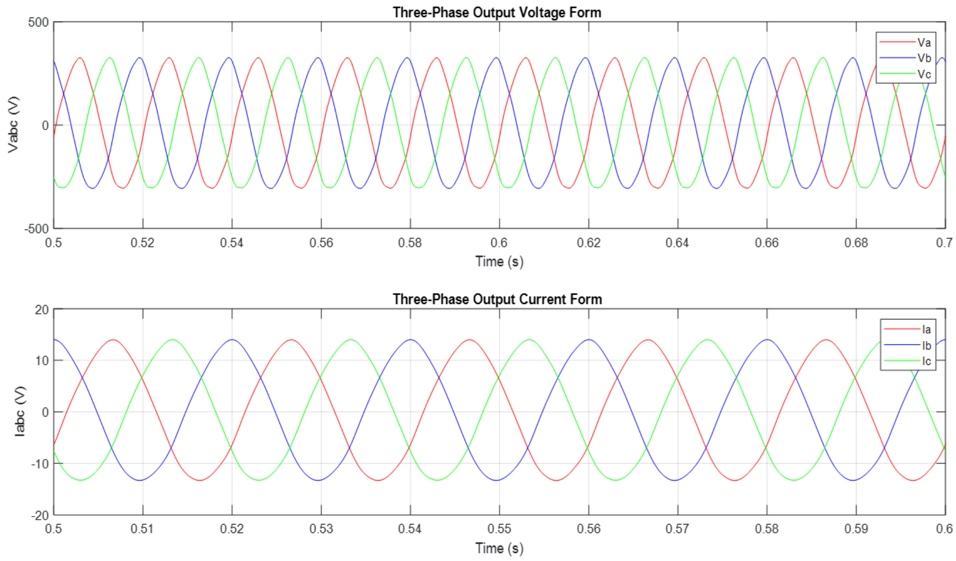

Figure 2.32: SI-SSI filtered output

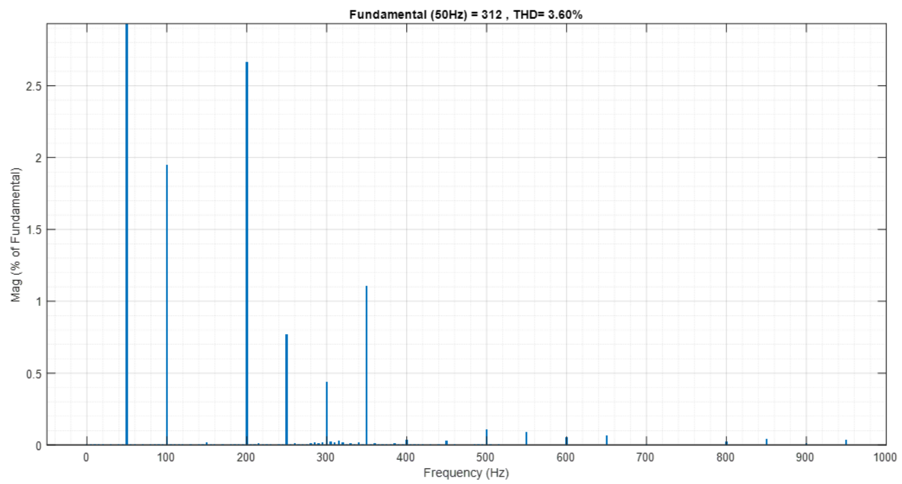

Figure 2.33: SI-SSI voltage THD profile

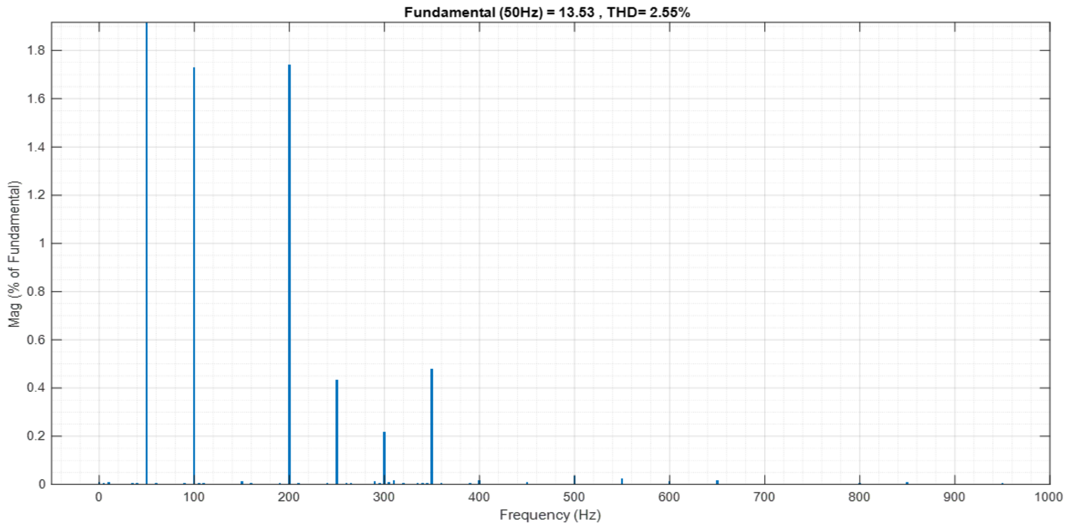

Figure 2.34: SI-SSI current THD profile

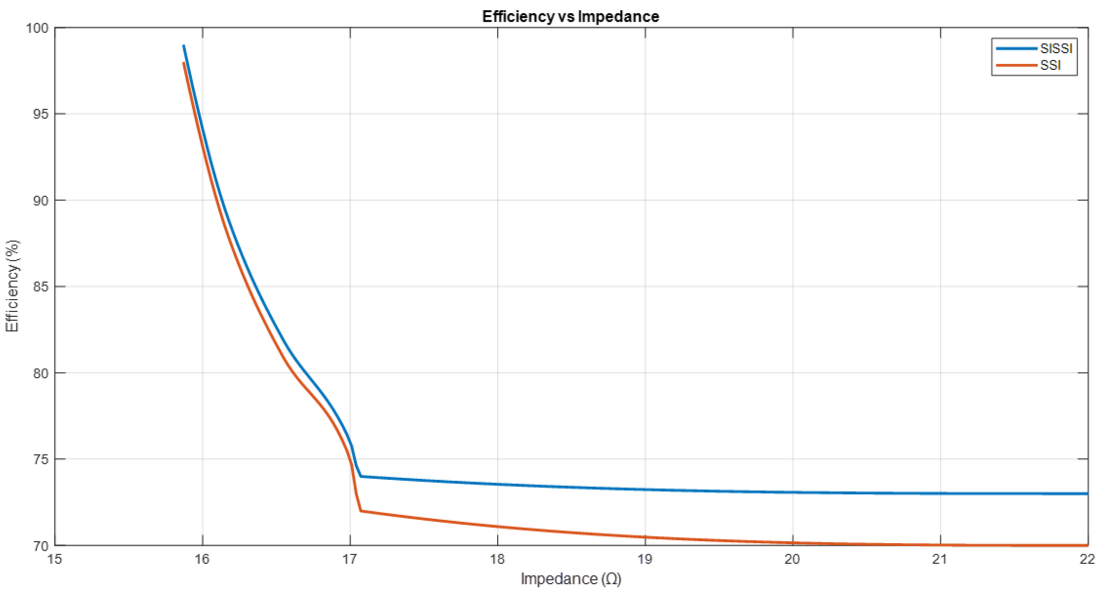

Figure 2.35: Efficiency profile SSI and SI-SSI vs impedance

2.5 Intepretation of results

From this simulation, the VSI produced a peak Voltage of 40.55V and peak current of 1.7A as shown in Figure 2.4, that is 28 V and 1.20 A RMS which are both extremely low for the desired system performance of 325 V peak voltage and 230 V RMS. The VSI also showed minimal THD levels of 1.03%, Figure 2.5 .Moreover, stepped sinusoidal output was observed for the unfiltered voltage waveforms Figure 2.3. Figure 2.4 shows the final waveforms after filtration by the LC filter which were smoother and cleaner with less distortion and noise. It is also observed that the current THD and voltage THD are similar, resistive load has no phase shift between current and voltage, and the current is an image of the voltage waveform.

The DC link voltage plays a crucial role in energy balance as shown in Figure 2.7 and Figure 2.15. The capacitor voltage remains stable with low ripple, confirming effective buffering and regulation across switching cycles. Figure 2.1 represents the sinusoidal reference signal with the carrier signal (triangular).

We can observe that the SI-SSI delivers approximately the same output voltage and current RMS values as were calculated in the theoretical modeling of the topology with the 15.87 Ω load. Simscape's RMS block was used to calculate the RMS value that produced 14.43 A and the peak of the 20.41 A phase as calculated in section 2.1.

It is also observed that both SSI and SI-SSI under the same load of (R = 15.87 Ω) displayed smooth output waveforms with reduced noise, Figure 2.9 and Figure 2.17. They also showed acceptable low THDs as indicated in Figure 2.18 for SI-SSI and Figure 2.10 for SSI, in which both meet the acceptable IEEE standards for interconnected and distributed energy resources [7]. For RL load with R = 15.87 Ω and L = (10 mH, 22 mH), both topologies in Figures 2.24, 2.25, 2.27 and 2.28 exhibited low THDs as the RL loads act as low-pass filters, thus smoothing the current waveforms, reducing the voltage and current ripples harmonics, and increasing the quality of the waveforms.

Without filtering, both the SSI and SI-SSI output waveforms exhibit stepped SPWM pattern with evident noise and harmonic distortion, Figure 2.11 and Figure 2.19. After filtration by the LC filters, the waveforms become cleaner and more sinusoidal with fewer ripples, confirming the effectiveness of the LC filter, Figure 2.12. The filtered SI-SSI waveforms exhibit similar characteristics to the SSI output but may experience minor overshoot depending on inductor size and switching dynamics. The SSI produced a Vpph of 324.6 V, 229.5 V RMS phase voltage which is close to the desired phase voltage of 230 V RMS. The SI-SSI produced peak phase voltage of 327.3 V and phase voltage of 231.6 V RMS which is slightly higher than the SSI due to its high boosting capability. The current follows the filtered voltage output profile and remains sinusoidal indicating good load tracking performance and are in phase with the output voltage waveforms.

The THD was calculated using the FFT analyses tool in Simulink's Powergui block over a steady state period after the startup transient. Figure 2.13 and Figure 2.21 shows the harmonic profile of the two topologies. Both exhibited THDs of $< 5\%$ with SSI 1.33 % and 3.86 % respectively. The SSI topology meets ultra-low distortion standards while the SISSI shows a slightly higher THD. This is due to the introduction of subharmonic ripples during the transition mode and additional ripples from the switched inductor network. The THDs meet the IEEE 519-2014 recommended limit of $< 5\%$.

Notable difference is observed when the RL $(\mathrm{R} = 22\,\Omega, \mathrm{L} = 10\,\mathrm{mH})$ load was introduced into the SISSI topology. A significant voltage drop is recorded as in illustrated in Figure 2.29. There is a 2.3% voltage drop from 327.3 V (resistive load) to 319.4 V, and the current slightly decreases by 0.94% from 14.88 A to 14.37 A, respectively. The drop confirms the theoretical expectations as the inductor's reactance increases the effective impedance to 22.2 Ω from 22 Ω. Furthermore, the voltage THD slightly improves from 3.86% in Figure 2.21 to 3.51% in Figure 2.30. The current THD is also low at 3.18% Figure 2.31. The reduction in harmonic distortion is due to the inductive load that acts as a low-pass filter, thus smoothing the output waveforms.

With an increased inductance of 22 mH, the total effective impedance is further augmented to 22 Ω that results to a significant drop in peak output voltage from 327.3 V to 312 V, as shown in Figure 2.32. In a similar manner, the peak current decreases from 14.88 A (resistive load) to 13.53 A , a 2.5% current drop. Additionally, the voltage THD Figure 2.33 is slightly lower at 3.60%. Figure 2.34 also indicates very low current THD, 2.55%. The THD performance is attributed to the inductive charge that filters out harmonics, hence reducing voltage distortion and smoothing the current waveform. Lastly, Figure 2.35 displays the efficiency comparison of the two topologies. The SI-SSI shows a slightly higher efficiency with variation in load impedance.

2.6 Conclusion

This study comprehensively analyzed and compared the power quality as measured by total harmonic distortion. Both topologies exhibit distinct characteristics in terms of harmonic performance.

The VSI showed very low THD levels which makes it suitable for sensitive applications such as hospital equipment but produces very low voltage without additional boosting stage making it unsuitable for medium or high-power usage scenarios.

The SSI topology achieved a THD of $< 1.33\,\%$, exceeding the performance criteria set by stringent standards such as IEEE 519. This low distortion is attributed to SSI's simple circuit structure, which results in simple switching transitions, reduced parasitic effects and lower frequency noise. These characteristics make the SSI particularly suitable for applications where minimal distortion is critical - such as medical devices, high-fidelity audio systems and military.

On the other hand, the SI-SSI topology, while offering enhanced voltage gain, produced a higher THD of $< 3.86\,\%$ mainly due to discontinuous currents and complex switching dynamics. While the THD of the SI-SSI is within the accepted limit, it can further be reduced by incorporation of LCL filters, dead-time compensation, and SVPWM techniques for better THD results. This makes the SI-SSI suitable where higher voltage boost and voltage gain is prioritized.

These results highlight the trade-off between voltage gain and power quality. The SSI is preferred for low-THD applications, while the SI-SSI fits systems requiring high voltage conversion. This study contributes to efficient inverter design by offering a practical comparison of the two topologies. Its findings support better topology selection in areas like renewable energy, electric vehicles, and smart grids.

2.7 Comparison between VSI and SI-SSI

In this section, performance metrics of both the VSI and the SI-SSI were compared, under similar operating conditions, to highlight the advantages and trade-offs of each inverter design.

In Table 2.3, the simulation results reveal that the VSI, though displaying a better THD level and cleaner output, it falls short on power delivery. It produces low voltage output that makes it unreliable for applications that require significant power delivery. On the other hand, the SI-SSI demonstrates higher voltage gain and higher current delivery but with slightly higher THD level. However, both inverters maintain low THD below the IEEE 519-2014 standard [7]

2.8 Comparison between SSI and SI-SSI

In the comparison Table 2.4, it was evident that both SSI and SI-SSI deliver waveforms within the acceptable THD limits as in [7]. However, the SI-SSI provides higher voltage gain compared to the SSI due to its switched inductor network configuration. On the

Table 2.3: Performance Comparison Between VSI and SI-SSI Topologies

Parameter	**VSI**	**SI-SSI**
Peak output voltage	40.55 V	327.3 V
RMS output voltage	28 V	231.6 V
Peak output current	1.7 A	14.88 A
RMS output current	1.20 A	10.52 A
Voltage THD	1.03 %	3.86 %
Current THD	1.03 %	3.86 %
DC-link voltage ripple	Low	Low
Output waveform quality	Clean sinusoidal	Clean sinusoidal with minor noise
Voltage boosting bapability	None	High

Table 2.4: Performance comparison between SSI and SI-SSI topologies

Parameter	**SSI**	**SI-SSI**
Output characteristics		
Peak output voltage	324.6 V	327.3 V
RMS output voltage (resistive load)	229.4 V	231.6 V
Peak output current	14.75 A	14.88 A
Capacitor voltage	727 V	895 V
Power quality		
Voltage THD (resistive load)	1.33 %	3.86 %
Topology features		
Switching complexity	Low	High
Voltage gain capability	Moderate	High
Filtering requirements	Standard	Precise tuning needed
THD sensitivity to load	Low	Moderate
Recommended applications		
	Low-THD systems	High-gain applications
	Audio/medical devices	Renewable energy systems

contrary, the SSI maintains lower THD levels 1.33% making it suitable for applications where power quality is important. The SI-SSI still exhibits higher efficiency in power delivery making it suitable for systems that require significant power delivery.

Chapter 3

SIMULATION OF SI-SSI IN PROTEUS

3.1 Introduction

This chapter presents the Implementation of SI-SSI in proteus. Our goal in this chapter was to model the inverter circuit , verify its operation and validate the output of our circuit. We implement both hardware and software components. The implementation process involves designing the SI-SSI logic, configuring the necessary components in Proteus, and validating the system through simulation. [42]

Proteus is an electronic design automation(EDA) tool that incorporates circuit simulation, schematic capture, and PCB design. It enables the construction, simulation, and evaluation of digital circuits all in one tool. This ensures reduced hardware prototyping costs and ensures design accuracy. Since a number of various tests are taken verifying its functionality prior to physical implementation. Proteus is preferred due to its enables hardware simulation through the use of electronic circuits. And also enables the building of circuits using actual electronic components under actual real world operating conditions.

This chapter will be covered into four main parts, first covering the selection of the hardware components required, followed by the design of our circuit, which will also include its simulation. Later the simulation results and interpretation of the results obtained. And finally a general conclusion of the chapter giving a general summary of the things that were covered in the chapter.

3.2 Selection of the hardware components required

The implementation of the inverter in Proteus requires careful selection of each of the required components. The circuit will be divided into parts, the part of the power supply, the part of control, driving component, the visualization component, and finally our inverter topology.

3.2.1 SG3525A

SG3525 is a driver used to control transistors using Pulse width modulation. It is designed to control the output voltage and frequency of a DC-AC converter. It provides a means of regulating the output voltage and frequency by adjusting the duty cycle of the PWM signal. It also includes protection features. SG3525A is an integrated circuit pulse width modulation controller used in switching in power switching power supplies, inverters, DC-DC converters. It generates PWM signals with an adjustable duty cycle and a stable frequency.

Characteristics of SG3525

SG3525 is a simple and reliable ntegrated chip that provides two PWM outputs with a programmable dead time. It also does not need an oscillator since we can set the switching frequency using RT and CT. This integrated circuit differs from other PWM controllers due to its ability to generate a PWM signal without the use of an external micro controller. It operates with a variable voltage ranging from 8-35 volts, thus it can be used in a wide range of applications. Equally, its output frequency can be adjusted from 50Hz to up to 400kHz, by varying the RC network. In addition, it has a soft start function that gradually increases the output voltage during startup[43].

Structure of the SG3525

The SG3525 is a voltage-mode PWM controller that operates from a single power supply over a variable number of voltages. It has all the usual functions for a basic PWM control circuit, including a precision voltage reference, error amplifier, oscillator,PWM comparator, and output drivers.The structure of an SG3525 consists of a numerous number of components for example; Internal Oscillator mainly used for the generation of a switching signal. Error amplifier which compares the input and output voltage and adjusts the input voltage to get the required output voltage. Thirdly, Double D flip-flop, used for the delay control , by changing the delay capacitor. And finally switching frequency, the frequency can be adjusted by adjusting the size of the internal resistor RT.

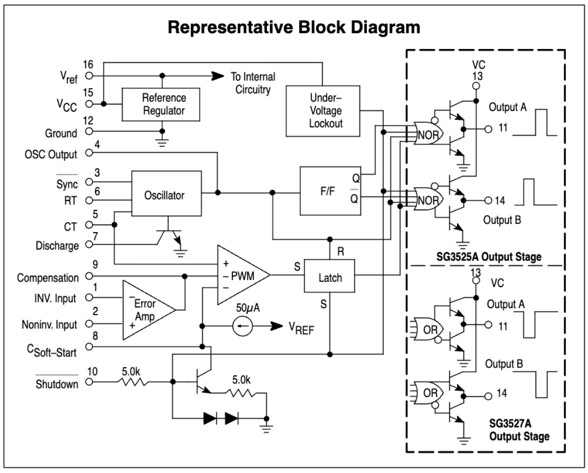

Figure 3.1: SG3525 internal overview

$$f_{\text{sw}} \approx \frac{1}{0.7 \times R_T \times C_T}$$

3.2.2 DRIVER

A MOSFET or IGBT gate driver is an electronic circuit designed to control power transistors in an inverter, chopper or any power converter. IR2112 is the most widely used in high and low-side driver for inverters. Most microcontrollers give 3.5-5V, which isn't sufficient to power MOSFETs thus the need for a driver. Drivers translate the logical signals to a higher voltage or current that facilitates the rapid switching of the gate.

Structure of the driver

The driver features a bootstrap circuit for voltage storage, enabling sufficient power for the high-side MOSFET, and a dual-channel capability for controlling both high-side and low-side MOSFETs. It also includes protection mechanisms like under voltage lockout to disable output when supply voltage is low. And finally, the pin configuration varies by package type, with PDIP having 14 pins and SOIC having 16 pins, ensuring reliable and efficient operation.

Symbol	Description
Vdd	Logic supply
HIN	Logic input for the high side driver output
SD	Logic input for shutdown
LIN	Logic input for the low side driver output
Vss	Logic ground
VB	High side floating supply
HO	Output for the high side gate drive
Vs	High side floating supply return
Vcc	Low side supply
LO	Output for the low side gate drive
COM	Low side supply return

Table 3.1: Driver IC pin description

Working operation

The high-side MOSFET is floating, thus it's not connected to the ground. To turn it on, the high side MOSFET needs to be at a higher voltage than the voltage at the drain, and this can only be achieved through the bootstrap circuit. When the low-side MOSFET is ON, the bootstrap capacitor charges through the diode. When the low-side MOSFET is OFF, the charged bootstrap provides voltage to turn ON the high-side MOSFET.

3.3 Design of the SI-SSI in proteus

The circuit of Switched Inductor split source inverter was modeled both in Simulink and ISIS. This chapter represents our ISIS model of our prototype. The prototype was a combination of the SG3525 PWM controller and also IR2112 driver. It also consisted of other key components like MOSFETS which were driven by our driver, 2 similar inductors, a battery, Capacitors, Oscilloscope for the visualization of the output, diodes, and finally numerous number of resistors with the majority of them being used in the protection of our prototype.

Principle of operation

The switched inductor split source inverter is an alternative to the conventional Split source Inverter. Capable of boosting the voltage without the need for a DC-DC booster. The operation in ISIS starts with input DC voltage could be a battery or a solar panel. This is essential in the powering of our inverter. The SG3525 PWM collector is then used to generate PWM signals which can be adjusted according to the value of the timing capacitor and timing resistor. The signals are then transferred to the MOSFETs using IR2112 which interprets the respective logic signals to provide the appropriate voltage signals to drive the MOSFETs. The opening and closing of the MOSFETs greatly influence the SI-SSI topology. During the OFF state, energy stored in the inductors is released to the capacitor through the diodes driven by the discharging of the inductors.

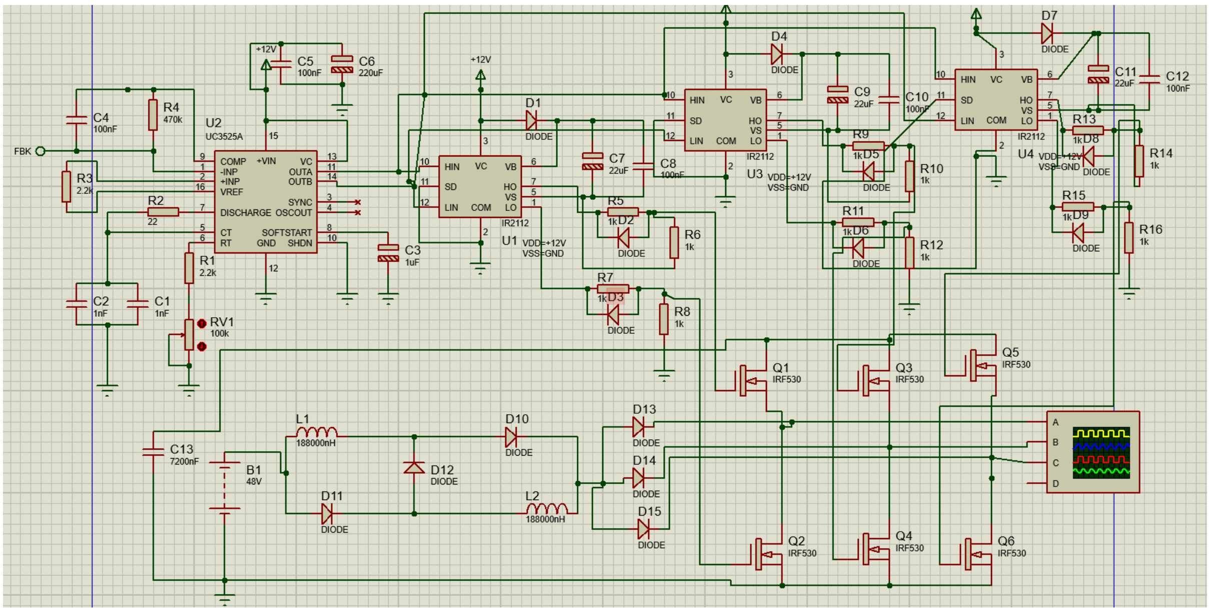

Figure 3.2: Three-phase SI-SSI inverter in ISIS

3.3.1 Simulation and results

The simulation of the SI-SSI in this chapter was done in Proteus, our main objective was to analyze our output wave form and verify our output through various conditions. First we shall cover the circuit setup and later the simulation results obtained from the oscilloscope.

The switches were driven by an IR2112 gate driver powered by an PWM collector, SG3525. The PWM driver produces a pulse width modulation that can be adjusted by varying the values of capacitor at RT and CT.

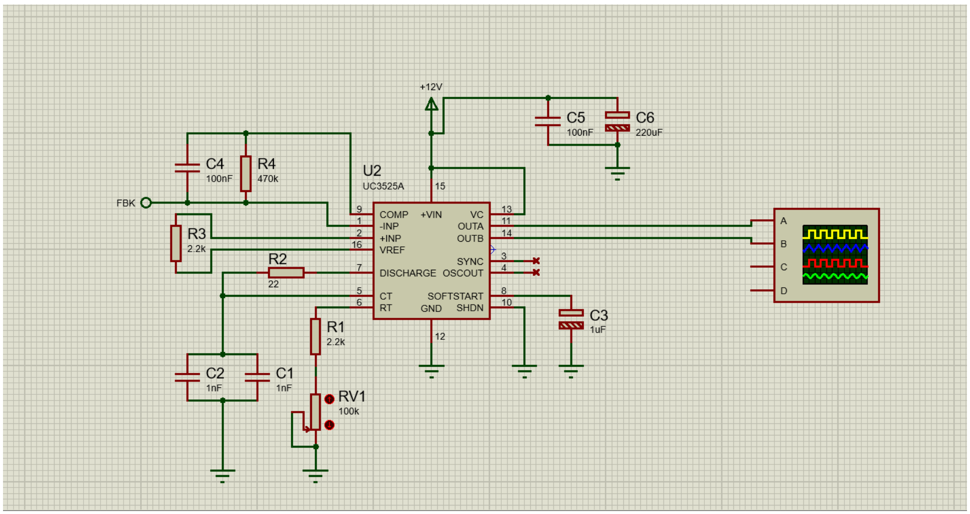

Figure 3.3: Circuit diagram of an SG3525

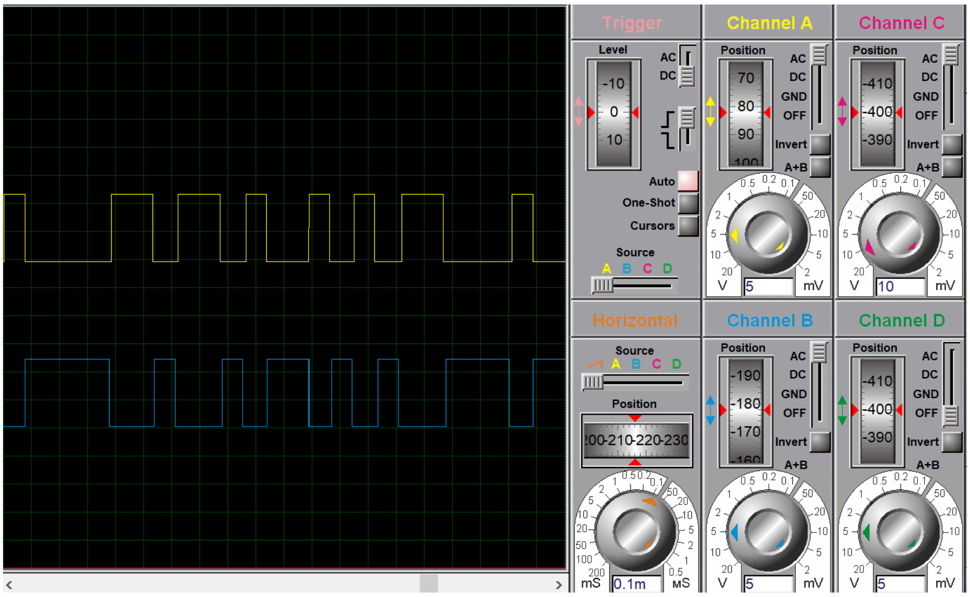

Figure 3.4: Oscilloscope output of SG3525

The output from the PWM driver is very minimal and insufficient to power the MOSFET, which necessitates the need for a driver, IR2112. This driver amplifies the signal obtained to a voltage sufficient to drive the MOSFET. Out A of SG3525 controller is connected to the HIN pin of the driver while Out B is connected to LIN.

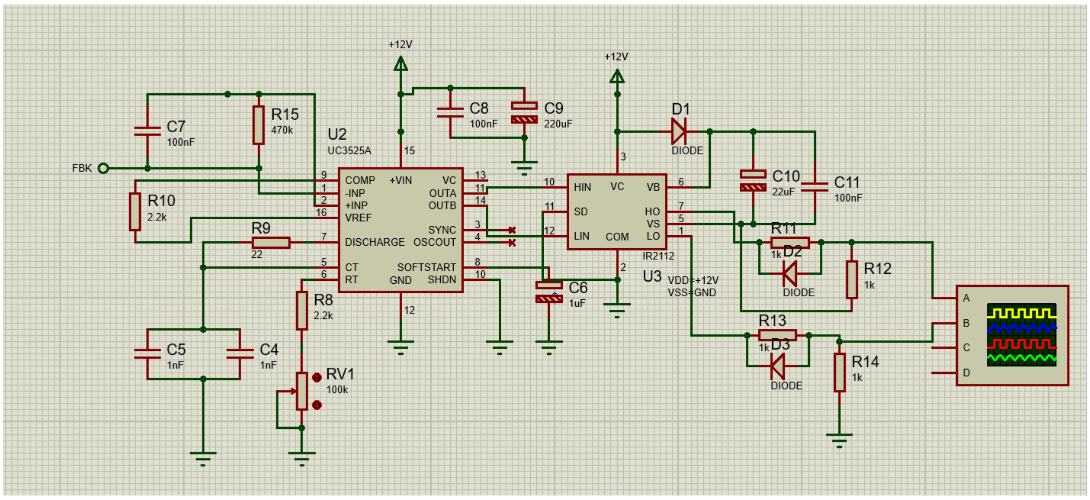

Figure 3.5: Circuit diagram of SG3525 connected to the driver

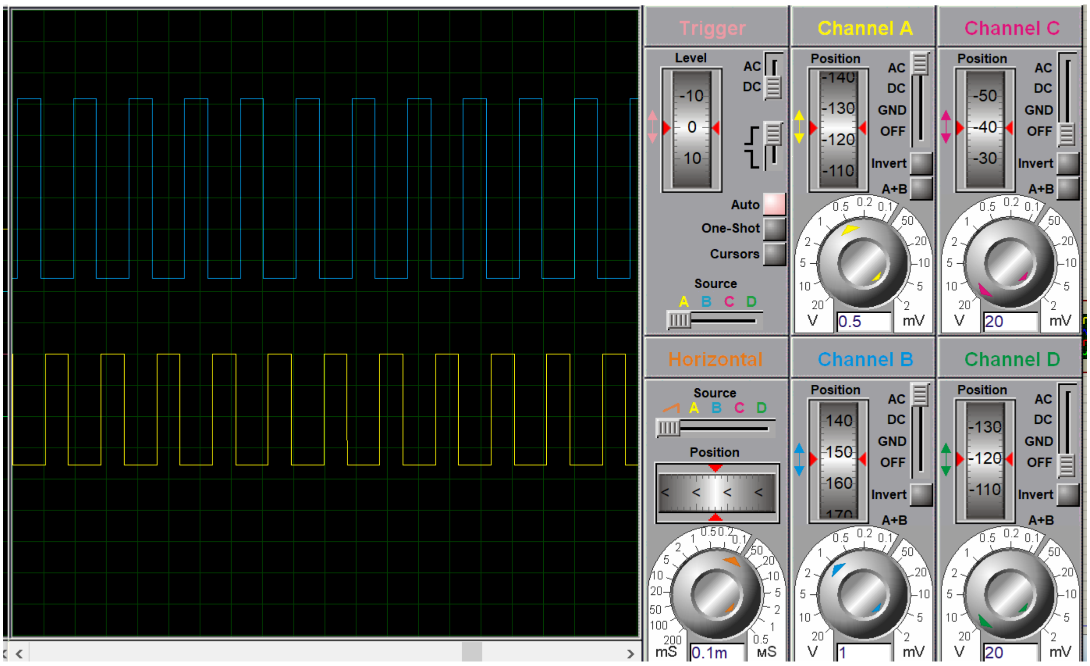

Figure 3.6: Oscilloscope output of the driver

The circuit is then connected to SI-SSI topology powered by a DC voltage source of 100V. The topology consisted of two inductors and two diodes with a capacitor connected in parallel with the topology. With the topology connected with both SG3525 and IR2112 driver, this outputs an AC wave form with a boosted voltage provided by the switching of the inductors.

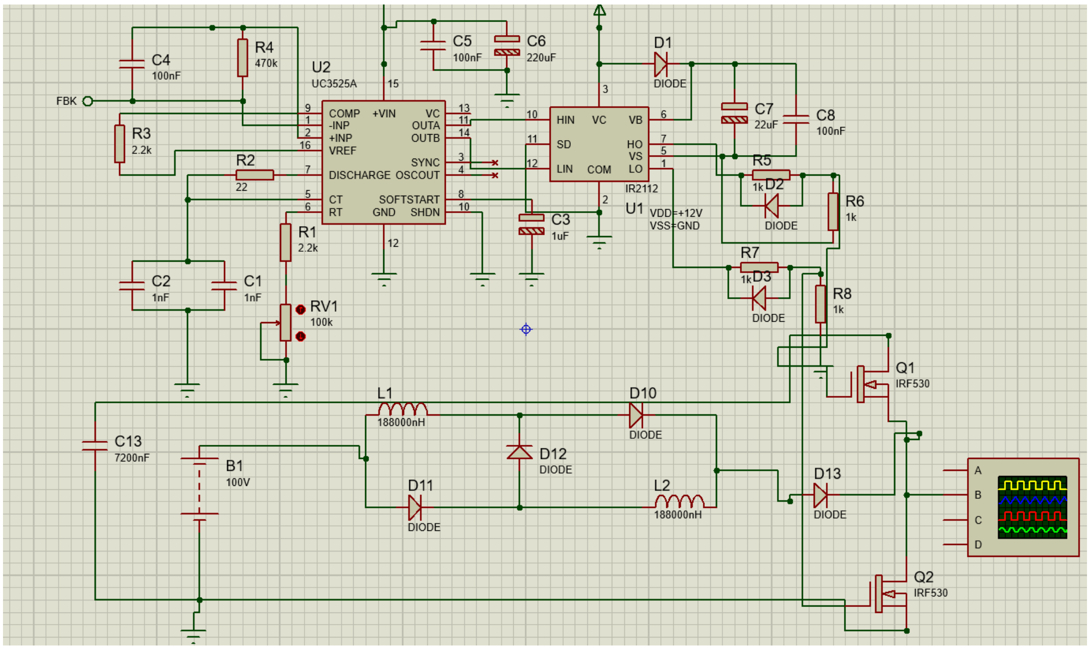

Figure 3.7: Mono-phase circuit diagram of SI-SSI

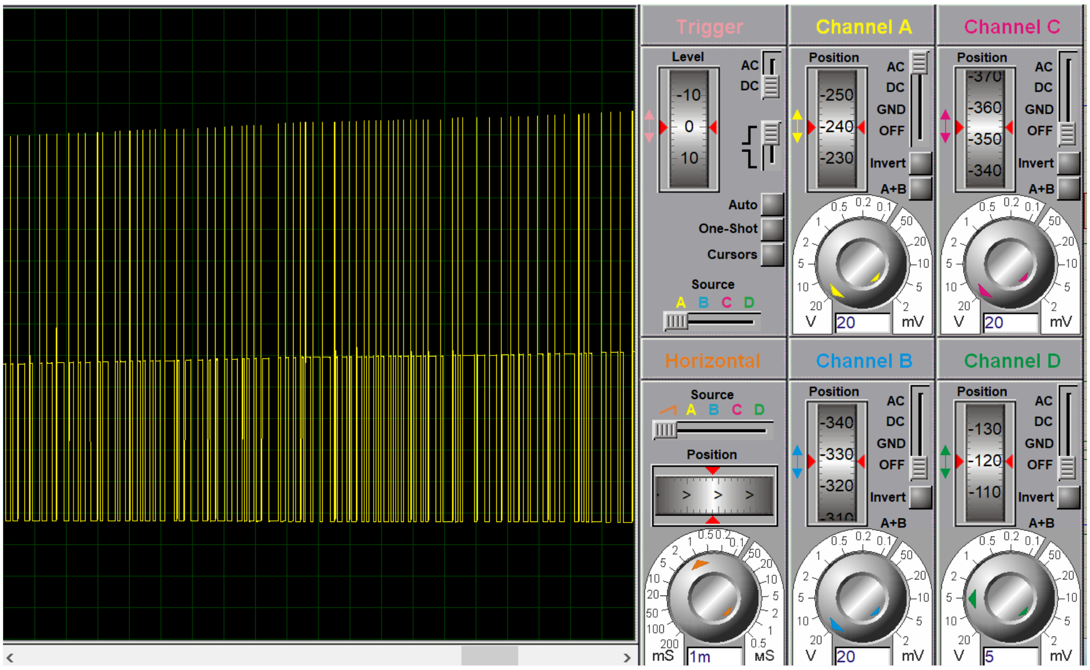

Figure 3.8: Oscilloscope output of the mono-phase circuit

When the circuit had a source of 100V, the wave form obtained was very hard to correctly visualize, since the maximum calibration of the oscilloscope is set to 20V. So the dc source was reduced to 12V to match the calibration of our oscilloscope. The capacitor and inductor values were also adjusted to match the dc voltage source.

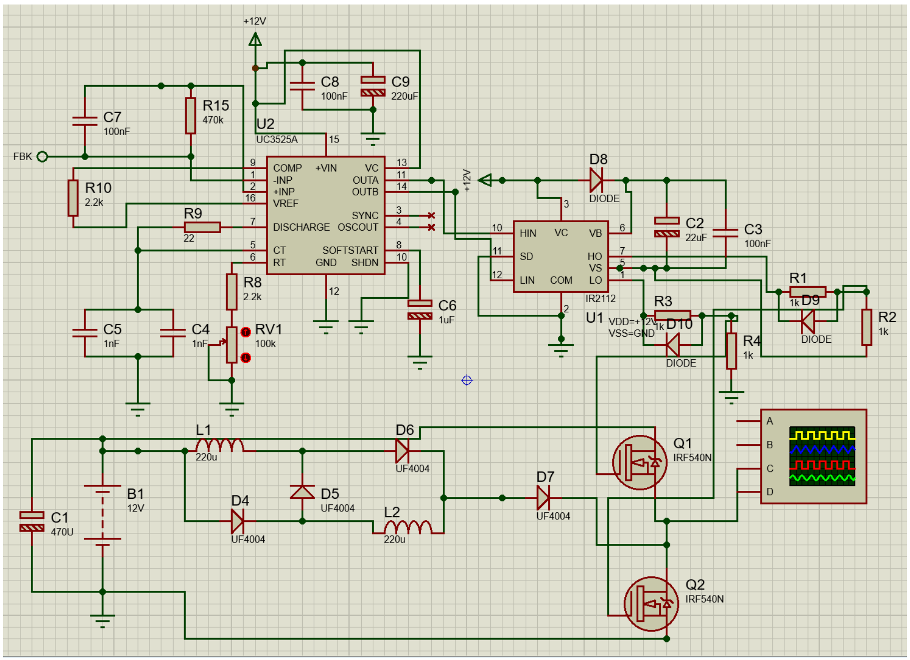

Figure 3.9: Monophase circuit of SISSI

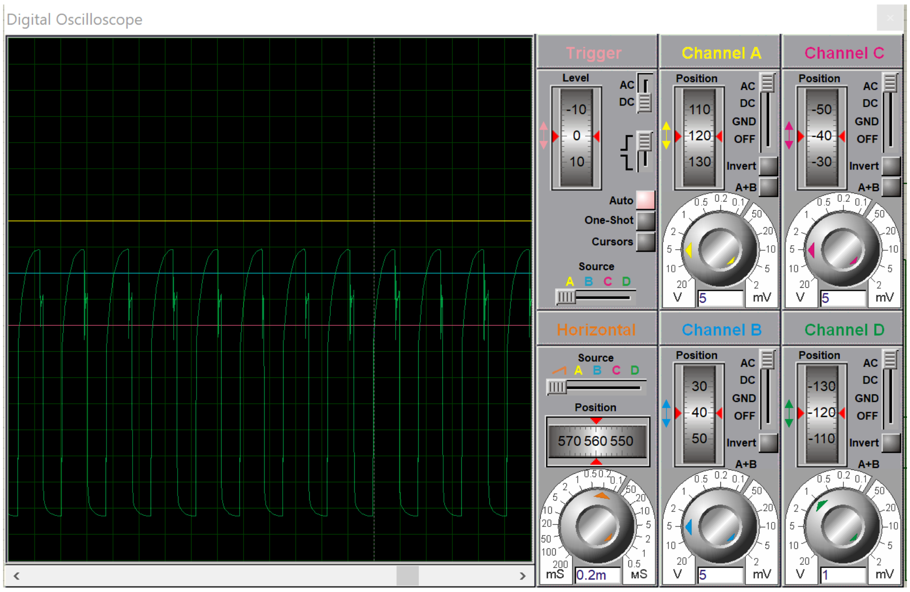

Figure 3.10: Monophase output of SISSI

Using the same values of resistors, capacitors used in the new monophase circuit of 12V. Using a capacitor of 470micro Farads and also two inductors of 220microFarads. The inital diodes were interchanged to have faster response diodes(UF4004) and also the MOSFETS were interchanged for IRF540N. From the monophase circuit, a 3phase circuit was constructed adding 2 drivers and 4 MOSFETs.

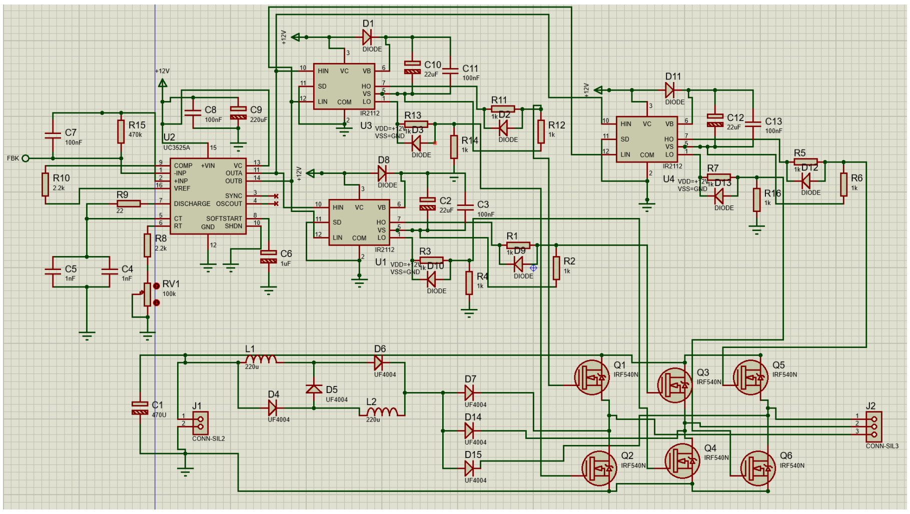

Figure 3.11: Three-phase circuit of SISSI

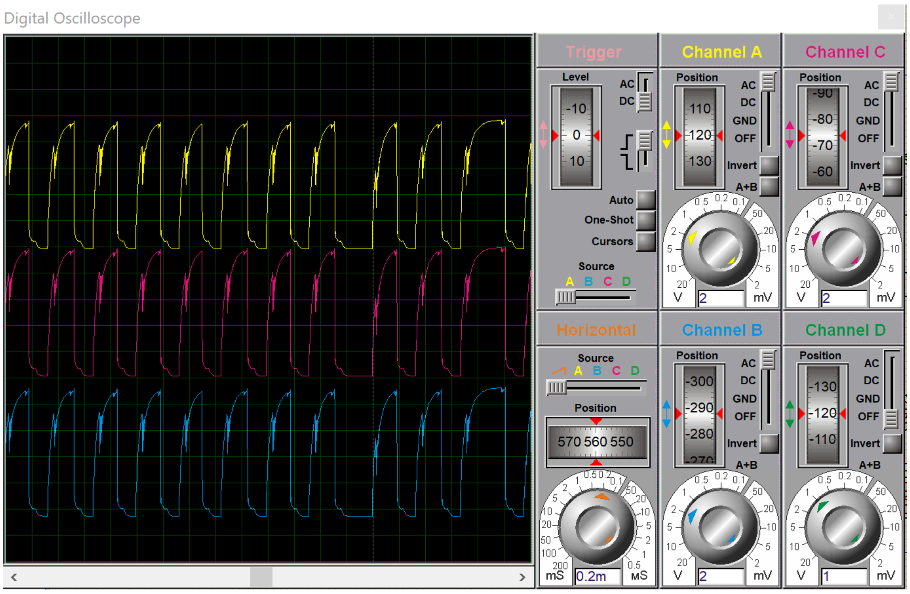

Figure 3.12: Output of the three-phase circuit

Simulation of the circuit with a LC filter.

From the output of the circuit, the waveforms contain several harmonics during the switching stages of the inverter. Thus the need to add an LC filter. The output of the inverter was connected to an LC low pass filter. The low pass filter contained an inductor of 3.3mH and a capacitor of 2.2microFarads. The low pass filter was calculated from the switching frequency which was estimated at 2OkHz. LC was calculated from the equations below.

$$f_s w = \frac{1}{2\pi\sqrt{LC}} \quad \Rightarrow \quad LC = \frac{1}{(2\pi f_s w)^2} \tag{3.2}$$

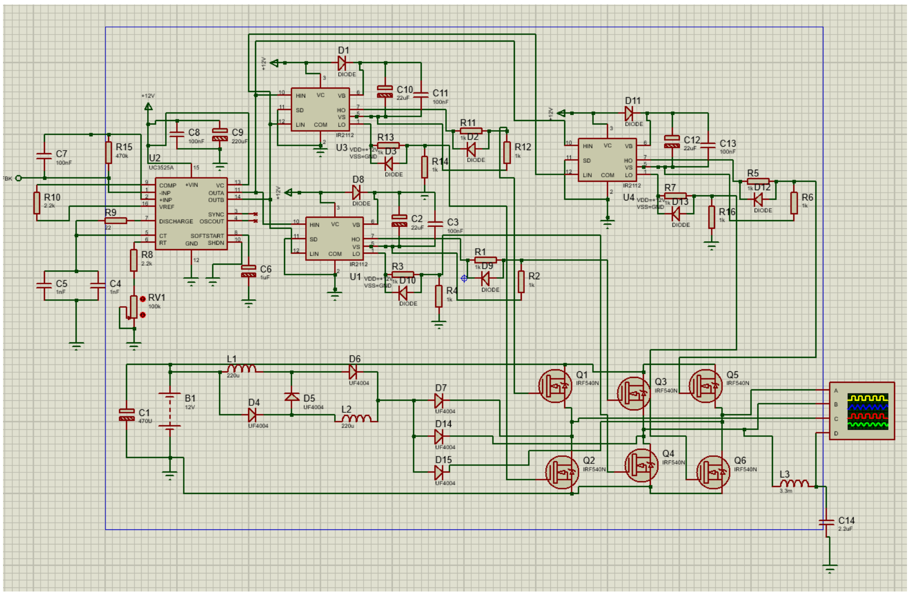

Figure 3.13: 3phase circuit with an LC filter

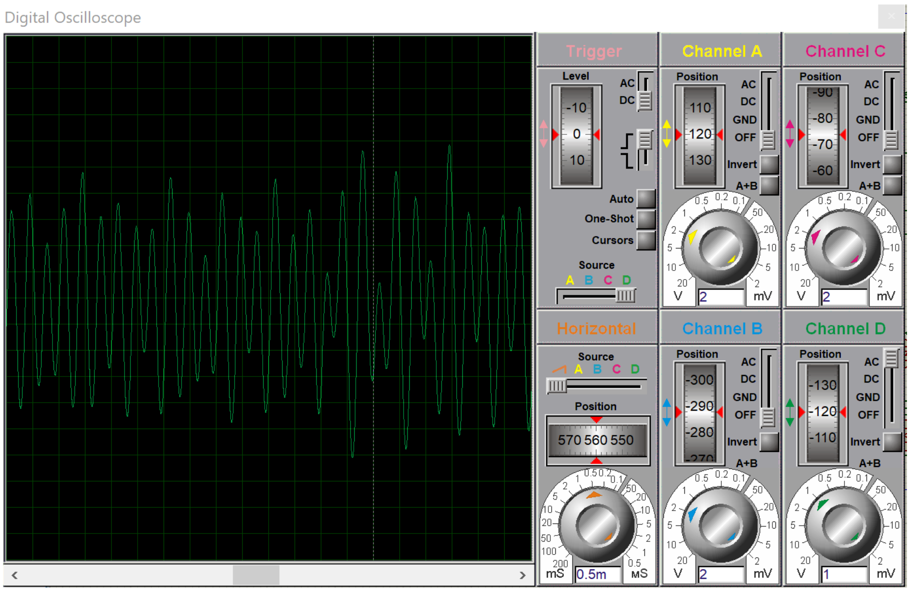

Figure 3.14: Output of the filtered circuit

3.3.2 Interpretation of Results

Upon simulation, the output from the oscilloscope before was observed to be an ac square pulse wave. The wave had a high frequency to the numerous number of switching patterns. The output had square pulses showing that the use of the SG3525 was a success. The switching frequency was also stable and consistent. Unfortunately, the waveform had sharp voltage spikes at the switching positions. The voltage spikes can be attributed to a number of several factors including, the fast switching transitions, the lack of a proper filter, switching of the inductors which dissipate energy during switching. Inductors are the most prominent cause of spikes. They store energy during charging, but when switches are turned off, these inductors release energy sharply, causing voltage spikes. Due to this, we added an LC filter to counter the harmonics in the circuit.

3.3.3 Implementation with the Arduino

Due to the spikes from the use of an SG3525, the replacement for the control was inevitable. The chosen controller was the arduino uno due to its simplicity and effective control. The arduino was then connected to the IR2112 driver to drive the MOSFETS.

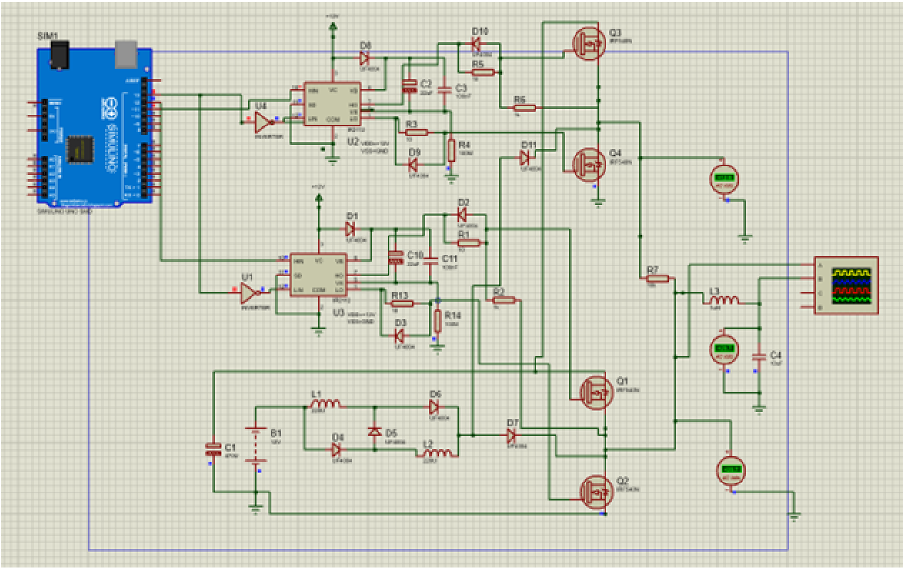

Figure 3.15: Arduino connected to SI-SSI topology

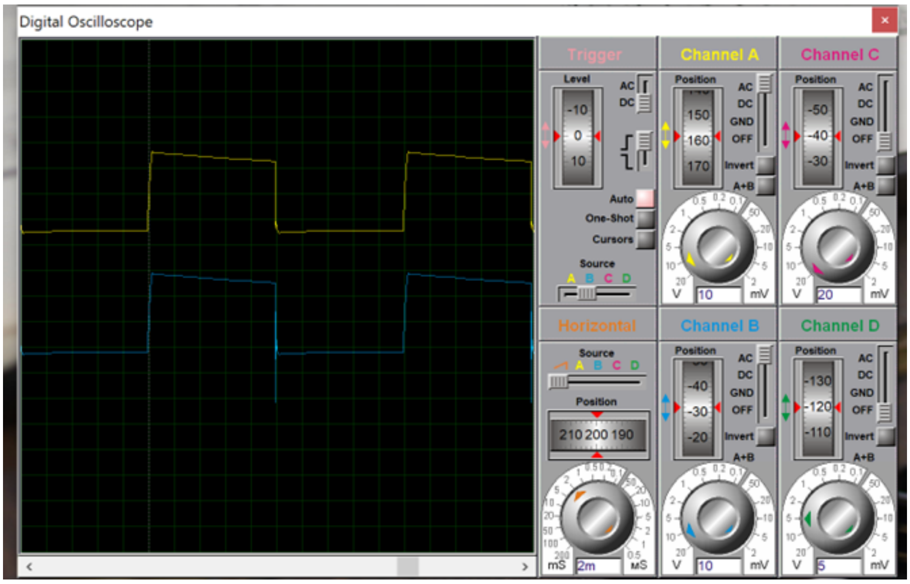

Figure 3.16: Output Voltage with Arduino

Interpretation of results

The output while using the arduino was boosted from 12V to about 20V. Also we can confirm that the DC-AC conversion was a success. The blue wave form represented the output with a load, and the yellow wave form was the output of one MOSFET leg.

3.3.4 Conclusion

The simulation of the SI-SSI topology in Proteus was a success with the successful conversion of DC-AC. The achievement of the AC square pulse wave was mainly influenced by the SG3525 controller, which outputted a square pulse wave, which was later boosted by the gate driver IR2112. Although the output achieved was an AC square pulse wave, it contained voltage spikes at the transitions. Due to this, we added an LC filter and also reduced the voltage to around 12V so that we can obtain an interpretable waveform. With the change of voltage, we also changed the inductors and capacitors plus replaced the diodes with faster recovery diodes.Upon adding the filter, the waveform immediately became sinusoidal. Although we added LC filter the output was not perfect. Thus we changed the controller in proteus and resorted to an arduino to generate the required pulse width modulation. The output voltage of the topology with the arduino connected was boosted and had fewer voltage spikes compared to SG3525

GENERAL CONCLUSION

This research presents a comprehensive study of the three-phase switched-inductor split-source inverter (SI-SSI) exploring its mathematical modeling, control strategies, and applications in power electronics. Through simulation studies and practical implementation in both the MATLAB/Simulink and Proteus ISIS softwares, we were able to perform and experimentally validate the theoretical analysis of the topology and further compare it to the other topologies explored in this study. Key findings include:

The SI-SSI has improved boost capability while maintaining high power quality. Compared to conventional voltage source inverters and split source inverters, the SI-SSI achieved a higher voltage gain due to its switched inductor network, as shown in equation (1.29). This makes it more suitable for application in renewable energy systems with fluctuating voltage sources or low voltage output, such as photovoltaic (PV) systems for grid integration.

The simulations revealed that the SI-SSI maintains the total harmonic distortion (THD) below 5%. The application of the SPWM modulation technique proved effective in managing the switching behavior, though slightly elevated THD (3.86%) was observed compared to 1.33% in SSI. This is largely due to the ripple effect induced by the presence of the switched-inductor network.

Hardware Validation

To validate the simulation results, hardware implementation was carried out in Proteus to validate the simulation findings. It was successfully established that DC-AC conversion was achieved. However, the output waveforms exhibited transient spikes, raising the need for an LC filter to smooth and mitigate high-frequency disturbances from switching operations.

Comparative Advantages

Overall, the SI-SSI outperformed traditional inverter topologies by enabling single-stage power conversion with high voltage gain, fewer passive components, reduced component stress, and reduced circuit complexity. These characteristics make it more suitable for medium- to high-power applications.

Suggestion for Future Work

Future work should explore space vector PWM (SVPWM) with microcontrollers such as DSP (e.g., TMS320F28379D) that could offer higher modulation precision and system adaptability; it is a solid control method for SI-SSI systems and could really tighten performance. Model Predictive Control (MPC) might also be worth testing, especially to boost dynamic response and reduce THD when loads shift around. AI-based controls such as fuzzy logic can also be explored as they provide adaptive control and may prove to be very efficient and beneficial for renewable energy systems with fluctuating input.

Further improvement of the SI-SSI design should involve the use of advanced semiconductors such as Gallium Nitride (GaN) and Silicon Carbide (SiC). Due to their fast switching and lower losses. They can ensure clean efficiency metrics. However, snubber circuits and fast recovery diodes should be implemented in the next development stages to minimize or eliminate the voltage overshoot and spike observed in the Proteus simulation.

Design and implementation of LCL filters and compliance testing based on [7] for real-world applications should be thoroughly examined and its performance in grid-connected configurations too. Evaluating its fault ride-through will provide insight into its dependence during electrical disturbances.

Additionally, to enhance the credibility of the SI-SSI topology as a valuable and reliable practical solution, future study should involve physical construction with discrete MOSFETs, integrated circuits drivers(ICs), and observations via scopes. Furthermore, electromagnetic interference (EMI) assessment and thermal profiling under variable loading conditions should be affected. These practical validations are necessary to ensure the reliability of the design in an industrial environment.

Bibliography

[1] M. Mubeen, "Design of z-source inverter for voltage boost application," *International Journal of Innovative Research in Electrical, Electronics, Instrumentation and Control Engineering (IJIREEICE)*, vol. 4, no. 2, pp. 157–161, Feb 2016.

[2] M. A. Ismeil, A. Abdelaleem, A. I. M. Ali, M. Nasrallah, H. S. Hussein, and E. E. M. Mohamed, "A comparison analysis of a new switched-inductor and conventional split source inverter structures," *IEEE Access*, vol. 12, pp. 28 013–28 024, 2024.

[3] B. K. Bose, *Modern Power Electronics and AC Drives.* Upper Saddle River, NJ, USA: Prentice Hall, 2006.

[4] M. H. Rashid, *Power Electronics: Circuits, Devices, and Applications*, 4th ed. Pearson, 2013.

[5] J. M. Carrasco, L. G. Franquelo, J. T. Bialasiewicz, R. C. Portillo-Guisado, and E. Galván, "Power-electronic systems for the grid integration of renewable energy sources: A survey," *IEEE Transactions on Industrial Electronics*, vol. 53, no. 4, pp. 1002–1016, August 2006.

[6] M. F. Blaabjerg, R. Teodorescu and A. Timbus, "Overview of control and grid synchronization for distributed power generation systems," *IEEE Transactions on Industrial Electronics*, vol. 53, no. 5, pp. 1398–1409, Oct 6.

[7] *IEEE Standard for Interconnecting Distributed Resources with Electric Power Systems*, IEEE Std. 1547-2018, 2018.

[8] P. K. Dewangan and U. T. Nagdeve, "Inverter for grid connected pv system: A review," *International Journal of Advanced Research in Electrical and Electronic Engineering and Instrumentation Engineering (IJAREEIE)*, vol. 3, no. 10, p. 5, Oct 2014.

[9] "Chapter 4," accessed: 2025-04-06. [Online]. Available: https://www.tntech.edu/engineering/pdf/cesr/ojo/asuri/Chapter4.pdf

[10] T. B. Shop. (2025) What is the difference between off-grid inverters, grid-tied inverters, and hybrid inverters. [Online]. Available: https://www.topbullshop.com/blogs/solar-energy-basics/what-is-the-difference-between-off-grid-inverters-grid-tied-inverters-and-hybrid-inverters

[11] R. L. Boylestad and L. Nashelsky, *Electronic Devices and Circuit Theory.* New Delhi: Prentice-Hall of India, 2000.

[12] R. W. Erickson and D. Maksimovic, *Fundamentals of Power Electronics*, 2nd ed. Springer, 2001.

[13] B. K. Bose, *Modern Power Electronics*, 3rd ed. Wiley, 2020.

[14] Y. Xue, L. Cha, S. B. Kjær, J. Bordonau, and T. Shimizu, "Topologies of single-phase inverters for small distributed power generators: An overview," *IEEE Transactions on Power Electronics*, vol. 19, no. 5, pp. 1305–1314, September 2004.

[15] P. Karuppusamy, G. Vijayakumar, and S. Sathishkumar, "Certain investigation on multilevel inverters for photovoltaic grid connected system," *J. Circuits Syst. Comput.*, vol. 25, no. 9, p. 1650108, 2016.

[16] M. M. Hoque, M. A. Hannan, and A. Mohamed, "Optimal algorithms for the charge equalisation controller of series connected lithium-ion battery cells in electric vehicle applications," *IET Electrical Systems in Transportation*, vol. 7, no. 4, pp. 267–277, 2017.

[17] S. Vavilapalli, S. Padmanaban, U. Subramaniam, and L. Mihet-Popa, "Power balancing control for grid energy storage system in photovoltaic applications—real time digital simulation implementation," *Energies*, vol. 10, no. 7, p. 928, 2017.

[18] D. C. Martins, "Analysis of a three-phase grid-connected PV power system using a modified dual-stage inverter," *ISRN Renewable Energy*, vol. 2013, Sep. 2013.

[19] A. Muszynski, "A refinement of the square wave phase noise evaluation," *Engineering, Technology & Applied Science Research*, vol. 9, no. 4, pp. 4429–4433, Aug 2019. [Online]. Available: https://etasr.com/index.php/ETASR/article/view/1733/pdf

[20] E. Hendawi and I. Bedir, "Analysis and simulation of three phase sinusoidal PWM inverter fed by PV array," *International Journal of Scientific & Engineering Research*, vol. 5, no. 6, pp. 948–949, 2014.

[21] S. Kouro, M. Malinowski, K. Gopakumar, J. Pou, L. G. Franquelo, and B. Wu, "Recent advances and industrial applications of multilevel converters," *IEEE Transactions on Industrial Electronics*, vol. 57, no. 8, pp. 2553–2580, August 2010.

[22] J. Holtz, "Pulse width modulation—a survey," *IEEE Transactions on Industrial Electronics*, vol. 39, no. 5, pp. 410–420, Oct 1994.

[23] V. Blasko, "Analysis of a hybrid pwm based on modified space-vector and triangle-comparison methods," *IEEE Transactions on Industry Applications*, vol. 33, no. 3, pp. 756–764, 1997.

[24] D. G. Holmes and T. A. Lipo, *Pulse Width Modulation for Power Converters: Principles and Practice.* Wiley-IEEE Press, 2003.

[25] Omron Corporation, *Inverter Technical Guide*, Omron Industrial Automation, 11 2010, accessed: [20th May 2025]. [Online]. Available: https://www.ia.omron.com/data_pdf/guide/9/inverter_tg_e_1_1.pdf

[26] H. Mao, X. Yang, Z. Chen, and Z. Wang, "A hysteresis current controller for single-phase three-level voltage source inverters," *IEEE Transactions on Power Electronics*, vol. 27, no. 7, pp. 3330–3339, 2012.

[27] M. A. Hannan, Z. A. Ghani, M. M. Hoque, P. J. Ker, A. Hussain, and A. Mohamed, "Fuzzy logic inverter controller in photovoltaic applications: Issues and recommendations," *IEEE Access*, vol. 7, pp. 24 934–24 955, 2019.

[28] D. K. Chaturvedi, *Modeling and Simulation of Systems Using MATLAB and Simulink*. Boca Raton, FL, USA: CRC Press, 2006.

[29] K. Zdenko and B. Stjepan, *Fuzzy Controller Design: Theory and Applications*. Boca Raton, FL, USA: CRC Press, 2006.

[30] H. Akagi, "New trends in power electronics for utility power systems," *IEEE Transactions on Industry Applications*, vol. 32, no. 6, pp. 1312–1322, Nov./Dec. 1996.

[31] N. Mohan, T. M. Undeland, and W. P. Robbins, *Power Electronics: Converters, Applications, and Design*, 3rd ed. New York, NY, USA: Wiley, 2002.

[32] S. Abbasian, M. Farsijani, M. T. Bina, and A. Shahirinia, "A non-isolated common-ground high step-up soft switching DC-DC converter with single active switch," *IEEE Transactions on Industrial Electronics*, vol. 69, no. 1, pp. 1–12, Jan 2022.

[33] A. Imanlou, E. S. Najmi, R. Behkam, M. Nazari-Heris, and G. B. Gharehpetian, "A new high voltage gain active switched–inductor based high step–up dc-dc converter with coupled–inductor," *IEEE Access*, vol. 11, pp. 56 749–56 765, 2023.

[34] S. Venkatesan and N. Arun, "Soft switched high gain trans inverse dc-dc converter based on three winding coupled inductor for renewable energy applications," *Scientific Reports*, vol. 15, p. 9951, 2025. [Online]. Available: https://www.nature.com/articles/s41598-025-92967-w

[35] S. Sadaf, N. Al-Emadi, A. Iqbal, M. S. Bhaskar, and M. Meraj, "Modelling, analysis, and implementation of a switched-inductor based dc/dc converter with reduced switch current stress," *IET Power Electronics*, vol. 14, no. 8, pp. 1504–1514, 2021.

[36] M. H. Rashid, *Power Electronics Handbook*, 4th ed. Butterworth-Heinemann, 2017.

[37] M. A. Ismeil, A. Abdelaleem, M. Nasrallah, and E. E. M. Mohamed, "Performance analysis of a novel high gain three-phase split source inverter," in *2022 23rd International Middle East Power Systems Conference (MEPCON)*. Cairo, Egypt: IEEE, 2022, pp. 1–6.

[38] F. A. M. Al-Qrimli and Y. S. Al-Hasnawi, "Three-phase split-source inverter (SSI)," *International Journal of Computer Applications*, vol. 168, no. 4, pp. 22–26, Jun 2017.

[39] M. A. Ismeil, A. Abdelaleem, and M. Nasrallah, "Split source inverter: Topology and switching modulation improvements—a review," *e-Prime - Advances in Electrical Engineering, Electronics and Energy*, 2023.

[40] University of British Columbia, Department of Mathematics. (2023) The Newton-Raphson method. University of British Columbia. Course notes for MATH 104. [Online]. Available: https://www.math.ubc.ca/~anstee/math104/newtonmethod.pdf

[41] Y. Zhou, W. Huang, P. Xu, and F. Blaabjerg, "A current-fed quasi-Z-source inverter with voltage buck–boost and regeneration capability," *IEEE Transactions on Industrial Electronics*, vol. 60, no. 10, pp. 4240–4247, Oct. 2013.

[42] S. Hameed, A. Khan, M. Rahman *et al.*, "Design and implementation of high-efficiency inverters," *IEEE Transactions on Power Electronics*, vol. 35, no. 4, pp. 1234–1245, April 2020.

[43] IC Components, "Sg3525: A deep dive into pulse width modulation control for renewable energy systems," https://www.ic-components.com/blog/sg3525-a-deep-dive-into-pulse-width-modulation-control-for-renewable-energy-systems.jsp, 2025, accessed: 25th May.

3.4 ANNEX

Annex pcb layout of the circuit

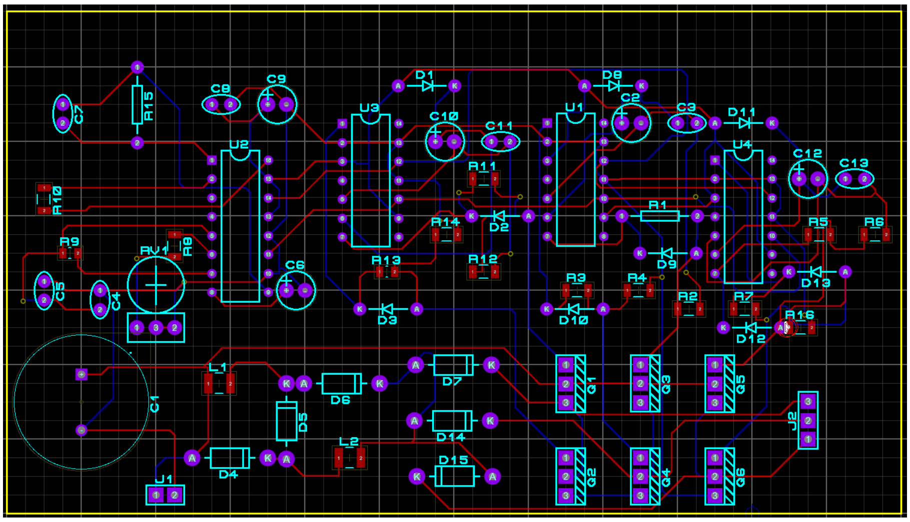

Figure 3.17: PCB layout of the three-phase circuit

3D visualisation of the circuit

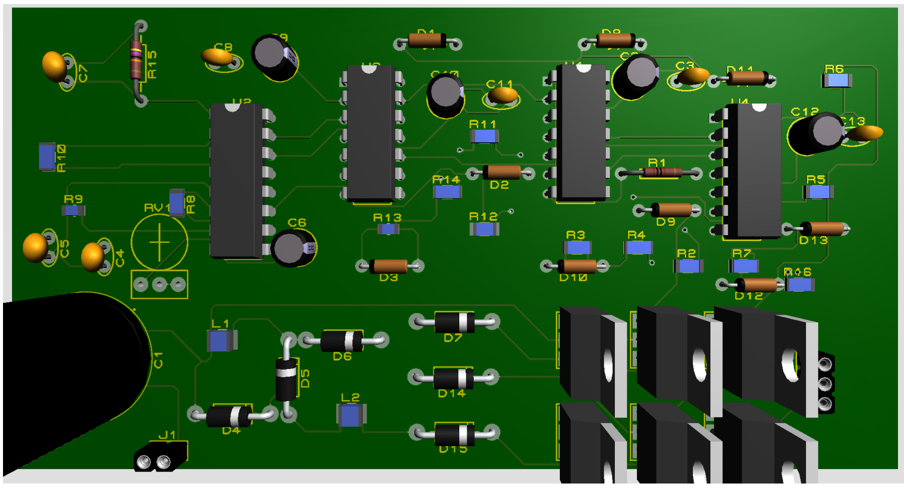

Figure 3.18: 3D visualisation of the circuit

The Arduino code used in this study

```
int output_1 = 11;  // Digital output pin 11
int output_2 = 12;  // Digital output pin 12
int output_3 = 13;  // Digital output pin 13
int t = 3310;       // Delay time in microseconds

void setup() {
  // Initialize all pins as outputs
  pinMode(output_1, OUTPUT);
  pinMode(output_2, OUTPUT);
  pinMode(output_3, OUTPUT);
}

void loop() {
  delayMicroseconds(t);
  digitalWrite(output_1, LOW);

  delayMicroseconds(t);
  digitalWrite(output_2, HIGH);

  delayMicroseconds(t);
  digitalWrite(output_3, LOW);

  delayMicroseconds(t);
  digitalWrite(output_1, HIGH);

  delayMicroseconds(t);
  digitalWrite(output_2, LOW);

  delayMicroseconds(t);
  digitalWrite(output_3, HIGH);
}
```

Listing 3.1: Arduino Pin Control Implementation

Figure 3.19: SG3525A

Figure 3.20: IR2112

Order this document by SG3525A/D

MOTOROLA

SG3525A
SG3527A

Pulse Width Modulator Control Circuits

PULSE WIDTH MODULATOR CONTROL CIRCUITS

SEMICONDUCTOR TECHNICAL DATA

The SG3525A, SG3527A pulse width modulator control circuits offer improved performance and lower external parts count when implemented for controlling all types of switching power supplies. The on–chip +5.1 V reference is trimmed to ±1% and the error amplifier has an input common–mode voltage range that includes the reference voltage, thus eliminating the need for external divider resistors. A sync input to the oscillator enables multiple units to be slaved or a single unit to be synchronized to an external system clock. A wide range of deadtime can be programmed by a single resistor connected between the C_T and Discharge pins. These devices also feature built–in soft–start circuitry, requiring only an external timing capacitor. A shutdown pin controls both the soft–start circuitry and the output stages, providing instantaneous turn off through the PWM latch with pulsed shutdown, as well as soft–start recycle with longer shutdown commands. The under voltage lockout inhibits the outputs and the changing of the soft–start capacitor when V_{CC} is below nominal. The output stages are totem–pole design capable of sinking and sourcing in excess of 200 mA. The output stage of the SG3525A features NOR logic resulting in a low output for an off–state while the SG3527A utilized OR logic which gives a high output when off.

- 8.0 V to 35 V Operation
- 5.1 V ± 1.0% Trimmed Reference
- 100 Hz to 400 kHz Oscillator Range
- Separate Oscillator Sync Pin
- Adjustable Deadtime Control
- Input Undervoltage Lockout
- Latching PWM to Prevent Multiple Pulses
- Pulse–by–Pulse Shutdown
- Dual Source/Sink Outputs: ±400 mA Peak

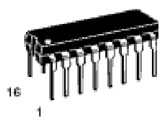

N SUFFIX
PLASTIC PACKAGE
CASE 648

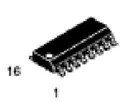

DW SUFFIX
PLASTIC PACKAGE
CASE 751B
(SO–16L)

PIN CONNECTIONS

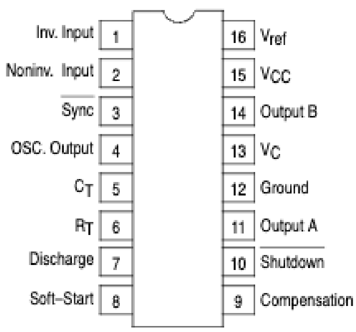

(Top View)

Representative Block Diagram

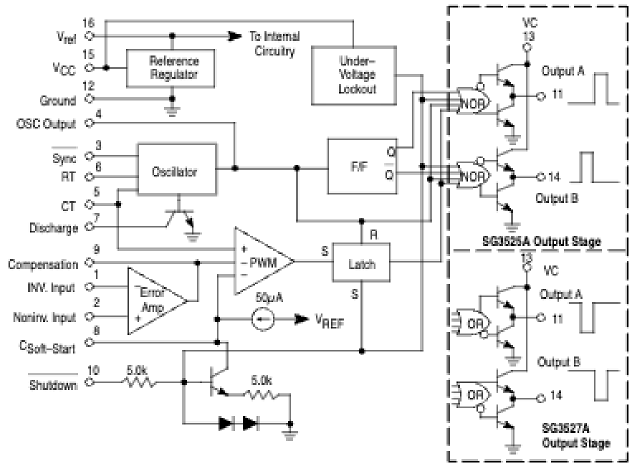

ORDERING INFORMATION

Device	Operating Temperature Range	Package
SG3525AN	T_A = 0° to +70°C	Plastic DIP
SG3525ADW		SO–16L
SG3527AN		Plastic DIP

 Rev 2

Figure 3.21: SG3525A Datasheet

SG3525A SG3527A

MAXIMUM RATINGS (Note 1)

Rating	Symbol	Value	Unit
Supply Voltage	V_{CC}	+40	Vdc
Collector Supply Voltage	V_C	+40	Vdc
Logic Inputs		–0.3 to +5.5	V
Analog Inputs		–0.3 to V_{CC}	V
Output Current, Source or Sink	I_O	±500	mA
Reference Output Current	I_{ref}	50	mA
Oscillator Charging Current		5.0	mA
Power Dissipation (Plastic & Ceramic Package) T_A = +25°C (Note 2) T_C = +25°C (Note 3)	P_D	 1000 2000	mW
Thermal Resistance Junction–to–Air	$R_{\theta JA}$	100	°C/W
Thermal Resistance Junction–to–Case	$R_{\theta JC}$	60	°C/W
Operating Junction Temperature	T_J	+150	°C
Storage Temperature Range	T_{stg}	–55 to +125	°C
Lead Temperature (Soldering, 10 seconds)	T_{Solder}	+300	°C

NOTES: 1. Values beyond which damage may occur.
2. Derate at 10 mW/°C for ambient temperatures above +50°C.
3. Derate at 16 mW/°C for case temperatures above +25°C.

RECOMMENDED OPERATING CONDITIONS

Characteristics	Symbol	Min	Max	Unit
Supply Voltage	V_{CC}	8.0	35	Vdc
Collector Supply Voltage	V_C	4.5	35	Vdc
Output Sink/Source Current (Steady State) (Peak)	I_O	 0 0	 ±100 ±400	mA
Reference Load Current	I_{ref}	0	20	mA
Oscillator Frequency Range	f_{osc}	0.1	400	kHz
Oscillator Timing Resistor	R_T	2.0	150	kΩ
Oscillator Timing Capacitor	C_T	0.001	0.2	μF
Deadtime Resistor Range	R_D	0	500	Ω
Operating Ambient Temperature Range	T_A	0	+70	°C

Figure 3.22: SG3525A maximum and operating conditions

International
IOR Rectifier

Data Sheet No. PD60026 revS

IR2112(-1-2)(S)PbF

HIGH AND LOW SIDE DRIVER

Features

- Floating channel designed for bootstrap operation
- Fully operational to +600V
- Tolerant to negative transient voltage
  dV/dt immune
- Gate drive supply range from 10 to 20V
- Undervoltage lockout for both channels
- 3.3V logic compatible
  Separate logic supply range from 3.3V to 20V
  Logic and power ground ±5V offset
- CMOS Schmitt-triggered inputs with pull-down
- Cycle by cycle edge-triggered shutdown logic
- Matched propagation delay for both channels
- Outputs in phase with inputs

Product Summary

V_{OFFSET}	600V max.
I_O+/-	200 mA / 420 mA
V_{OUT}	10 - 20V
$t_{on/off}$ (typ.)	125 & 105 ns
Delay Matching	30 ns

Packages

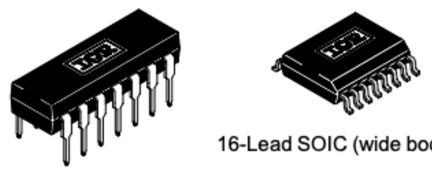

14-Lead PDIP

16-Lead SOIC (wide body)

Description

The IR2112(S) is a high voltage, high speed power MOSFET and IGBT driver with independent high and low side referenced output channels. Proprietary HVIC and latch immune CMOS technologies enable ruggedized monolithic construction. Logic inputs are compatible with standard CMOS or LSTTL outputs, down to 3.3V logic.
The output drivers feature a high pulse current buffer stage designed for minimum driver cross-conduction. Propagation delays are matched to simplify use in high frequency applications. The floating channel can be used to drive an N-channel power MOSFET or IGBT in the high side configuration which operates up to 600 volts.

Typical Connection

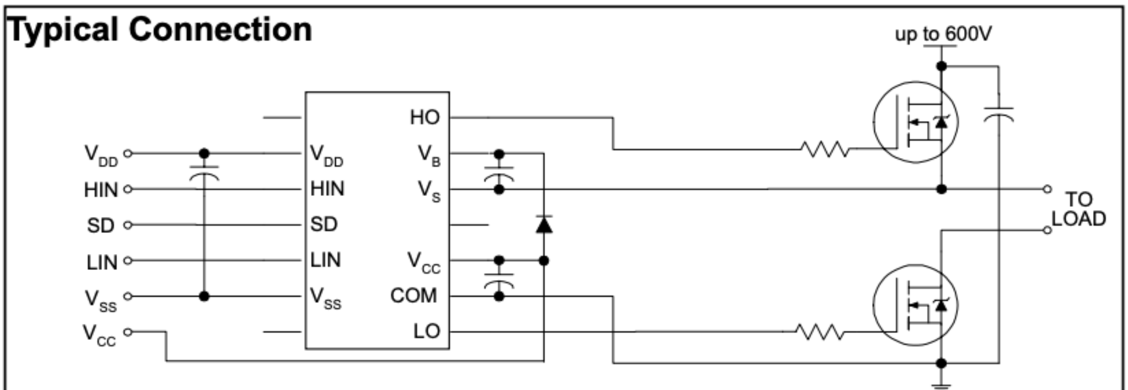

(Refer to Lead Assignments for correct pin configuration). This/These diagram(s) show electrical connections only.
Please refer to our Application Notes and DesignTips for proper circuit board layout.

Figure 3.23: IR2112 Datasheet

IR2112(-1-2)(S)PbF

International IOR Rectifier

Absolute Maximum Ratings

Absolute Maximum Ratings indicate sustained limits beyond which damage to the device may occur. All voltage parameters are absolute voltages referenced to COM. The Thermal Resistance and Power Dissipation ratings are measured under board mounted and still air conditions. Additional information is shown in Figures 28 through 35.

Symbol	Definition		Min.	Max.	Units
V_B	High Side Floating Supply Voltage		-0.3	625	
V_S	High Side Floating Supply Offset Voltage		V_B - 25	V_B + 0.3	
V_{HO}	High Side Floating Output Voltage		V_S - 0.3	V_B + 0.3	
V_{CC}	Low Side Fixed Supply Voltage		-0.3	25	V
V_{LO}	Low Side Output Voltage		-0.3	V_{CC} + 0.3	
V_{DD}	Logic Supply Voltage		-0.3	V_{SS} + 25	
V_{SS}	Logic Supply Offset Voltage		V_{CC} - 25	V_{CC} + 0.3	
V_{IN}	Logic Input Voltage (HIN, LIN & SD)		V_{SS} - 0.3	V_{DD} + 0.3	
dV_s/dt	Allowable Offset Supply Voltage Transient (Figure 2)		—	50	V/ns
P_D	Package Power Dissipation @ $T_A \leq$ +25°C	(14 Lead DIP)	—	1.6	W
		(16 Lead SOIC)	—	1.25	
R_{THJA}	Thermal Resistance, Junction to Ambient	(14 Lead DIP)	—	75	°C/W
		(16 Lead SOIC)	—	100	
T_J	Junction Temperature		—	150	
T_S	Storage Temperature		-55	150	°C
T_L	Lead Temperature (Soldering, 10 seconds)		—	300	

Recommended Operating Conditions

The Input/Output logic timing diagram is shown in Figure 1. For proper operation the device should be used within the recommended conditions. The V_S and V_{SS} offset ratings are tested with all supplies biased at 15V differential. Typical ratings at other bias conditions are shown in Figures 36 and 37.

Symbol	Definition	Min.	Max.	Units
V_B	High Side Floating Supply Absolute Voltage	V_S + 10	V_S + 20	
V_S	High Side Floating Supply Offset Voltage	Note 1	600	
V_{HO}	High Side Floating Output Voltage	V_S	V_B	
V_{CC}	Low Side Fixed Supply Voltage	10	20	
V_{LO}	Low Side Output Voltage	0	VCC	V
V_{DD}	Logic Supply Voltage	V_{SS} + 3	V_{SS} + 20	
V_{SS}	Logic Supply Offset Voltage	-5 (Note 2)	5	
V_{IN}	Logic Input Voltage (HIN, LIN & SD)	V_{SS}	V_{DD}	
T_A	Ambient Temperature	-40	125	°C

Note 1: Logic operational for V_S of -5 to +600V. Logic state held for V_S of -5V to -V_{BS}. (Please refer to the Design Tip DT97-3 for more details).
Note 2: When V_{DD} < 5V, the minimum V_{SS} offset is limited to -V_{DD}.

Figure 3.24: IR2112 Maximum and operating conditons

IR2112(S) & (PbF)

International IOR Rectifier

Functional Block Diagram

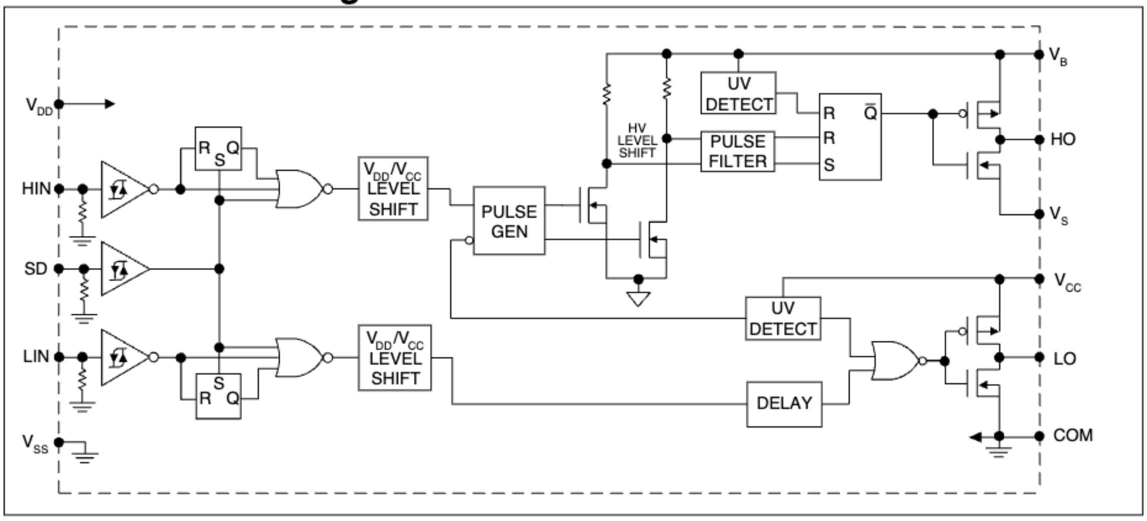

Lead Definitions

Symbol	Description
V_{DD}	Logic supply
HIN	Logic input for high side gate driver output (HO), in phase
SD	Logic input for shutdown
LIN	Logic input for low side gate driver output (LO), in phase
V_{SS}	Logic ground
V_B	High side floating supply
HO	High side gate drive output
V_S	High side floating supply return
V_{CC}	Low side supply
LO	Low side gate drive output
COM	Low side return

Lead Assignments

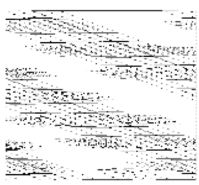

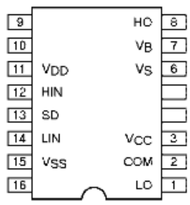

14 Lead DIP	16 Lead SOIC (Wide Body)
IR2112	**IR2112S**
Part Number	

Figure 3.25: Functional block diagram

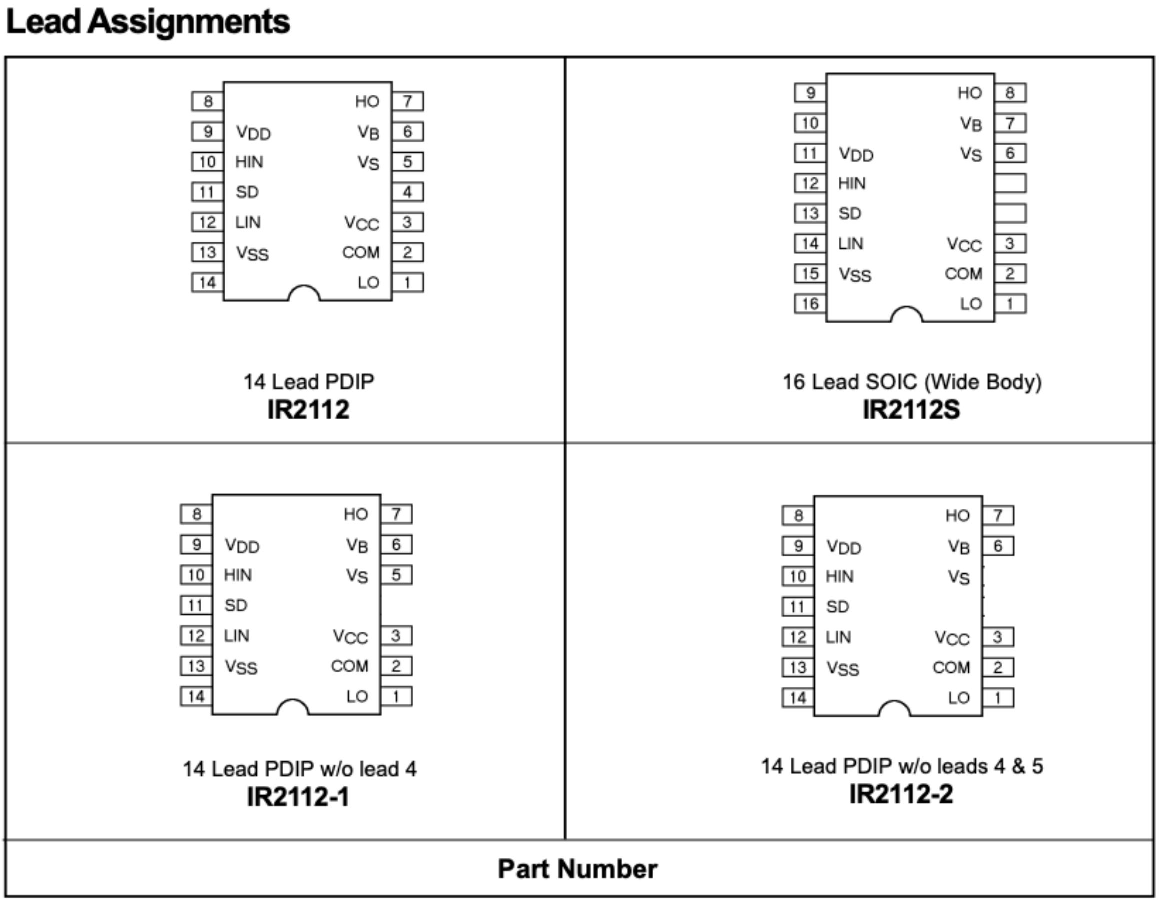

Figure 3.26: IR2112 Lead Assignments

Abstract

Traditional inverters are bulky, less efficient, and have complex control systems, making them unsuitable for compact renewable energy solutions. This thesis proposes a Switched-Inductor Split-Source Inverter (SI-SSI)—a single-stage, transformerless design that combines voltage boosting and DC-AC conversion. Using a 100V input, it delivers 10kW output, modeled in MATLAB with SPWM control. Hardware implementation uses the SG3525A PWM IC, enabling adjustable switching frequency with simple RT/CT components. Tests show a stable three-phase output and 40% fewer components than traditional systems, with comparable performance. The SI-SSI is compact, efficient, and ideal for clean energy systems. Keywords: SI-SSI, SPWM, Single-Stage, Voltage Boost

Keywords
Split-Source Inverter (SSI), Switched-Inductor Split-Source Inverter, Sinusoidal PWM (SPWM), Voltage Boosting, Single-Stage Converter.

Résumé:

Les onduleurs traditionnels sont encombrants, moins efficaces, et nécessitent des systèmes de contrôle complexes, ce qui les rend peu adaptés aux énergies renouvelables. Cette thèse introduit le SI-SSI, un onduleur monostage sans transformateur intégrant élévation de tension et conversion DC-AC. Avec une entrée de 100V, il fournit 10kW, modélisé sous MATLAB avec commande PWM sinusoïdale. L'implémentation matérielle utilise le circuit SG3525A, permettant une fréquence ajustable via des composants RT/CT simples. Les tests montrent une sortie triphasée stable et une réduction de 40% des composants, pour une efficacité équivalente.

Mots clés:
Onduleur à source divisée (SSI), onduleur (SSI), onduleur à source divisée à inductance commutée (SI-SSI), convertisseur à un étage, inductance commutée (SI), PWM sinusoïdal (SPWM), convertisseur monostade.

ملخص

هذه تقترح .المعقدة التحكم وأنظمة المراحل متعدد والتحويل الضخمة المحولات بسبب تحديات التقليدية العاكسات تواجه مرحلة في متردد إلى المستمر التيار وتحويل الجهد رفع بين يجمع محول بدون جديد تصميم وهو ،SI-SSI عاكس الأطروحة MATLAB/Simulink باستخدام النظام نمذجة تم .كيلوواط 10 بقدرة الطور ثلاثي خرجًا يحقق ،فولت 100 بمدخل .واحدة عبر للتعديل قابل تبديل تردد النتائج أظهرت .التكلفة منخفضة SG3525A دارة باستخدام تنفيذه وتم ،جيبية PWM تقنية مع ذات التقليدية بالأنظمة مقارنة ٪40 بنسبة المكونات عدد بتقليل التصميم يسمح.مستقرًا وخرجًا بسيطة RT/CT مكونات وكفاءة بساطة تتطلب التي المتجددة الطاقة لتطبيقات مناسبًا يجعله مما ،نفسها الكفاءة على الحفاظ مع المرحلتين.

المفتاحية الكلمات

،رفع الجهد ،(SPWM) عاكس مصدر مقسوم بمحاثة مبدّلة، تعديل عرض النبضة الجيبي ،(SSI) عاكس مصدر مقسوم
محول أحادي المرحلة